

University of Rhode Island

DigitalCommons@URI

Open Access Master's Theses

2004

BIOACTIVE SECONDARY METABOLITES PRODUCED BY MARINE MICROORGANISMS: THEIR ISOLATION, STRUCTURAL ELUCIDATION AND FUNCTION

Jiayuan Liu

University of Rhode Island

Follow this and additional works at: <https://digitalcommons.uri.edu/theses>

Terms of Use

All rights reserved under copyright.

Recommended Citation

Liu, Jiayuan, "BIOACTIVE SECONDARY METABOLITES PRODUCED BY MARINE MICROORGANISMS: THEIR ISOLATION, STRUCTURAL ELUCIDATION AND FUNCTION" (2004). *Open Access Master's Theses*. Paper 262.

<https://digitalcommons.uri.edu/theses/262>

This Thesis is brought to you by the University of Rhode Island. It has been accepted for inclusion in Open Access Master's Theses by an authorized administrator of DigitalCommons@URI. For more information, please contact digitalcommons-group@uri.edu. For permission to reuse copyrighted content, contact the author directly.

**BIOACTIVE SECONDARY METABOLITES PRODUCED BY MARINE
MICROORGANISMS: THEIR ISOLATION, STRUCTURAL
ELUCIDATION AND FUNCTION**

**BY
JIAYUAN LIU**

**A THESIS SUBMITTED IN PARTIAL FULFILLMENT OF THE
REQUIREMENTS FOR THE DEGREE OF MASTER IN
PHARMACOGNOSY**

UNIVERSITY OF RHODE ISLAND

2004

MASTER OF SCIENCE THESIS

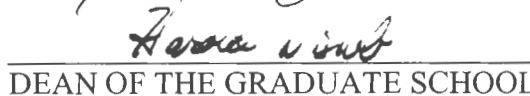
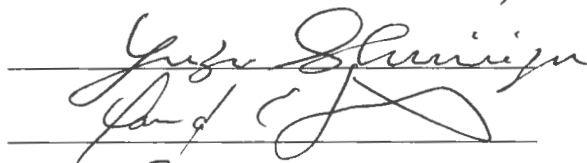
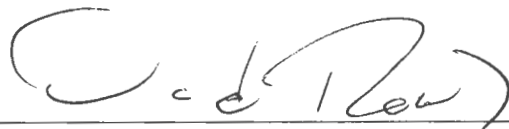
OF

JIAYUAN LIU

APPROVED:

Thesis Committee:

Major Professor



DEAN OF THE GRADUATE SCHOOL

UNIVERSITY OF RHODE ISLAND

2004

ABSTRACTS

Compared to their terrestrial counterparts, marine microorganisms seem to be a relatively unexplored resource for novel bioactive metabolites. This thesis research aimed to discover new bioactive compounds of pharmaceutical value from the secondary metabolites produced by marine bacteria and fungi. The ecological role of marine bacteria involving the production of antibacterial metabolites was also investigated.

This thesis describes three different studies, all of which are focused on the secondary metabolites produced by marine bacteria or fungi. First, bacteria-bacteria antagonism as a mechanism limiting the spread of *Vibrio cholerae* in the ocean was investigated using a marine particle-attached bacterial model, SWAT3, for its ability to prevent the colonization of particles and hence the growth of *V. cholerae*, by producing an antibacterial agent, andrimid. Second, the biosynthesis of CNC352.223, a novel metabolite derived from a marine fungus was explored using stable isotopic feeding experiments. Third, a marine-derived *Halobacillus* sp. culture C42, was investigated for its production of bacterial cell-cell signaling-antagonists since compounds possessing this type of activity may lead to a new generation of antibiotics. Two bioactive metabolites were isolated from C42 culture. Their bioactivity against bacterial cell-cell communication system was also examined.

ACKNOWLEDGEMENTS

I would like to give my appreciation to my graduate advisor Dr. David Rowley. His kindness, encouragement and knowledge have supported me throughout the course of this graduate study.

I would also like to acknowledge to Dr. Yuzuru Shimizu. He kindly allowed me to use his instruments and chemical solutions in my research. He also gave me tremendous guidance in biosynthetic research.

I thank Dr. David Smith. His course, *Marine Microbial Ecology*, helped me fully appreciate the marine ecology project. I also thank him for being my thesis committee member.

Thanks to Dr. Gongqin Sun, who kindly chaired my thesis defense.

Thanks to Dr. Aftab Ahmed and Ms. Rebecca Pitts for their kind help in instrumentation in BRIN core facility.

I would also like to give my appreciation to my collaborators Dr. Farooq Azam, Dr. Douglas Bartlett, and Mr. Eric Zamora of the Scripps Institution of Oceanography, UCSD, and Dr. Richard Long at Texas A&M. Without their sincere cooperation, the first chapter of my thesis would not be here.

During my research on Quorum Sensing which is described in the third chapter of this thesis, Dr. David Nelson supplied me with the biosensor strains, culture medium nutrients and spectroscopic instrumentation. His former PhD student, Dr. Steve Denkin also helped me greatly in this research.

Help from my colleagues and friends also contributed very much to my research. Mr. Dioscaris Garcia did the Gram Stain and 16s rRNA sequencing of C42. Ms.

Margaret Teasdale and Ms. Joselynn Wallace assisted me with the Quorum Sensing reporter assay. Mr. Aaron Socha graciously edited my thesis. Dr. Tianle Yang and Dr. Katherine Drainville-Higgins also helped me greatly with their suggestive tips.

Finally, I would like to give my love to my husband Tony (Xu) Han. His encouragement has supported me to finish this two years graduate study.

TABLE OF CONTENTS

ABSTRACT	ii
ACKNOWLEDGEMENTS.....	iii
TABLE OF CONTENTS.....	v
LIST OF TABLES.....	viii
LIST OF FIGURES.....	x

CHAPTER	PAGE
1 Bacteria-Bacteria Antagonism as a Mechanism Limiting the Spread of <i>Vibrio cholerae</i> in the Ocean.....	1
1.1 Introduction.....	2
1.2 Methods and Results.....	8
1.2.1 Isolation and Purification of Anti- <i>Vibrio cholerae</i> Metabolites Produced by SWAT3, a Marine <i>Vibrio</i> sp.	8
1.2.2 Assessment of the Anti- <i>Vibrio cholerae</i> Activity of Andrimid.....	12
1.2.3 Exploration of the Relationship Between the Anti- <i>V. cholerae</i> Activity of SWAT3 and Its Andrimid Production.....	17
1.3 Summary and Discussion.....	26
1.4 References.....	27
2 Biosynthesis of CNC352.223, a Novel Metabolite of Polyketide Origin Produced by a Marine-Derived <i>Aspergillus niger</i>.....	30
2.1 Introduction.....	30

2.2	Methods and Results.....	33
2.2.1	Stable Isotopic Feeding Experiments.....	33
2.2.2	Isolation and Structural Examination of ¹³ C-Labeled CNC352.223 Substrates.....	33
2.2.3	Investigation of the Biosynthesis of CNC352.223 by ¹³ C NMR Analyses of Labeled Substrates.....	34
2.3	Summary and Discussion.....	42
2.4	References.....	43
3	Inhibition of Bacterial Cell-Cell Signaling by Metabolites Produced by a Marine <i>Halobacillus</i> sp.	45
3.1	Introduction.....	45
3.2	Methods and Results.....	51
3.2.1	QS-Antagonism Screening of the Library of Crude Extracts Produced by Marine Bacteria.....	51
3.2.1.1	Agar disk diffusion assay for violacein inhibition.....	54
3.2.1.2	CV026 screening assay in microtiter plates.....	54
3.2.2	Isolation of Quorum Sensing Inhibitory Compounds C42.191 and C42.205 Produced by <i>Halobacillus</i> sp. Culture C42.....	58
3.2.3	Structural Elucidation of C42.191 and C42.205.....	62
3.2.4	QS-Inhibition Activity of C42.191 and C42.205.....	78
3.2.4.1	CV026-violacein inhibition assay.....	78
3.2.4.2	Green fluorescence protein assay.....	86

3.3 Summary and Discussion.....	89
3.4 References.....	90
BIBLIOGRAPHY.....	97

LIST OF TABLES

TABLE	PAGE
1.1	The Effect of Temperature on <i>Vibrio cholerae</i> Inhibition by Marine Bacteria..... 5
1.2	The Effect of Temperature on SWAT3 Antagonism Against <i>Vibrio cholerae</i> 5
1.3	Proton NMR Data of Andrimid in DMSO- <i>d</i> ₆ (400 MHz)..... 12
1.4	The 4-fold Serial Dilution Set Up Scheme for the Broth Dilution Assay... 14
1.5	The Concentration of the Samples in Each Well..... 15
1.6	The Diameter of Antibacterial Zone Induced by SWAT3 Crude Extracts.. 19
1.7	UV Absorbance of Andrimid at Different Concentrations..... 22
1.8	The Yield of Crude Extracts of SWAT3-wt Cultures Grown at 24° C and 30° C..... 23
1.9	The Absorbance of Andrimid in the Crude Extracts of SWAT3-wt Culture Incubated at Two Different Temperatures..... 25
1.10	The Calculated Concentration of Andrimid in the Crude Extract Solution 25
1.11	The Average Yield of Andrimid per 100 mL of SWAT3-wt Culture at Two Different Temperatures..... 25
1.12	The Correlation Between the Production of Andrimid and the Bioactivity of SWAT3-wt, SWAT3-4 and SWAT3-111..... 26
2.1	Stable Isotopic Incorporations Resulting from Feeding Experiment with ¹³ C-Labelled Acetates..... 41

3.1	Autoinducers Utilized by Bacteria in Quorum Sensing.....	49
3.2	^1H and ^{13}C NMR Assignments for C42.191 in MeOD- d_4	64
3.3	^1H and ^{13}C NMR Assignments for C42.205 in MeOD- d_4	65
3.4	The GFP Assay Set Up and the Serial Concentration of C42.205.....	87
3.5	Measured Fluorescence and Optical Density.....	88

LIST OF FIGURES

FIGURE	PAGE
1.1 The Antagonistic Activity by SWAT3 Strains.....	6
1.2 The Antagonistic Activity of SWAT3 Strains Against the Colonization of <i>V. cholerae</i> in Liquid.....	7
1.3 The Flow Chart of the Isolation of Andrimid from a 39 L SWAT3 Culture	10
1.4 Proton NMR of Andrimid in DMSO- <i>d</i> ₆ (400 MHz).....	11
1.5 Sensitivity of <i>V. cholerae</i> to Andrimid at 28°C.....	16
1.6 Sensitivity of <i>V. cholerae</i> to Andrimid as a Function of Temperature.....	18
1.7 HPLC Chromatograms of Andrimid and the Crude Extracts of Three SWAT3 Strains.....	20
1.8 Standard Curve of Andrimid, Absorbance vs. Concentration.....	23
2.1 Structure of CNC352.223.....	31
2.2 The Hypothesized Biosynthetic Pathway of CNC352.223 (<i>I</i>).....	32
2.3 The Flow Chart of the Isolation and Purification of CNC352.223 from All Three Different Feeding Experiments.....	35
2.4 ¹³ C NMR Spectrum of CNC352.223-N in DMSO- <i>d</i> ₆	36
2.5 ¹³ C NMR Spectrum of CNC352.223-S in DMSO- <i>d</i> ₆	37
2.6 ¹³ C NMR Spectrum of CNC352.223-D in DMSO- <i>d</i> ₆	38
2.7 Labeling Pattern of CNC352.223 from Stable Isotopic Experiments.....	40
3.1 A Typical QS Pathway in Gram-negative Bacteria Using LuxI/LuxR Circuit.....	48

3.2	Some Brominated Furanones with QS-Antagonistic Activity.....	50
3.3	RNAIII-Inhibiting Peptides (RIP) Isolated from <i>Staphylococcus xylosus</i> ...	51
3.4	<i>N</i> -Hexanoyl-L-Homoserine Lactone (HHL).....	53
3.5	HHL Induction of Violacein Production by CV026.....	53
3.6	The Plating Scheme for QS-Inhibition Broth Assay.....	57
3.7	QS-Inhibitory Activity of C42 Crude Extracts vs. Fermentation Time.....	59
3.8	Bioassay Guided Fractionation of C42 Culture.....	61
3.9	The Structures of C42.191 and C42.205.....	62
3.10	Mass Chromatogram (Positive Ion) of C42.191.....	66
3.11	¹ H NMR Spectrum (400 MHz) of C42.191 in MeOD- <i>d</i> ₄	67
3.12	¹³ C NMR Spectrum (100 MHz) of C42.191 in MeOD- <i>d</i> ₄	68
3.13	Dept135 NMR Spectrum of C42.191 in MeOD- <i>d</i> ₄	69
3.14	COSY Spectrum of C42.191 in MeOD- <i>d</i> ₄	70
3.15	HMQC Spectrum of C42.191 in MeOD- <i>d</i> ₄	71
3.16	Mass Chromatogram (Positive Ion) of C42.205.....	72
3.17	¹ H NMR Spectrum (400 MHz) of C42.205 in MeOD- <i>d</i> ₄	73
3.18	¹³ C NMR Spectrum (100 MHz) of C42.205 in MeOD- <i>d</i> ₄	74
3.19	Dept135 NMR Spectrum of C42.205 in MeOD- <i>d</i> ₄	75
3.20	COSY Spectrum of C42.205 in MeOD- <i>d</i> ₄	76
3.21	HMQC Spectrum of C42.205 in MeOD- <i>d</i> ₄	77
3.22	Synthesis of HHL.....	79
3.23	Purification of Synthetic HHL.....	80

3.24	<i>N</i> -Decanoyl-L-Homoserine Lactone (DHL).....	81
3.25	4-Bromo-5-(Bromomethylene)-2(<i>5H</i>)-Furanone.....	81
3.26	Synthesis of Brominated Furanones.....	83
3.27	Purification of 4-Bromo-5-(Bromomethylene)-2(<i>5H</i>)-Furanone.....	84
3.28	QS-Antagonistic Activity of DHL, C42.191 and C42.205.....	86
3.29	C42.205 Inhibition of QS-mediated GFP production	88

CHAPTER 1

Bacteria-Bacteria Antagonism as a Mechanism Limiting the Spread of *Vibrio cholerae* in the Ocean

Evidence suggests that *Vibrio cholerae*, the etiologic agent of cholera, proliferates much faster at higher sea surface temperatures (Colwell, 1996). Thus, there is a concern that global climate warming will lead to increases in the frequency and geographic distributions of cholera epidemics (Harvell *et al.*, 2002; Epstein, 1999). However, the mechanisms for the temperature-dependent abundance of *V. cholerae* in ocean are unknown. This chapter describes a study designed to explore whether autochthonous marine bacteria play a role in limiting the proliferation of *V. cholerae* through bacteria-bacteria antagonism. Further, this study sought to explore the effect of temperature on these types of bacterial interactions.

The investigation described in this chapter was conducted in collaboration with Dr. Farooq Azam, Dr. Douglas Bartlett, and Mr. Eric Zamora of the Scripps Institution of Oceanography, UCSD, and Dr. Richard Long at Texas A&M University. The investigation can be roughly divided into two parts. The first part, conducted by my collaborators listed above, included collecting and screening a diverse panel of marine bacteria for their anti-*V. cholerae* activity, building a model system employing bacteria labeled with Green Fluorescent Protein (GFP), and conducting *V. cholerae* colonization inhibition assays. A brief review of these components will be presented in the Introduction. My contribution to this study was the identification of the chemical mechanisms behind the observed bacteria-bacteria antagonistic interactions, and is described in detail in the ensuing sections of this chapter.

1.1 Introduction

The Gram-negative bacterium *Vibrio cholerae* is notorious for its pathogenic biotypes that cause the severe and sometimes fatal diarrheal disease known as cholera. In 1883, Robert Koch isolated the classical biotype of *V. cholerae* (*V. cholerae* 01) which caused the first six pandemics of cholera lasting until 1923 (Madigan *et al.*, 2003a). The seventh outbreak of cholera started in 1961 and several more pathogenic biotypes, notably *V. cholerae* 01 El Tor, *V. cholerae* non 01, and *V. cholerae* 0139, have since been discovered (Colwell, 1996; Ramamurthy *et al.*, 1993; Shimada *et al.*, 1993; Waldor *et al.*, 1994). *V. cholerae* is an aquatic bacterium, and people consuming contaminated water are in danger of becoming infected (Madigan *et al.*, 2003a). Pathogenic biotypes of *V. cholerae* proliferate and transport on marine particles, especially zooplankton. These associations assist *V. cholerae* in proliferating quickly during plankton blooms (Colwell 1996). Transport of *V. cholerae* in the ballast water of cargo ships is a concern for the introduction of the pathogen to previously unaffected coastlines (Ruiz *et al.*, 2000).

The frequency of cholera outbreaks has been linked with increases in sea surface temperatures (Colwell, 1996). For example, cholera outbreaks have followed the sea surface temperature elevations associated with El Niño-Southern Oscillation (ENSO) events (Pascual *et al.*, 2000). Thus, there is a concern that global climate change may lead to the emergence and resurgence of cholera pandemics. However, the reasons for rapid proliferation of *V. cholerae* during ocean warming events still remained undiscovered.

It was previously reported that over 50% of marine bacteria exhibit antagonistic activity against other marine strains (Long & Azam 2001). Considering this pervasive antibiosis in nature, it was hypothesized by Dr. Long and Azam that antagonistic behavior by indigenous marine bacteria might limit colonization of marine particles by *V. cholerae* and thus its rapid proliferation in marine ecosystems. Dr. Richard Long and coworkers tested bacteria-bacteria antagonism as a possible mechanism to retard the proliferation of *V. cholerae*. In this study, 74 marine bacterial isolates representing phylogenetically diverse species of cultivable marine bacteria were tested for antagonistic activity against eight biotypes (both clinical and environmental) of *V. cholerae*. Both particle-attached and free living bacterial species were examined. A modified Burkholder inhibition assay was used (Long & Azam 2001). Briefly, growing cultures of test isolates were spotted onto lawns of *V. cholerae* imbedded in soft ZoBell 2216 agar, and then zones of growth inhibition were measured after an incubation period. At 20 °C, a mean of 23% of the particle-attached marine bacteria inhibited the growth of *V. cholerae* while only 6% of free-living bacteria showed similar antagonistic behavior (Table 1.1). Clinical and environmental biotypes of *V. cholerae* were equally inhibited, including both classical and El Tor strains. Furthermore, the results were temperature dependent. Antagonistic interactions decreased dramatically when the assay was increased to 30 °C.

SWAT3 (Sea Water ATtached 3), a particle attached marine *Vibrio* sp., was selected as a model strain to study the effects of bacteria-bacteria antagonism on particle colonization by *V. cholerae*. SWAT3 displayed a temperature-dependent antagonistic activity against the *V. cholerae* panel (Table 1.2). GFP-producing mutants

of SWAT3 were created by mutagenesis with a Tn10-based transposon derivative containing a promoterless-green fluorescent protein (Stretton *et al.*, 1998). The GFP-mutants could be microscopically distinguished from *V. cholerae*. SWAT3-4 and SWAT3-111 were selected for further study from the 2000 mutants screened due to their (1) strong GFP signal and (2) ability (SWAT3-4) or inability (SWAT3-111) to antagonize the growth of *V. cholerae* N16961 (Figure 1.1). Both mutants displayed similar growth properties as the wild type.

The mutant strains were next examined for their ability to inhibit the colonization of model particles by *V. cholerae* N16961. Sterile seawater Petri dishes including nutrient-enriched, agarose particles were inoculated with one of the SWAT3 mutants and incubated over night. The cultures were then inoculated with *V. cholerae*. The density of SWAT3 on the particles at the time of *V. cholerae* inoculation was 10^8 mL⁻¹, which falls within the range of bacterial density on marine particles (10^7 - 10^{10} mL⁻¹; Alldredge, 1986). *V. cholerae* was also inoculated into a control Petri dish with sterile agarose particles. The antagonistic mutant, SWAT3-4, completely inhibited the colonization of particles by *V. cholerae*, while particles in the presence of the non-antagonistic mutant (SWAT3-111) had similar levels of attached *V. cholerae* as the control (Fig 1.2). The experiment was then repeated with particles embedded with freeze-thawed-lysed cells of the dinoflagellate *Lingulodinium polyedrum* with similar results.

Table 1.1

The Effect of Temperature on *Vibrio cholerae* Inhibition by Marine Bacteria

<i>V. cholerae</i> strain ¹	20 °C		30 °C	
	Attached	Free-living	Attached	Free-living
N16961	22.9	3.2	20	0
01	22.9	3.2	8.6	0
139	17.1	6.5	17.1	0
non01	22.9	6.5	17.1	0
395	31.4	16.1	20	3.2
1st case	25.7	6.5	14.3	0
G2	22.9	3.2	11.4	3.2
Dino	20	3.2	31.4	22.6

Note. Numbers refer to the percent of particle-attached and free-living marine bacterial isolates that inhibited *V. cholerae* growth as determined by a modified Burkholder inhibition assay (see text). The assay was scored positive when a zone of inhibition was greater than 2 mm from the edge of the test isolate. ¹*V. cholerae* isolates Vc N16961 and Vc 0395 were gifts from John J. Mekalanos. Isolates Vc01, Vc0139, Vc Non01 and Vc 1st case are part of an unpublished strain collection of Leonardo Lizaraga (CICSESE, Ensenda Mexico). Isolates Vc TP and Vc SIO are environmental strains isolated off Scripps Pier (Purdy *et al.*; manuscript in preparation; GenBank accession numbers AY494843 & AY494842)

Table 1.2

The Effect of Temperature on SWAT3 Antagonism Against *Vibrio cholerae*

<i>V. cholerae</i> Strains	25 °C	30 °C
N16961	5 mm ^a	Hazy Zone ^b
01	6 mm	None
0139	6 mm	None
Non01	5 mm	None
1st Case	4 mm	Hazy Zone
G2	7 mm	Hazy Zone
Dino	4 mm	Hazy Zone

Note. ^aThe numbers represent the radius from the edge of the SWAT3 colony to where the lawns become translucent. ^bHazy Zone indicates minimal inhibition, with a clear lawn of less than 2 mm.

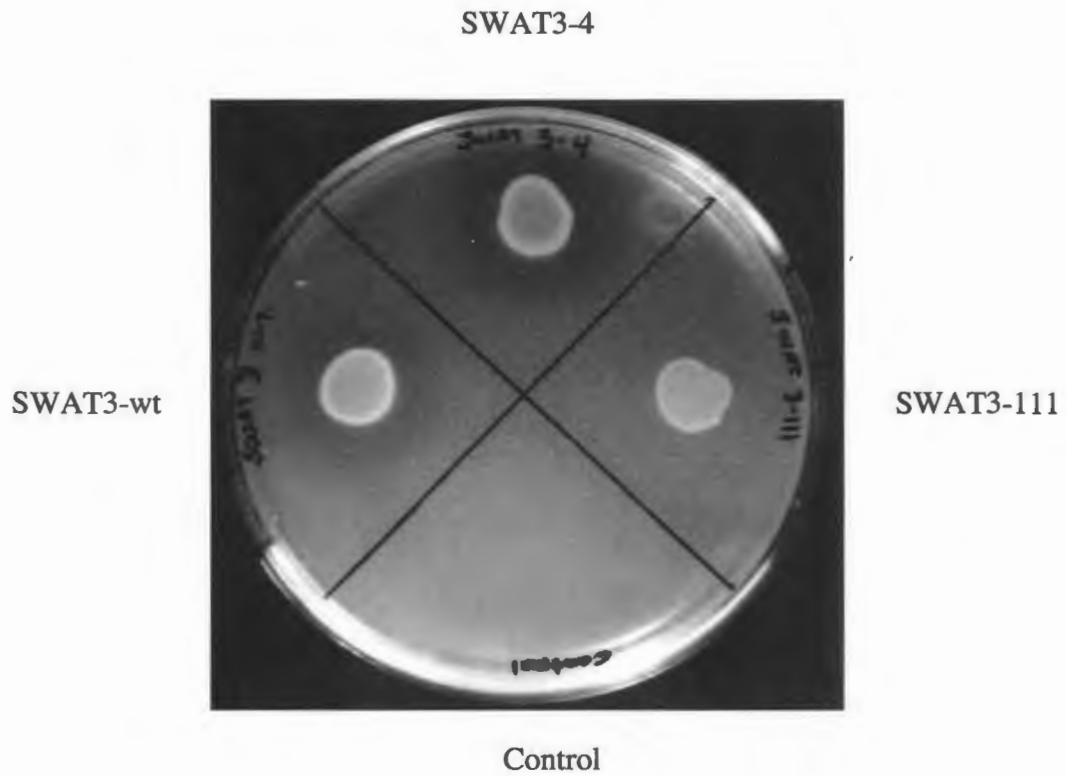


Figure 1.1. The Antagonistic Activity by SWAT3 Strains

Note. Colonies of SWAT3-wt and GFP-mutants which inhibit (SWAT3-4) and do not inhibit (SWAT3-111)

V. cholerae were spotted onto a lawn of *V. cholerae* N16961 and incubated at 20 °C.

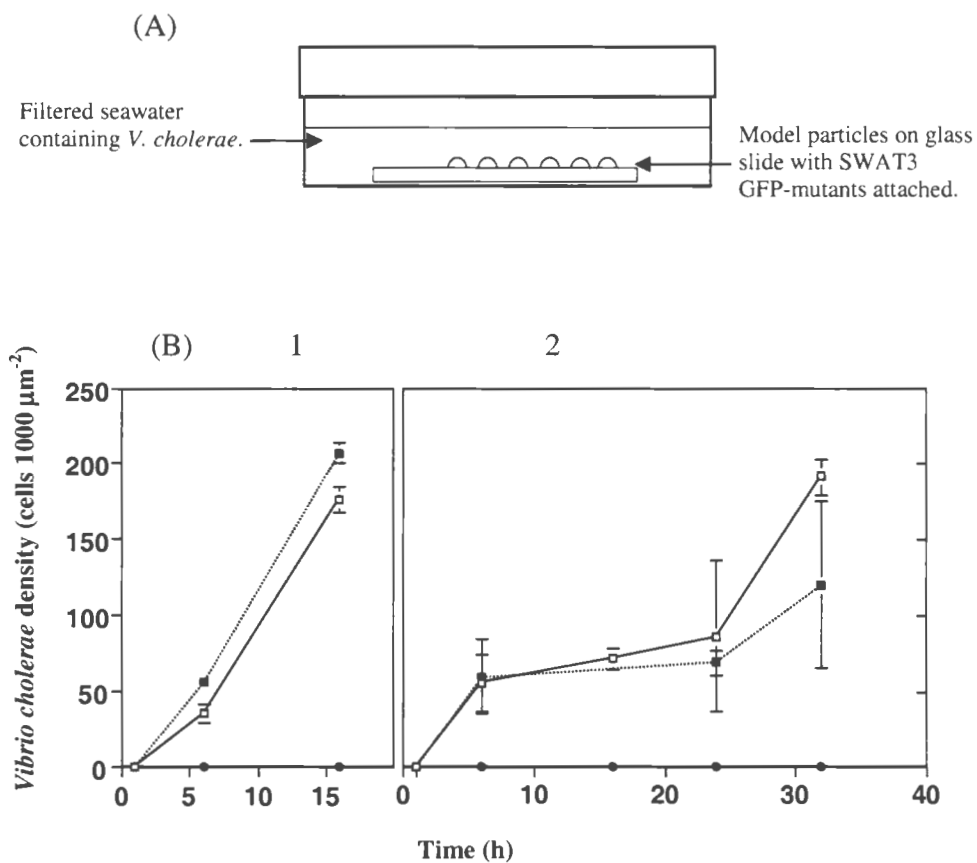


Figure 1.2. The Antagonistic Activity of SWAT3 Strains Against the Colonization of *V. cholerae* in Liquid

Note. (A) Particle Colonization Assay set up. ZoBell agarose particles were inoculated with a SWAT3 GFP-mutant and then spotted onto glass slides. Slides were incubated in 100kD filtered seawater with or without *V. cholerae*, formalin fixed, and stained with DAPI. *V. cholerae* abundance was determined by subtracting SWAT3 (GFP) counts from total bacteria (DAPI) counts. A second experiment used agarose particles embedded with lysed dinoflagellate cells (*Lingulodinium polyedrum*) in stead of nutrients. (B) Inhibition of *V. cholerae* colonization. Model particles were inoculated with either SWAT3-4 (filled circle) or SWAT3-111 (filled square). Control blanks appear as open squares. Replicates (n=3) were removed at each time point, and error bars represent standard deviations. 1, agarose particles amended with nutrients; and 2, agarose particles embedded with freeze-thaw-lysed cells of *L. polyedrum*.

My role in this project was to investigate (1) the underlying chemical mechanisms of the observed bacteria-bacteria antagonism, and (2) the temperature dependency of these interactions. The model system comprising SWAT3-wt (wild type), SWAT3-4 and SWAT3-111 was chosen to help accomplish these objectives. Prior to my involvement in this project, my former lab partner Ms. Ying Wang had studied SWAT3 due to a broad-spectrum antagonism it displayed against a panel of other marine bacterial strains (Long & Azam, 2001). By way of bioassay-guided fractionation, she had isolated the previously described antibacterial agent andrimid (Fredenhagen *et al.*, 1987; Needham *et al.*, 1994; Singh *et al.*, 1997) from crude extracts of SWAT3 fermentations (Wang, 2003a). My initial hypothesis was that the *V. cholerae* inhibition by SWAT3 was due to its production of andrimid.

1.2 Methods and Results

1.2.1 Isolation and Purification of Anti-Vibrio cholerae Metabolites Produced by SWAT3, a Marine Vibrio sp.

A 39 L culture of SWAT3 grown in YP medium (also called ZoBell medium, consisting of 1 g of yeast extract and 5 g of peptone in 1 liter of filtered sea water) was extracted with ethyl acetate to give 1.96 grams of crude extract (Wang, 2003a). Solvent partitioning of the crude extract between water and, sequentially, trimethylpentane (TMP), dichloromethane (DCM), ethyl acetate (EtOAc), and butanol (BuOH) concentrated the antibacterial activity in the DCM fraction (1.5 g) (Wang, 2003a). 813 mg of the DCM fraction was applied to column chromatography (Kontes[®] 100 x 25 mm column packed with Amberchrom[®] CG-161m, Lot: 32510129) and eluted using

aqueous methanol in gradient concentrations: 50% (150 mL) →75% (150 mL) →90% (150 mL) →100% (300 mL). The 90% methanol fraction yielded 82 mg of yellow amorphous solid which was further purified by reverse phase HPLC (X-Terra[®] Prep RP C₁₈ column, 100 × 19 mm, flow rate of 10 mL/min, λ=292 nm) using gradient aqueous methanol 45% → 80% over 20 minutes. The major peak eluting at 15.3 minutes was collected and concentrated *in vacuo* to yield the active material as a yellow amorphous solid (33.9 mg, Figure 1.3). This substance was verified as pure andrimid by comparison of its ¹H NMR spectrum with literature values (Needham *et al.*, 1994) (Figure 1.4; Table 1.3).

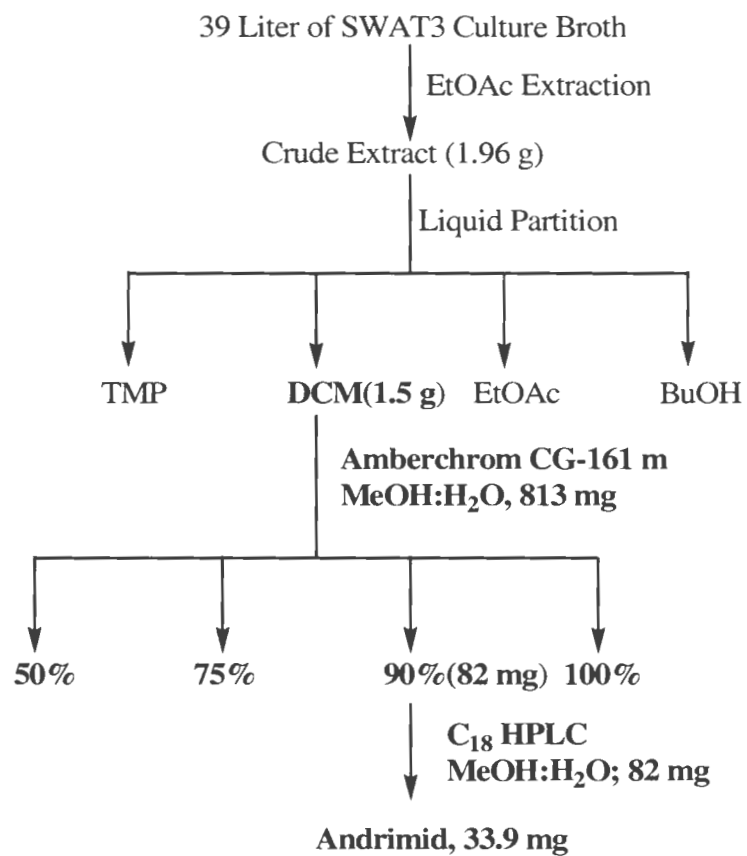


Figure 1.3. The Flow Chart of the Isolation of Andrimid from a 39 L SWAT3 Culture

Note. The bold part was conducted as part of this thesis. The extraction and solvent partitioning steps were done by Ms. Ying Wang (Wang, 2003a).

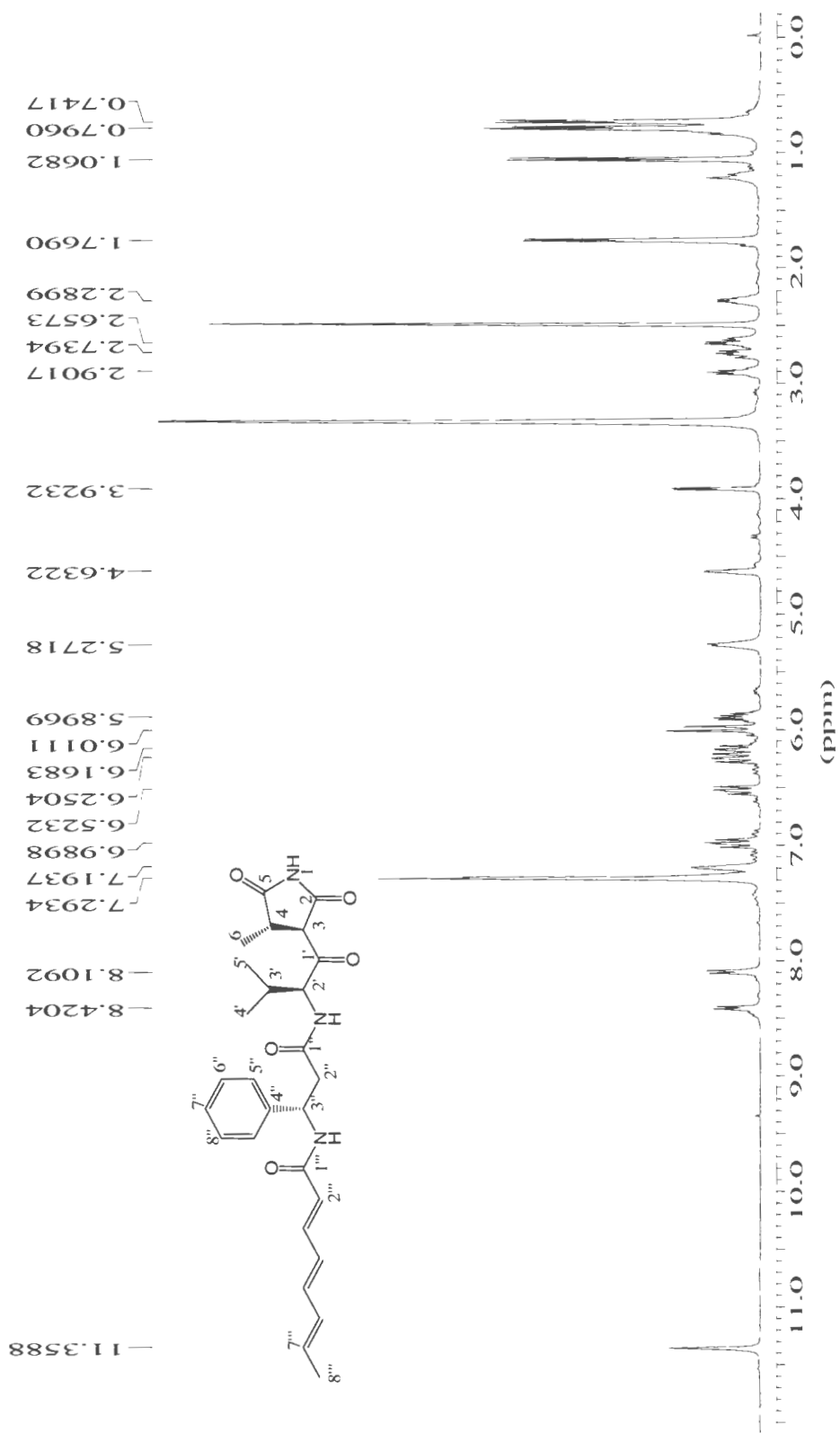


Figure 1.4. Proton NMR of Andrimid in DMSO-*d*₆ (400 MHz)

Note. This spectrum was reprinted from Wang, 2003a.

Table 1.3

Proton NMR Data of Andrimid in DMSO-*d*₆ (400 MHz)

Carbon	δH	Carbon	δH	Carbon	δH	Carbon	δH
1-NH	11.36	1'		1''		1'''	
2		2'	4.63	2''	2.66, 2.74	2'''	6.01
3	3.92	3'	2.29	3''	5.27	3'''	6.99
4	2.90	4'	0.74	4''		4'''	6.25
5		5'	0.80	5''	7.29	5'''	6.52
6	1.07	2'-NH	8.11	6''	7.29	6'''	6.17
				7''	7.19	7'''	5.90
				8''	7.29	8'''	1.77
				9''	7.29		
				3''-NH	8.42		

1.2.2 Assessment of the Anti-*Vibrio cholerae* Activity of Andrimid

The anti-*Vibrio cholerae* activity of purified andrimid was initially examined using a disk diffusion assay. *V. cholerae* was cultured in 10 mL broth (1% NaCl + 1% Tryptone) and incubated at 30 °C with shaking overnight. The next day, a loop of the culture was evenly streaked over the top of a solid agar plate (1% NaCl + 1% Tryptone). Andrimid was dissolved in methanol at 25 mg/mL and 20 μL was applied to a paper disk (BBL™, 6mm diameter). A second disk treated with 20 μL of pure methanol served as the control. After solvent evaporation, the two paper disks were applied to the inoculated agar plate and incubated at 30 °C overnight. Andrimid produced a clear 27 mm zone of inhibition. No zone was observed for the control disk.

A broth dilution assay was next performed to determine the IC₅₀ (inhibitory concentration that results in a 50% reduction in growth) of andrimid versus *V. cholerae*. An overnight culture of *V. cholerae* was diluted with fresh culture medium to

OD₆₀₀=0.043 and then further diluted 10-fold. This diluted culture is hereafter referred to as *cell suspension* (CS). In 96-well microtiter plates, 120 μ L aliquots of the CS were treated with four-fold serial dilutions of andrimid. Tetracycline, methanol, and fresh broth (1% NaCl+1% Tryptone) were used as the antibiotic, solvent, and blank controls, respectively. Table 1.4 shows the assay plate set up. The final concentrations of andrimid, tetracycline and methanol in each well of the plate are shown in Table 1.5. Duplicate plates were then incubated at 28 °C overnight. The next day, the optical density of the treated cultures was measured at 630 nm. The percent growth of *V. cholerae* in response to andrimid was calculated using the following the equation:

$$\% \text{ growth} = 100\% \times (\text{OD}_{\text{sample}} - \text{OD}_{\text{blank}}) / (\text{OD}_{\text{solvent}} - \text{OD}_{\text{blank}}) \quad (1)$$

Figure 1.5 shows percent growth as a function of andrimid concentration. At 28 °C, *V. cholerae* was sensitive to andrimid with an IC₅₀ of 0.12 μ M, slightly lower than tetracycline (0.13 μ M).

Table 1.4

The 4-Fold Serial Dilution Set Up Scheme for the Broth Dilution Assay

	1	2	3	4	5	6	7	8	9	10	11	12
A	155 μ L CS* + 5 μ L Andrimid	155 μ L CS + 5 μ L Andrimid	155 μ L CS + 5 μ L Andrimid	155 μ L CS + 5 μ L Andrimid	155 μ L CS + 5 μ L Andrimid	4 \times dilution from H1	4 \times dilution from H2	4 \times dilution from H3	4 \times dilution from H4	4 \times dilution from H5	155 μ L CS + 5 μ L Tetracycline	155 μ L CS + 5 μ L MeOH
B	120 μ L CS	120 μ L CS	120 μ L CS	120 μ L CS	120 μ L CS	120 μ L CS	120 μ L CS	120 μ L CS	120 μ L CS	120 μ L CS	120 μ L CS	120 μ L CS
C	120 μ L CS	120 μ L CS	120 μ L CS	120 μ L CS	120 μ L CS	120 μ L CS	120 μ L CS	120 μ L CS	120 μ L CS	120 μ L CS	120 μ L CS	120 μ L CS
D	120 μ L CS	120 μ L CS	120 μ L CS	120 μ L CS	120 μ L CS	120 μ L CS	120 μ L CS	120 μ L CS	120 μ L CS	120 μ L CS	120 μ L CS	120 μ L CS
E	120 μ L CS	120 μ L CS	120 μ L CS	120 μ L CS	120 μ L CS	120 μ L CS	120 μ L CS	120 μ L CS	120 μ L CS	120 μ L CS	120 μ L CS	120 μ L CS
F	120 μ L CS	120 μ L CS	120 μ L CS	120 μ L CS	120 μ L CS	120 μ L CS	120 μ L CS	120 μ L CS	120 μ L CS	120 μ L CS	120 μ L CS	120 μ L CS
G	120 μ L CS	120 μ L CS	120 μ L CS	120 μ L CS	120 μ L CS	120 μ L CS	120 μ L CS	120 μ L CS	120 μ L CS	120 μ L CS	120 μ L CS	100 μ L broth
H	120 μ L CS	120 μ L CS	120 μ L CS	120 μ L CS	120 μ L CS	120 μ L CS	120 μ L CS	120 μ L CS	120 μ L CS	120 μ L CS	120 μ L CS	100 μ L broth

Note. CS: cell suspension, diluted *V. cholerae* culture. Serial dilution was accomplished by transferring 40 μ L of A1-A5 to B1-B5, mixing, transferring 40 μ L to C1-C5, and so on.

Table 1.5

The Concentration of the Samples in Each Well

	Andrimid (μM)		Tetracycline (μM)	MeOH
	1-5	6-10	11	12
A	65.226	0.001	64.982	3.125% (v/v)
B	16.307	2.5×10^{-4}	16.246	0.781%
C	4.076	6.25×10^{-5}	4.061	0.195%
D	1.019	1.56×10^{-5}	1.015	0.049%
E	0.255	3.9×10^{-6}	0.254	0.012%
F	0.064	9.75×10^{-7}	0.063	0.003%
G	0.016	2.44×10^{-7}	0.016	Blank
H	0.004	6.1×10^{-8}	0.004	Blank

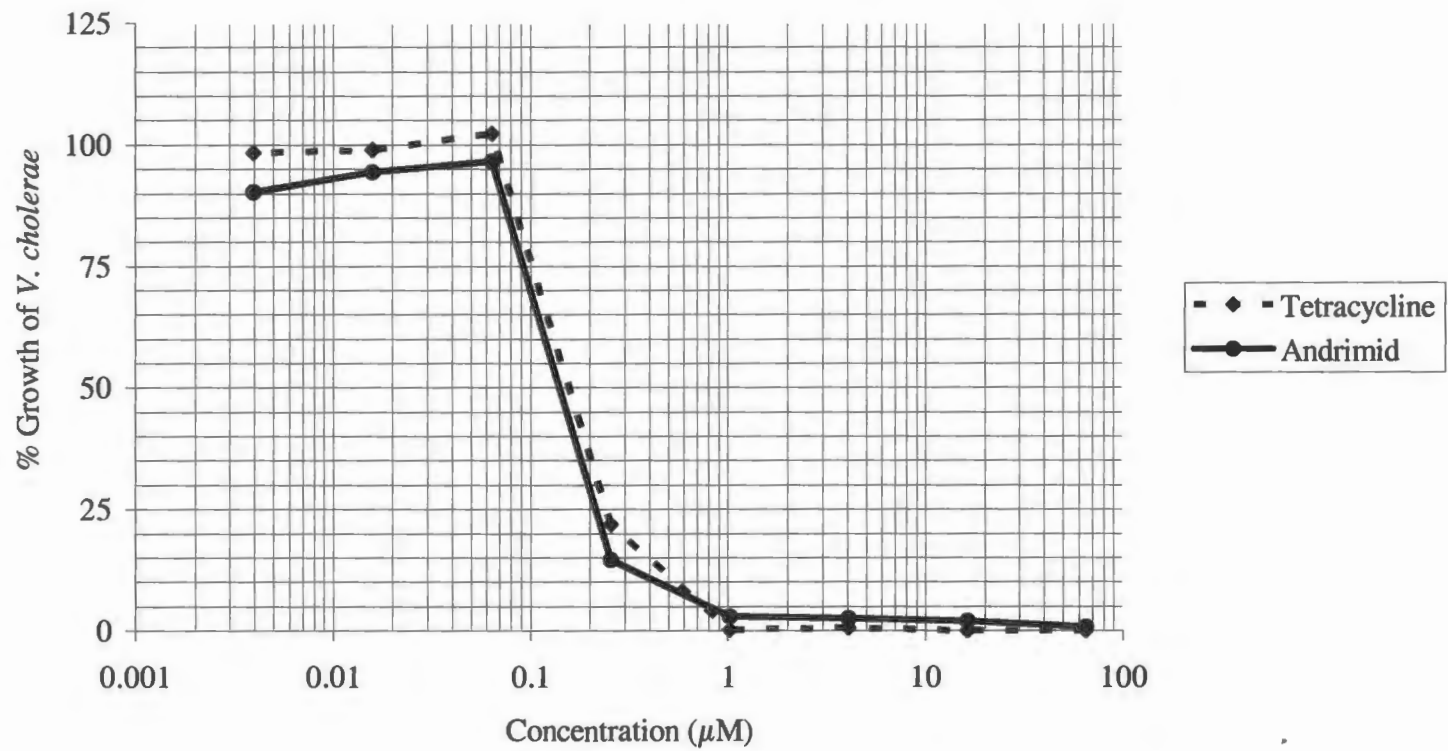


Figure 1.5. Sensitivity of *V. cholerae* to Andrimid at 28 °C (n=10)

To explore the temperature dependency of SWAT3 antagonism of *V. cholerae*, a 2-fold broth dilution assay was performed as described above, but incubated at two different temperatures: 24 °C and 30 °C. The IC₅₀ of andrimid against *V. cholerae* was 0.08 μM at 24 °C and 0.14 μM at 30 °C (Figure 1.6). This result did not show a significant difference between the two values, which suggested that temperature was not critical to the antibacterial potency of andrimid against *V. cholerae*. The slight differences in IC₅₀ were likely due to faster growth of *V. cholerae* at higher temperatures.

1.2.3 Exploration of the Relationship Between the Anti-V. cholerae Activity of SWAT3 and Its Andrimid Production

The following experiments were conducted to determine if the differences in antagonistic behaviors between the GFP-mutants SWAT3-4 and SWAT3-111 related to their ability to produce andrimid. As previously discussed SWAT3-4 prevented the colonization of particles by *V. cholerae* while SWAT3-111 did not. SWAT3-wt (wild type), SWAT3-4, and SWAT3-111 were each cultured in 1 L of YP broth, and incubated at approximate 24 °C on a rotary shaker. After four days, the turbid, light yellow cultures were each filtered through Celite521 (ACROS ORGANISCS, lot: A016788001) to remove the cells, and the resulting clear supernatants were then each extracted with 2 × 500 mL of ethyl acetate. The three ethyl acetate portions were dried over Na₂SO₄ and then concentrated *in vacuo*.

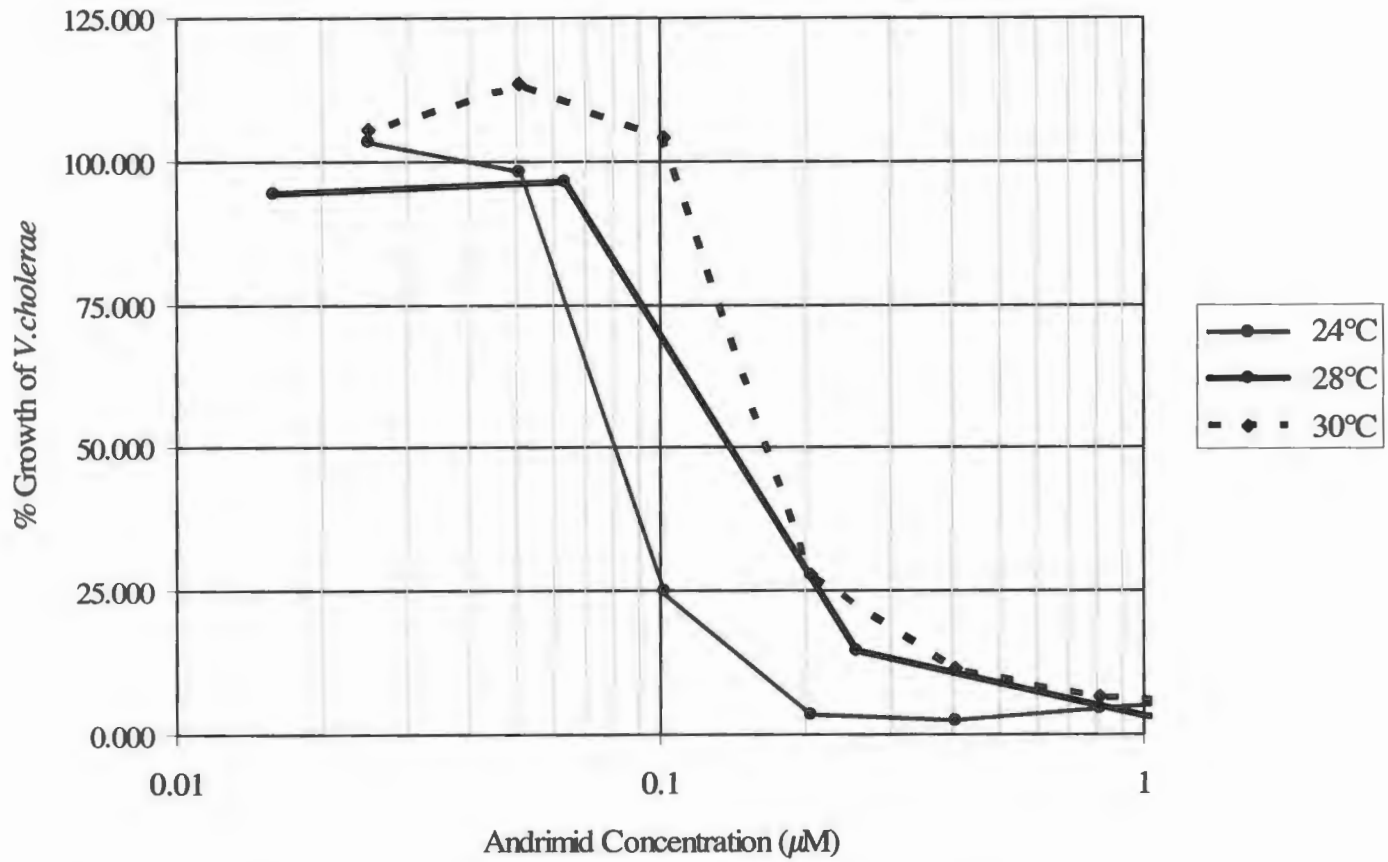


Figure 1.6. Sensitivity of *V. cholerae* to Andrimid as a Function of Temperature

These cultures yielded 84.3 mg of SWAT3-wt extract, 85.8 mg of SWAT3-4 extract, and 74.7 mg of SWAT3-111 extract, all three as light brown solids.

Paper disk diffusion assays (as described above) showed that the SWAT3-wt and SWAT3-4 extracts equally inhibited the growth of *V. cholerae* (ZOI = 22 mm), while the SWAT3-111 extract was inactive (Table 1.6).

Table 1.6

The Diameter of Antibacterial Zone Induced by SWAT3 Crude Extracts

Test sample	MeOH	Andrimid	SWAT3-wt	SWAT3-4	SWAT3-111
Diameter of the inhibitory zone(mm)*	N/A	27	22	22	N/A

Note. * The diameter of the paper disk (6 mm) was included.

Following the assays, all three crude extracts were examined by analytical HPLC (Hitachi[®] equipped with L-7455 diode array detector, column: X-Terra[®] RP C₁₈ column, 3.0 × 100 mm) to examine the concentrations of andrimid in the crude extracts. Andrimid and three crude extracts were each dissolved in methanol at a concentration of 3.3 mg/mL. The HPLC analysis of all four samples were conducted using identical conditions: 10 µL of the injection volume, gradient aqueous methanol (with 0.1 % formic acid) (45% → 80%) system, a flow rate of 1 mL/min, and UV monitoring at λ₂₉₂ nm. The multi-display chromatograms (Figure 1.7) verified that SWAT3-wt and SWAT3-4 both produced andrimid, while SWAT3-111 did not. This result is consistent with the *V. cholerae*-antagonistic activity of SWAT3-wt and SWAT3-4 and the lack thereof by SWAT3-111.

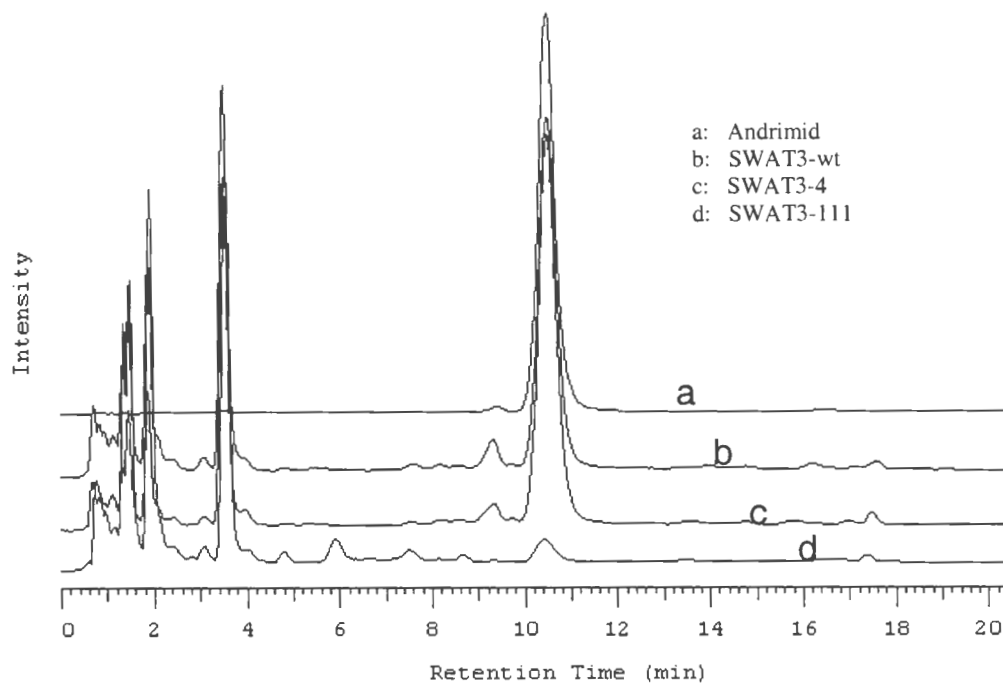


Figure 1.7. HPLC Chromatograms of Andrimid and the Crude Extracts of Three SWAT3 Strains

The effect of temperature on andrimid production by SWAT3 was next examined. This aim was achieved by quantitative HPLC. The Beer-Lambert Law states the linear relationship between absorbance and concentration of a species in the equation (2):

$$A = a \cdot b \cdot c \quad (2)$$

where A stands for the measured absorbance, a (λ) is a wavelength-dependent absorptivity coefficient, b is the path (cell) length, and c is the concentration of the compound giving the absorbance. To calculate the concentration of andrimid in crude extracts, a standard curve of absorbance versus concentration was first plotted using a pure andrimid standard. Serial dilutions of andrimid in methanol (MeOH) were analyzed by HPLC (Hitachi[®] equipped with L-7455 diode array detector and L-7200 autosampler; Symmetry[®] C₁₈ 3.5 μ m, 4.6 \times 75mm column) using the following conditions: 10 μ L of the injection volume, gradient aqueous methanol (with 0.1 % formic acid) (40% \rightarrow 65% over 15 minutes and then 65% \rightarrow 100% over 5 minutes), a flow rate of 1 mL/min, UV detection at λ 292 nm. The andrimid peak eluted at 17 minutes. UV absorbance was measured for three replicates at each concentration (Table 1.7). The standard curve was then plotted using the absorbance average of each replicate set (Figure 1.8). The standard curve equation (3) was calculated to be:

$$y = 13531059 x + 277399 \quad (3)$$

where y represents the absorbance of the andrimid, x represents the concentration of andrimid, and $R^2 = 0.99853$.

Table 1.7

UV Absorbance of Andrimid at Different Concentrations

Concentration	Absorbance1	Absorbance2	Absorbance3	Average	SD
0.825 mg/mL	10723009	11817314	11435248	11325190	555392
0.400 mg/mL	6169920	6252562	5115765	5846082	633822
0.200 mg/mL	4341035	2409038	2813440	3187838	1018962
0.100 mg/mL	1829021	1324538	1661728	1605096	256965
0.050 mg/mL	1111343	869316	861500	947386	142044
0.025 mg/mL	491461	351179	364860	402500	77346

Note. The replicate average and the standard deviation (SD) are also shown (Raw data, n=3). Absorbance was measured using a Hitachi L-7455 diode-array detector monitoring at a 292 nm wavelength.

Ten replicate cultures of SWAT3-wt were inoculated into 100 mL of sterile YP broth. These ten replicates were divided into two groups of five. Group A was incubated at 24 °C, and group B was incubated at 30 °C. All other conditions were kept constant. After four days incubation, 100 mL culture was extracted with 2 x 50 mL of ethyl acetate, dried over Na₂SO₄, and concentrated *in vacuo*. All ten dried crude extracts had the same physical properties (brown-yellow solid) and were weighed (Table 1.8).

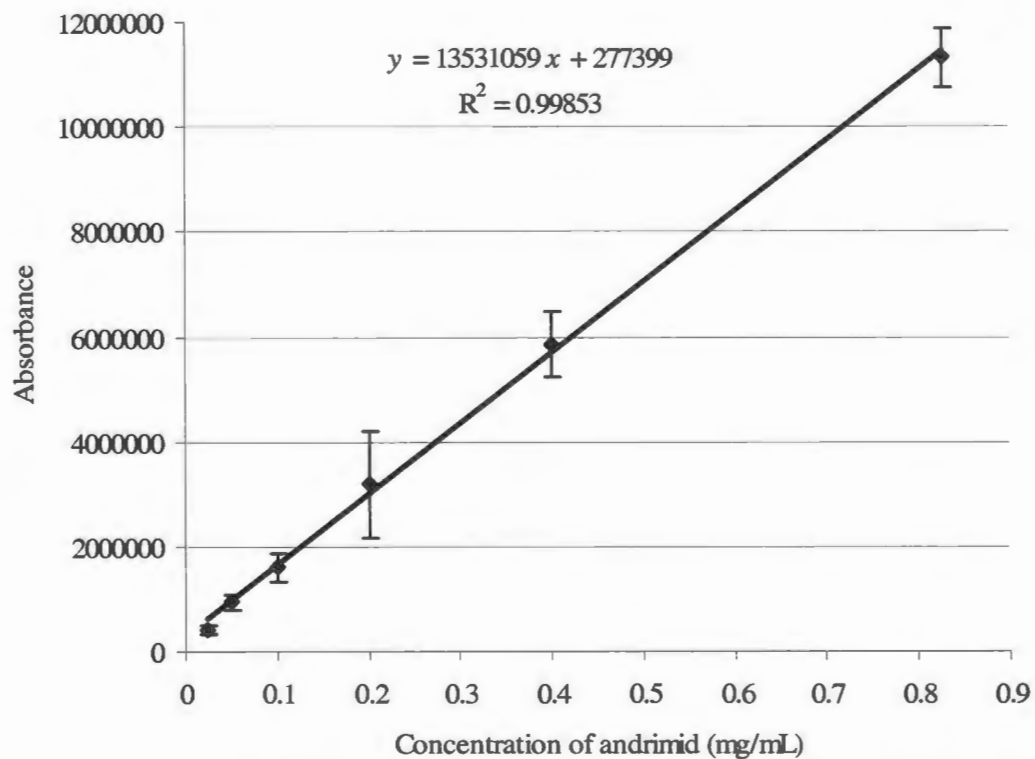


Figure 1.8. Standard Curve of Andrimid, Absorbance vs. Concentration

Note. The error bars are the standard deviation, n=3.

Table 1.8

The Yield of Crude Extracts of SWAT3-wt Cultures Grown at 24 °C and 30 °C

Replicates	1	2	3	4	5	average
Group A-24°C	8.7 mg	8.8 mg	8.2 mg	8.8 mg	7.9 mg	8.5 mg
Group B-30°C	7.6 mg	7.8 mg	7.0 mg	7.6 mg	8.0 mg	7.6 mg

Each of the ten extracts was dissolved in methanol at 3.3 mg/mL and analyzed by HPLC using the identical conditions as above. Table 1.9 shows the absorbance of the andrimid peaks in the crude extracts. Concentrations of andrimid in the crude extract solutions were then calculated using equation (3). The mean concentration of andrimid for group A (24 °C) was 0.166 ± 0.029 mg/mL and for group B (30 °C) was 0.021 ± 0.017 mg/mL (Table 1.10). Using equation (4), the percentages of andrimid in the crude extracts were calculated to be 5.03% in group A and 0.64% in group B (Table 1.11).

$$\frac{\text{Concentration}_{\text{andrimid}}}{\text{Concentration}_{\text{crude extract}}} \times 100\% = \% \text{ andrimid in crude extract} \quad (4)$$

The average of andrimid yielded per 100mL of SWAT3-wt culture was 0.43 mg for group A and 0.05 mg for group B (Table 1.11, Equation 5).

$$\text{Mass}_{\text{crude extract}} \times \% \text{ andrimid in crude extract} = \text{Mass}_{\text{andrimid}} \quad (5)$$

Table 1.9

The Absorbance of Andrimid in the Crude Extracts of SWAT3-wt Culture Incubated at Two Different Temperatures (n=5)

Absorbance	1	2	3	4	5	Average ± SD
Group A-24 °C	3030300	2326155	2030394	2404887	2800203	2518388 ± 354809
Group B-30 °C	868534	729108	324281	353192	562911	567605 ± 210638

Table 1.10

The Calculated Concentration of Andrimid in the Crude Extract Solution (mg/mL) (n = 5)

Concentration	1	2	3	4	5	Average ± SD
Group A-24 °C	0.203	0.151	0.130	0.157	0.186	0.166 ± 0.029
Group B-30 °C	0.044	0.033	0.003	0.006	0.021	0.021 ± 0.017

Table 1.11

The Average Yield of Andrimid per 100 mL of SWAT3-wt Culture at Two Different Temperatures

Temperature	Concentration ¹ _{andrimid}	Concentration _{crude}	% of andrimid in crude extract	Yield ² _{crude extract}	Yield ³ _{andrimid}
Group A-24 °C	0.166 ± 0.029 mg/mL	3.30 mg/mL	5.03%	8.5 mg	0.43 mg
Group B-30 °C	0.021 ± 0.017 mg/mL	3.30 mg/mL	0.64%	7.6 mg	0.05 mg

Note. ¹ Refer to table 1.10. ^{2,3} Yield of crude extract or andrimid per 100 mL of SWAT3-wt culture.

1.3 Summary and Discussion

Several lines of evidence support that andrimid is the agent responsible for the observed antagonistic interaction directed at *V. cholerae* by SWAT3. First, andrimid is a potent inhibitor of *V. cholerae* growth. Vc N16961 was susceptible to the antibiotic at a concentration of $\sim 0.1 \mu\text{M}$, comparable to the potency of tetracycline against this bacterium. Second, the antagonistic GFP-mutant SWAT3-4 produces andrimid in a quantity comparable to the wild-type, while the non-antagonistic mutant SWAT3-111 does not produce the antibiotic. The production of andrimid by SWAT3-4 is therefore the likely mechanism by which it inhibits colonization of model particles by Vc N16961.

Table 1.12

The Correlation Between the Production of Andrimid and the Bioactivity of SWAT3-wt, SWAT3-4 and SWAT3-111.

	<i>V. cholerae</i> -antagonistic activity		Andrimid in crude extract (HPLC)
	Burkholder Assay ¹	Crude extract	
SWAT3-wt	+	+	+
SWAT3-4	+	+	+
SWAT3-111	-	-	-

Note. ¹ This assay was done by the collaborators.

The temperature dependency of the SWAT3 antagonism of *V. cholerae* appears to be related to a decrease in andrimid production at higher temperatures. In fact, an eight-fold decrease in compound biosynthesis was observed as the incubation temperature was raised from 24 °C to 30 °C. *V. cholerae* was only slightly less sensitive to andrimid at higher temperatures in the broth dilution assay ($\text{IC}_{50} = 0.08 \mu\text{M}$ at 24 °C,

0.12 μM at 28 °C, and 0.14 μM at 30 °C). These small decreases in susceptibility are likely due to faster growth rates of the bacterium at higher temperatures, and should not account for the significant differences in bacteria-bacteria antagonism observed in the modified Burkholder assay (Table 1.1).

The combined results of this study (Table 1.12) suggest that bacteria-bacteria antagonism by indigenous bacteria may be a mechanism that keeps the proliferation of *V. cholerae* in check in the marine environment. However, the observed temperature dependencies of these interactions suggest that *V. cholerae* may gain a competitive advantage under warmer conditions.

1.4 References

- Allredge, A. L., Cole J. and Caron D. A. Production of heterotrophic bacteria inhabiting organic aggregates (marine snow) from surface waters. *Limnology and Oceanography*. 1986 (31): 68-78.
- Colwell R. R. Global climate and infectious disease: The cholera paradigm. *Science*. 1996 (274): 2025-2031.
- Epstein P. R. Climate and health. *Science*. 1999 (285): 347-348.
- Fredenhagen A., Tamura S. Y., Kenny P. T. M., Komura H., Naya Y., and Nakanishi K. Andrimid, a new peptide antibiotic produced by an intracellular bacterial symbiont isolated from a brown planthopper. *Journal of American Chemical Society*. 1987 (109): 4409-4411.

- Harvell C. D., Mitchell C. E., Ward J. R., Altizer S., Dobson A. P., Ostfeld R. S., and Samuel M. D. Climate warming and disease risks for terrestrial and marine biota. *Science*. 2002 (296): 2158-2162.
- Long R. A. and Azam F. Antagonistic interactions among marine pelagic bacteria. *Applied and Environmental Microbiology*. 2001 (67): 4975-4983.
- Madigan M. T., Martinko J. M., and Parker J. Cholera, In *Brock Biology of Microorganisms*. Pearson Education, Inc. 2003a (10th Ed): pp943-944.
- Needham J., Kelly M. T., Ishige M., and Andersen R. J. Andrimid and moiramides A-C, metabolites produced in culture by a marine isolate of the bacterium *Pseudomonas fluorescens*: structure elucidation and biosynthesis. *Journal of Organic Chemistry*. 1994 (59): 2058-2063.
- Pascual M., Rodó X., Ellner S. P., Colwell, R. and Bouma M. J. Cholera dynamics and El Niño-Southern oscillation. *Science*. 2000 (289): 1766-1769.
- Ramamurthy T., Garg S., Sharma R., Bhattacharya S. K., Nair G. B., Shimada T., Takeda T., Karasawa T., Kurazano H., Pal A., and Takeda Y. Emergence of novel strain of *Vibrio cholerae* with epidemic potential in southern and eastern India. *Lancet*. 1993(341): 703-704.
- Ruiz G. M., Rawlings T. K., Dobbs F. C., Drake L. A., Mullady T., Huq A., and Colwell R. R. Global spread of microorganisms by ships. *Nature*. 2000 (408): 49-50.
- Shimada T., Nair G., Deb B. C., Albert M. J., Sack R. B., and Takeda Y. Outbreak of *Vibrio cholerae* non-01 in India and Bangladesh. *Lancet*. 1993(341): 1347.

- Singh M. P., Mroczenski-Willey M. J., Steinberg D. A., Andersen R. J., Maiese W. M., and Greenstein M. Biological activity and mechanistic studies of andrimid. *The Journal of Antibiotics*. 1997 (50): 270-273.
- Stretton S., Techkarnjanaruk S., McLennan A. M., and Goodman A. E. Use of green fluorescent protein to tag and investigate gene expression in marine bacteria. *Applied and Environmental Microbiology*. 1998 (64): 2554-2559.
- Waldor M. K., Colwell R. R., and Mekalanos J. J. The *Vibrio cholerae* O139 serogroup antigen includes an O-antigen capsule and lipopolysaccharide virulence determinants. *National Academy of Sciences Proceedings in USA*. 1994 (91): 11388 -11392.
- Wang Y. Biologically active secondary metabolites from marine microorganisms. A thesis submitted in partial fulfillment of the requirements for the degree of master in pharmacognosy. University of Rhode Island. 2003a: pp27-59.

CHAPTER 2

Biosynthesis of CNC352.223, a Novel Metabolite of Polyketide Origin

Produced by a Marine-Derived *Aspergillus niger*

A structurally novel compound was isolated from a marine fungus *Aspergillus niger* in a previous study. The carbon skeleton of this molecule was predicted of pentaketide origin. This chapter describes my studies of the biosynthetic pathway of this compound. Methods included the conduction of the stable isotopic feeding experiments using ^{13}C singly and doubly labeled sodium acetate, the isolation and purification of the target substrates, and ^{13}C NMR analyses of labeled substrates.

2.1 Introduction

During the course of an investigation to discover novel inhibitors of the viral enzymes HIV integrase and the topoisomerase of the *Molluscum contagiosum* virus, a structurally novel compound, CNC352.223 (*I*, Figure 2.1), was isolated from the mycelium of a marine-derived *Aspergillus niger* van Tieghem (Wang, 2003b). Although (*I*) lacked inhibitory activity against the two targets, it was proposed to be a structurally unique metabolite. An unprecedented structural feature of (*I*) is a fused bicyclic ring system comprising pyrone and pyrrolinone heterocycles. CNC352.223 possesses a novel carbon skeleton, and with the inclusion of the nitrogen atom, derives from mixed biosynthetic pathways.

A plausible biogenic origin of the carbon skeleton is hypothesized in figure 2.2. Given that the molecule contains ten carbons, a pentaketide precursor can be easily imagined. Pentaketides are formed by sequential enzyme mediated condensation

reactions of an acetyl CoA starter unit with four molecules of malonyl-CoA (Herbert, 1989a). Classic Dieckmann cyclization (McMurry, 1988) of pentaketide (**2**) followed by aromatization would result in the proposed precursor (**3**). Bayer-Villiger type ring expansion via an arene oxide intermediate (Iijima *et al.*, 1983; Herbert, 1989b) could lead to the substituted 7*H*-oxepin-2-one (**4**). Ring opening via ester hydrolysis followed by isomerization of the alkene bond and subsequent reformation of the lactone with the C9 hydroxyl would result in pyrone (**5**). Hydroxylation of C3 and ring closure of the pyrrolinone ring via introduction of a nitrogen atom would give the completed metabolite (**1**).

To explore the above hypothetical biogenic origin of (**1**), feeding experiments of the producing *A. niger* isolate were undertaken using ¹³C-labelled substrates. Specifically, singly and doubly labeled sodium acetates were provided to the fungus over a period of ten days, and the labeled compound (**1**) was then isolated from each experiment and analyzed by ¹³C NMR spectroscopy.

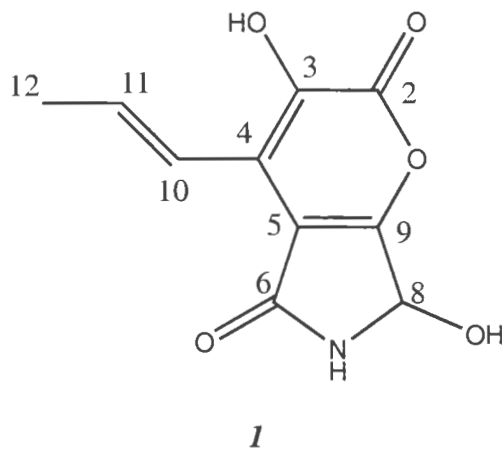


Figure 2.1. Structure of CNC352.223

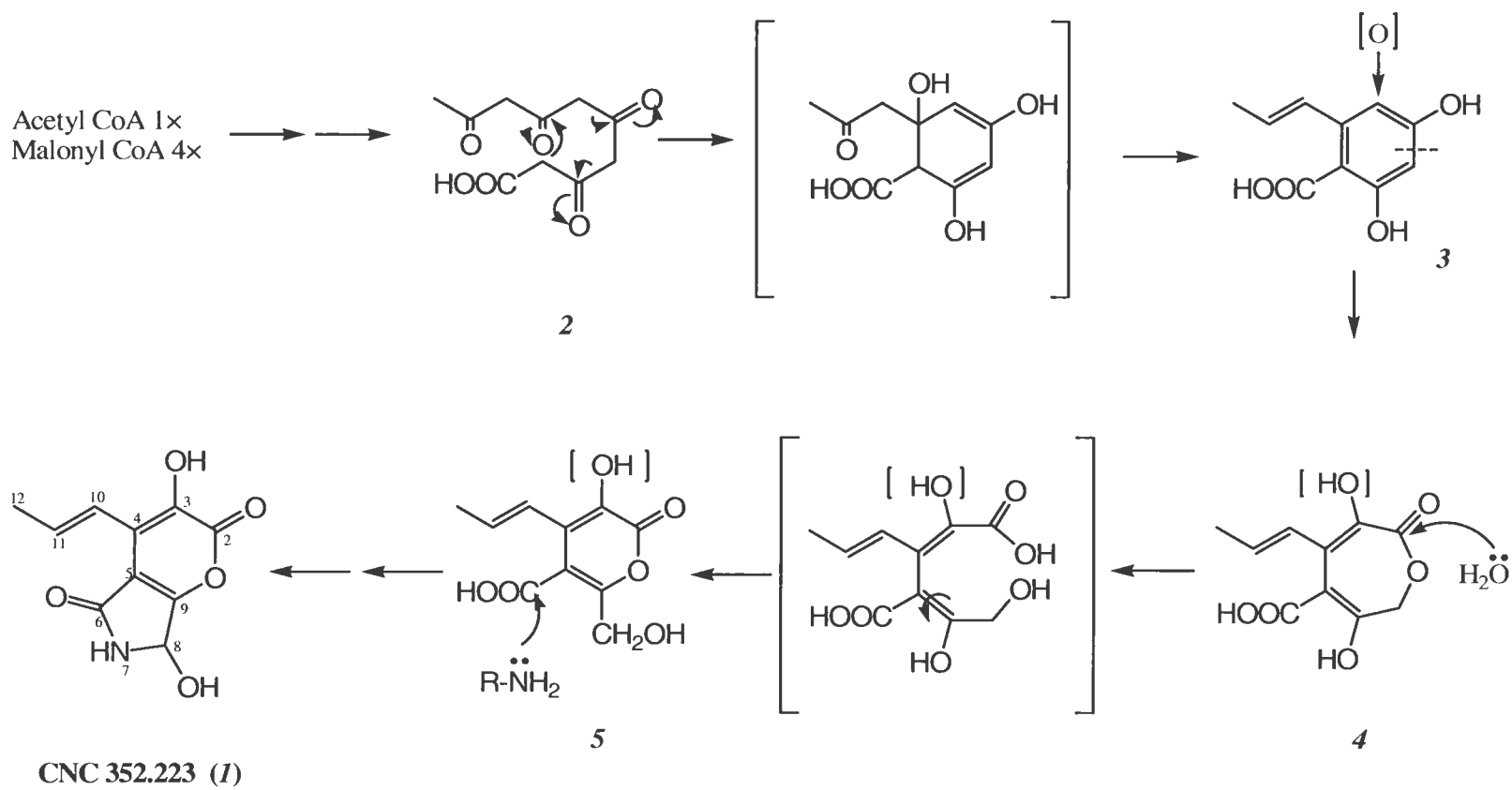


Figure 2.2. The Hypothesized Biosynthetic Pathway of CNC352.223 (*I*)

2.2 *Methods and Results*

2.2.1 *Stable Isotopic Feeding Experiments*

Frozen stock (-80 °C) of a marine fungal strain identified as *Aspergillus niger* van Tieghem was thawed at room temperature and transferred into 20 mL of YPM broth (2 g peptone, 2 g yeast extract, 4 g mannitol in 1 L of filtered seawater). After five days of static incubation at 24 °C, the fungal mycelium was macerated with a spatula and evenly distributed into 6 L (6 x 1 L) of fresh YPM broth. The inoculated cultures were then divided into three groups (2 x 1 L each) that were each cultivated using different isotopic feeding schemes over ten days. Group A was fed with 250 mg of singly labeled sodium acetate ($\text{CH}_3\text{COONa-1-}^{13}\text{C}$) on days two, four, six and eight. Group B was fed with doubly labeled sodium acetate ($\text{CH}_3\text{COONa-1,2-}^{13}\text{C}_2$) using the identical schedule. Group C received no additional nutrient. All one-liter cultures formed mycelial mats thick with black hyphae over the ten day experiment with no obvious morphological differences between them. On the tenth day of incubation, the cultures were each filtered through cheese cloth and the liquid portions were discarded. The mats from Groups A, B, and C were each frozen and lyophilized for chemical investigation.

2.2.2 *Isolation and Structural Examination of ^{13}C -Labeled CNC352.223 Substrates*

Figure 2.3 outlines the isolation and purification of CNC352.223 from the three different feeding experiments. The dried mats were extracted with methanol and dichloromethane (1:1), and concentrated *in vacuo* to yield crude extracts (yellow-green chunky solids). Fractionations were pursued using reverse phase column

chromatography (Flex[®] 30 x 200 mm columns packed BAKERBOND[™] Octadecyl resin, 40 μ m, Prep LC packing, LOT: T27085) using a stepwise methanol gradient in water (10% - 20% - 30% - 40% - 50% - 60% - 75% - 100%, 200 mL/each). ¹H NMR spectra of these fractions suggested that (*I*) was concentrated in the 10% and 20% fractions. The 10% fraction from Group B (doubly-labeled) was further purified by HPLC (X-Terra[®] Prep RP C₁₈ column, 100 x 19 mm) using a linear 15% - 30% gradient of methanol in water (25 minutes, 10 mL/minute flow rate, 0.1% formic acid was added to each solvent). Fractions were collected based on UV monitoring at a wavelength of 217 nm. The desired material eluted after eight minutes. Trituration of the dried, light brown solids with methanol yielded pure (*I*) from Group B. Trituration of the 10% and 20% fractions of Groups A and C directly led to purification of (*I*). For the purposes of discussion, compound (*I*) isolated from each treatment group will be referred to as CNC352.223-S (Singly-labeled, from Group A), CNC352.223-D (Doubly-labeled, from Group B), and CNC352.223-N (Non-labeled, from Group C).

2.2.3 Investigation of the Biosynthesis of CNC352.223 by ¹³C NMR Analyses of Labeled Substrates

CNC352.223 obtained from each labeling experiment was dissolved in DMSO-*d*₆ at a concentration of 19.5 mg/mL, and ¹³C NMR spectra were acquired using 3700 scans (Figures 2.4-2.6).

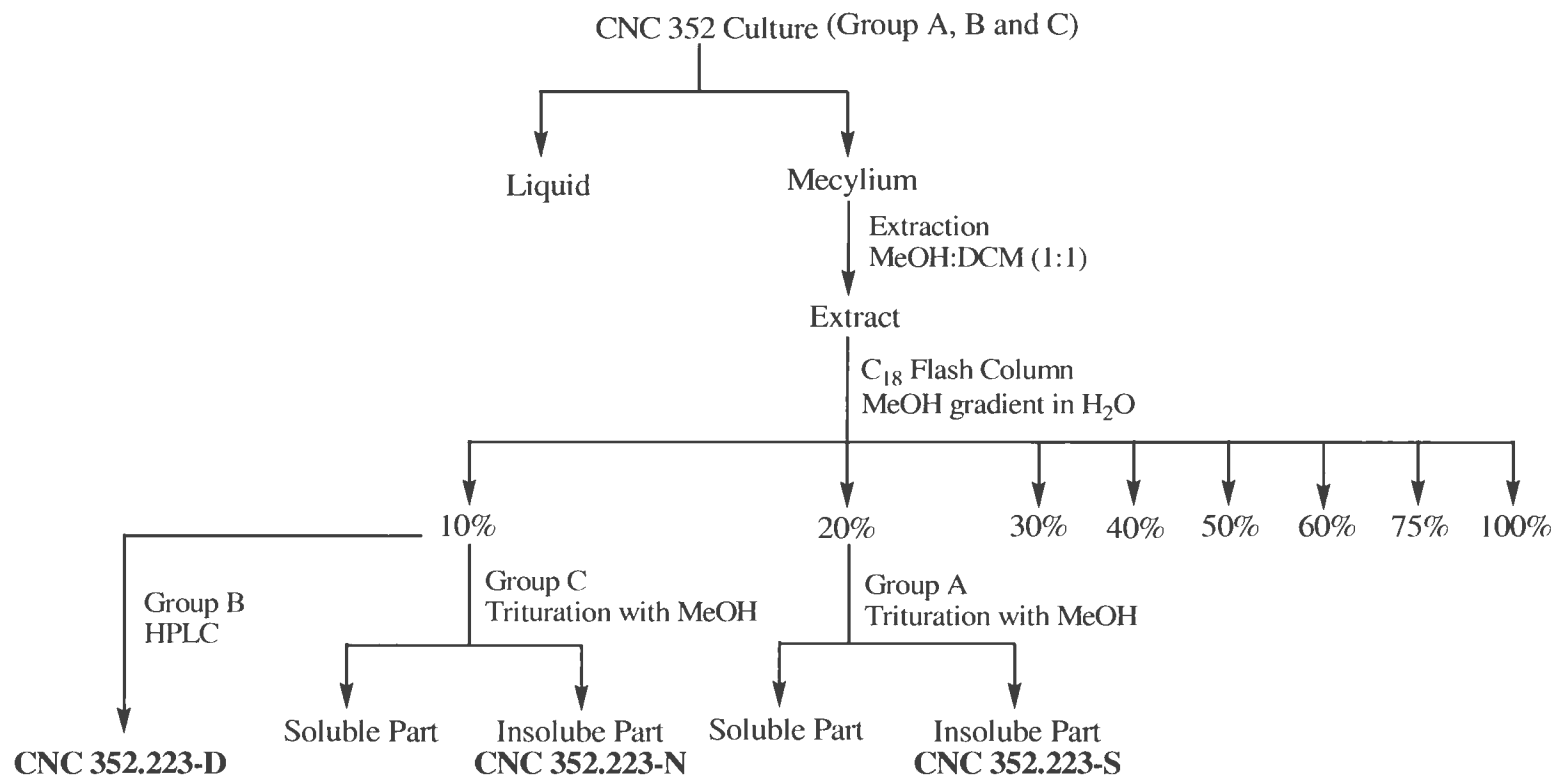


Figure 2.3. The Flow Chart of the Isolation and Purification of CNC352.223 from All Three Different Feeding Experiments

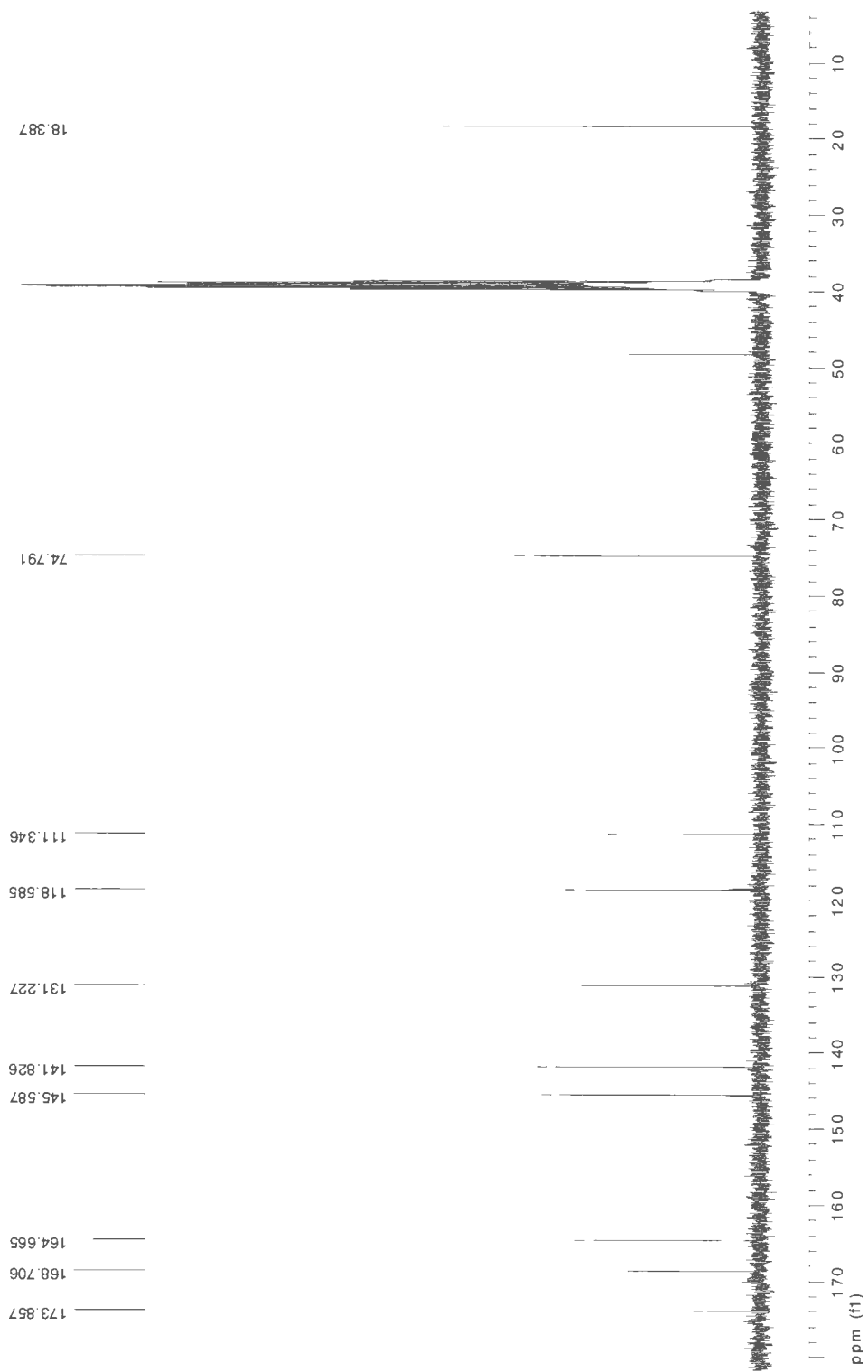


Figure 2.4. ^{13}C NMR Spectrum of CNC352.223-N in $\text{DMSO-}d_6$.

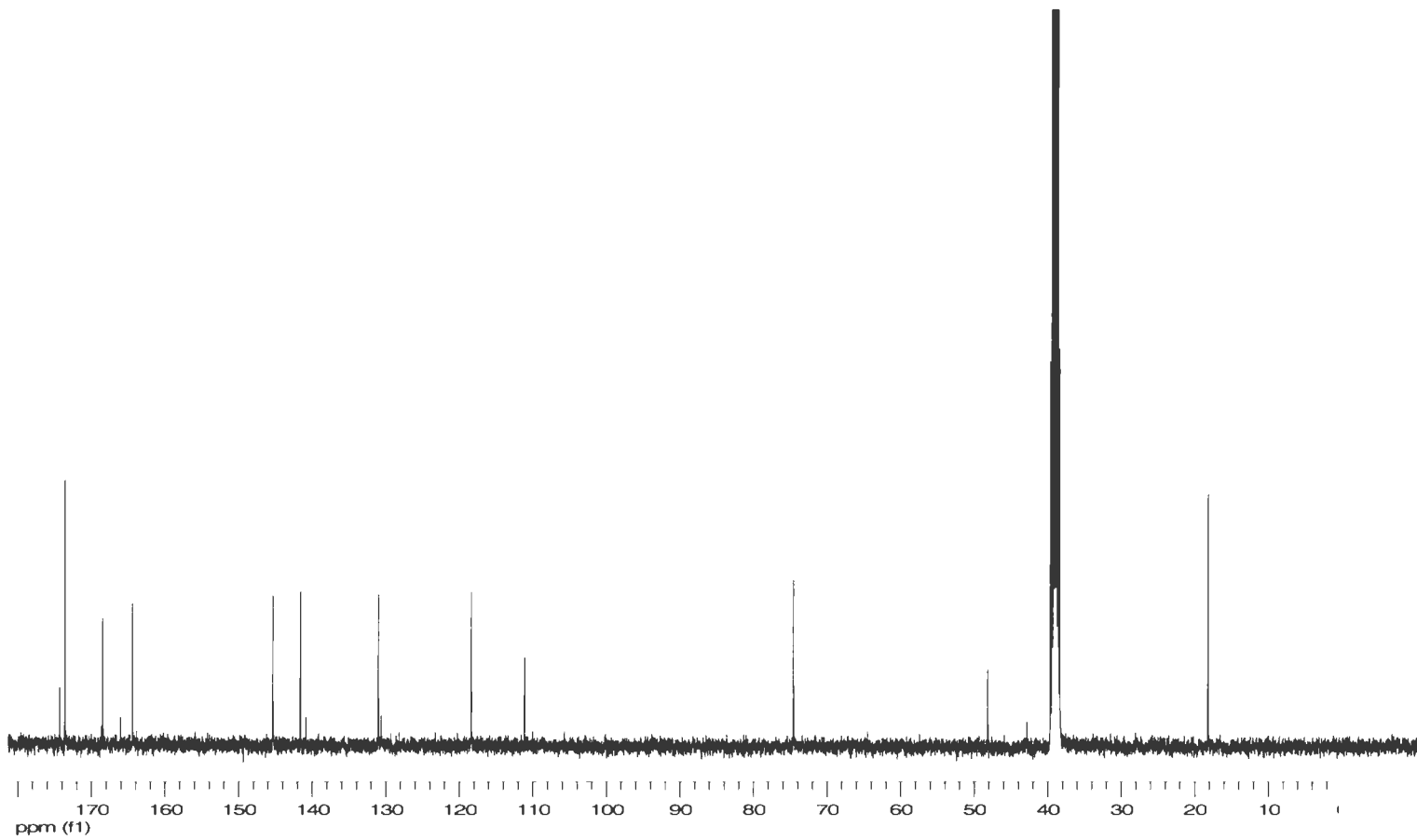


Figure 2.5. ^{13}C NMR Spectrum of CNC352.223-S in $\text{DMSO-}d_6$.

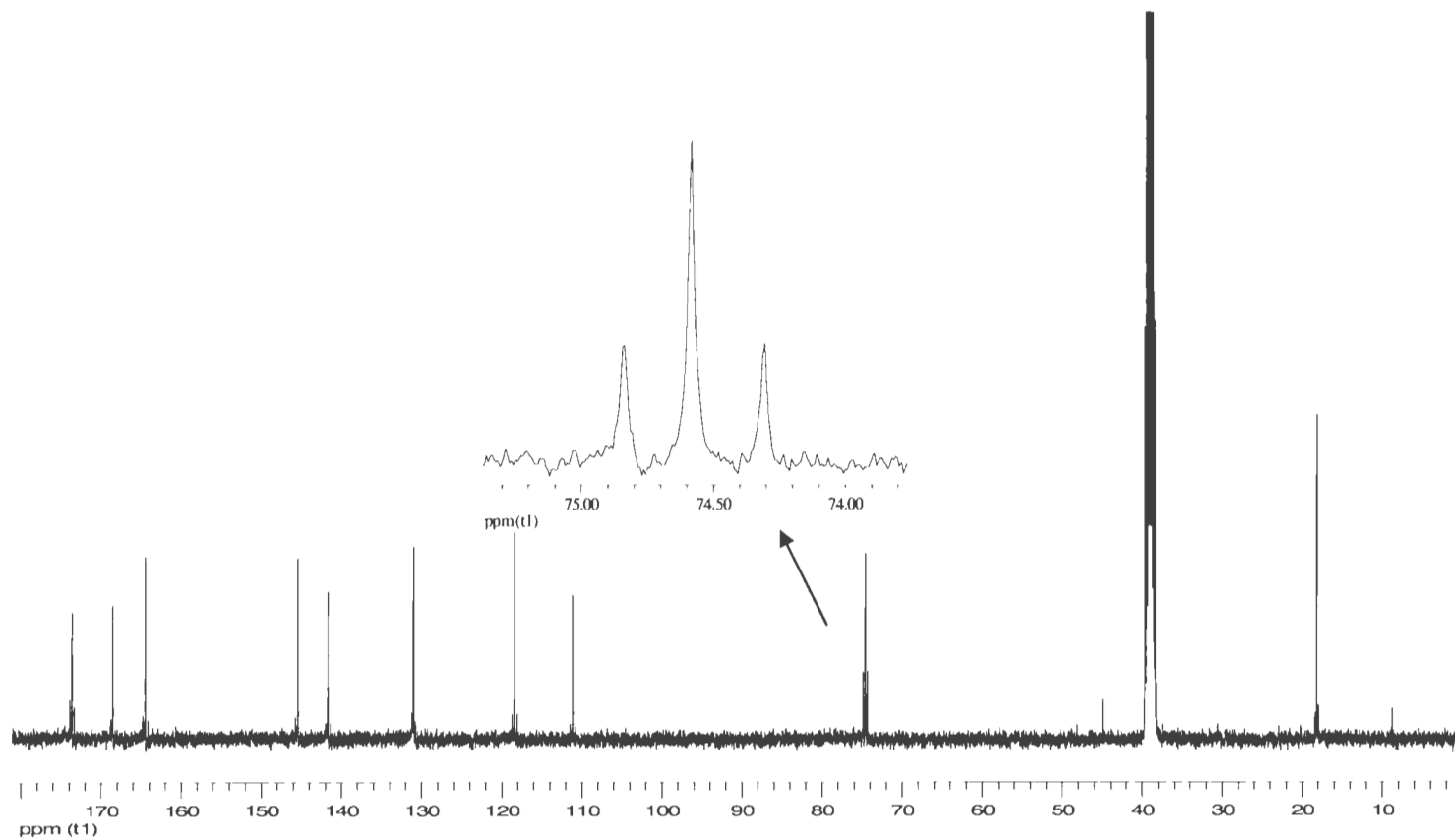


Figure 2.6. ^{13}C NMR Spectrum of CNC352.223-D in $\text{DMSO-}d_6$.

Note. The amplified peak at $\delta 74.8$ is displayed as a diagram. The peak in the center is the singlet resulted from the resonance of natural abundant ^{13}C . The two smaller peaks on either side are the doublets (also called satellites) resulted from the ^{13}C - ^{13}C coupling of two adjacent ^{13}C s.

The ^{13}C incorporations from the labeled acetate feeding experiments are consistent with the proposed biosynthetic hypothesis. In the ^{13}C NMR spectrum of CNC352.223-D (experiment 2, fungus fed with 1,2- $^{13}\text{C}_2$ labeled sodium acetate), doublets from ^{13}C - ^{13}C coupling could be observed in all ten resonances (Figure 2.6). ^{13}C - ^{13}C coupling arising from naturally abundant ^{13}C isotope (1.1% of all carbon) is essentially negligible ($1.1\% \times 1.1\% = 0.0121\%$). Thus, the obvious doublets shown in figure 2.6 are the result of incorporations of doubly labeled acetate by the fungus in the biosynthesis of (*I*) (Casey *et al.* 1976). The specific incorporations (Renner *et al.*, 2000) and coupling constants (Table 2.1) are consistent with a pentaketide precursor and the hypothetical biosynthetic pathway (Figure 2.2). The following carbon-carbon pairs share similar specific incorporation values and the coupling constants, demonstrating that each derives from an intact acetate unit: C2-C3, C4-C10, C5-C6, C8-C9, and C11-C12. This coupling pattern is entirely consistent with the proposed structure (Figure 2.1).

Instead of the satellites that are observed in the ^{13}C NMR spectrum of CNC352.223-D, enriched singlets are present in the ^{13}C NMR spectrum of CNC352.223-S. Since the culture was fed with singly labeled sodium acetate [$1\text{-}^{13}\text{C}$], only the carbons in the molecule that originate from the carbonyl carbon of the labeled acetate should show enrichment over natural abundance. Based on the proposed biosynthetic pathway (Figure 2.2), carbon atoms C2, C4, C6, C9, and C11 were predicted to show enrichment. Indeed, isotopic enrichments in C2 (0.30%) and C9 (1.16%) are consistent with the hypothesized biosynthesis. However, enrichments of less than 0.22% (or 20% relative height over the natural abundant signal) were

measured for the C4, C6, and C11, which are lower than the generally acceptable limit (Herbert, 1989c) and are therefore not significant. This result is consistent with the lower incorporations observed with carbon pairs C4-C10 (around 0.17%), C5-C6 (around 0.17%) and C11-C12 (around 0.13%) in experiment 2. Curiously, the enrichment difference between C8 and C9 is very high (1.16%) which is also consistent with the high enrichment (around 0.5-0.7%) of C8-C9 in experiment 2. The labeled pattern obtained from both singly labeled and doubly labeled experiments is displayed in figure 2.7.

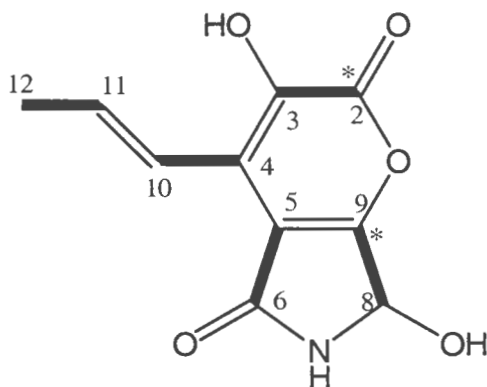


Figure 2.7. Labeling Pattern of CNC352.223 from Stable Isotopic Experiments

Note. Darkened bonds show carbons coupled from [1,2-¹³C₂] acetate incorporation. The asterisks represent significant enrichment from [1-¹³C] acetate.

Table 2.1

Stable Isotopic Incorporations Resulting from Feeding Experiment with ^{13}C -

Labelled Acetates.

Position	$\delta^{13}\text{C}$	[1,2- $^{13}\text{C}_2$]-acetate		[1- ^{13}C]-acetate
		Specific incorp ^a	$^1J_{c,c}$ (Hz)	Specific incorp ^b
2	168.7	0.26	55.2	0.30
3	141.8	0.26	56.6	
4	145.6	0.17	65.3	NSE ^c
5	111.3	0.17	64.5	
6	164.7	0.17	64.9	NSE
8	74.8	0.70	53.2	
9	173.9	0.52	53.4	1.16
10	118.6	0.18	67.1	
11	131.2	0.15	42.3	NSE
12	18.4	0.12	42.5	

Note. ^aSpecific incorporations (doubly labeled) = % enrichments above natural abundance = $1.1\% \times (\text{combined peak height of enriched satellites} - \text{the combined theoretical peak height for the same satellites resulting from natural abundance coupling}) / (\text{peak height of the natural abundance singlet} + \text{the combined theoretical peak height for all satellites resulting from natural abundance coupling})$ (Renner *et al.*, 2000). ^bSpecific incorporations (Singly labeled) = % enrichments above natural abundance = $1.1\% \times (\text{peak height of enriched singlet} - \text{peak height of natural abundance singlet}) / \text{peak height of natural abundance singlet}$. ^cNo significant enrichment (NSE): % enrichment was less than the lower limit for accurate determination of incorporation (Herbert, 1989c) and so was not considered.

2.3 Summary and Discussion

Isotopic labeling studies of CNC352.223 with singly and doubly labeled ^{13}C -acetate supported the original biosynthetic hypothesis. From the studies conducted with the ^{13}C doubly labeled sodium acetate (experiment 2), satellites were observed on all ten resonances, which is consistent with the fungus using acetate derivatives (acetyl CoA and malonyl CoA) as precursors to synthesize the metabolite. Comparison of the enrichments and coupling constants (J) helped to establish that the following carbon pairs were derived from the same molecules of acetate: C2 and C3; C4 and C10; C5 and C6; C8 and C9; C11 and C12. This coupling pattern strongly supports the proposed structure of (*I*). Different carbon pairs possessed different specific incorporations. This was because the uptake rates of the labeled acetate to form individual carbon pairs by the fungus were different. The ^{13}C - ^{13}C coupling constants for the three labeled sp^2 - sp^2 bonds varied based on the substitution patterns ($J_{2,3} = 55\sim 56$, $J_{4,10} = 65\sim 67$, $J_{5,6} = 64$). The sp^2 - sp^3 bond of C11-C12 was found to have a relatively low coupling constant ($J_{11,12} = 42$).

The biosynthetic pathway of the molecule CNC352.223 was further traced through the analysis of ^{13}C NMR spectrum of CNC352.223-S. In this case, the carbons on the molecule originating from the carbonyl carbon of acetate should show enriched singlets compared to those from the non-labeled substrate (CNC352.223-N). This incorporation pattern clearly showed that C2 and C9 originate from the carbonyl carbons in acetate. Unfortunately, insignificant enrichment prohibits carbons C4, C6 and C11 from similarly being assigned.

The specific incorporations from the doubly-labeled acetate feeding experiment (experiment 2, sodium acetate-1,2- $^{13}\text{C}_2$) and the enrichment from the singly-labeled acetate feeding experiment (experiment 1, sodium acetate-1- ^{13}C) agreed. Carbon pair C8-C9 showed the highest specific incorporation (~0.6%) in experiment 2 as well as the highest enrichment of C9 (1.16%) in experiment 1. It was found that the first acetate on a skeleton, “starter unit”, tends to get more incorporation than the successive ones (Herbert, 1989a). The carbons in the C8 and C9 positions would correspond to the fourth acetate unit in the hypothetical pentaketide precursor. It is not clear at this point why there is much higher incorporation of labeled substrate at the C8-C9 position.

In accordance with the proposed biosynthetic pathway, the oxygens at C3-OH and C8-OH should not be derived from acetate. The source of these oxygens could potentially be revealed through further feeding experiments using ^{18}O .

2.4 References

- Casey M. L., Paulick R. C., and Whitlock H. W. Jr. A carbon-13 nuclear magnetic resonance study of mollisin and its biosynthesis. *Journal of the American Chemical Society*. 1976 (98): 2636-2640.
- Herbert R. B. Polyketides. In *The Biosynthesis of Secondary metabolites*. Chapman and Hall Ltd. 1989a (2nd Ed): pp33-34.
- Herbert R. B. Polyketides. In *The Biosynthesis of Secondary metabolites*. Chapman and Hall Ltd. 1989b (2nd Ed): pp38-42.
- Herbert R. B. Technique for biosynthesis. In *The biosynthesis of Secondary Metabolites*. Chapman and Hall Ltd. 1989c (2nd Ed): pp22.

- Iijima H., Noguchi H., Ebizuka Y., Sankawa U., and Seto H. The biosynthesis of Patulin: the mechanism of oxidative aromatic ring cleavage and loss of side chain protons from aromatic intermediates. *Chemical and Pharmaceutical Bulletin*. 1983 (31): 362-365.
- McMurry J. Intramolecular claisen condensations: the dieckmann cyclization. In *Organic Chemistry*. Brooks/Cole Publishing Company. 1988 (2nd Ed): pp837-839.
- Renner M. K., Jensen P. R., and Fenical W. Mangicols: structures and biosynthesis of a new class of sesterterpene polyols from a marine fungus of the genus *Fusarium*. *Journal of Organic Chemistry*. 2000 (65): 4843-4852.
- Wang Y. Biologically active secondary metabolites from marine microorganisms. A thesis submitted in partial fulfillment of the requirements for the degree of master in pharmacognosy. University of Rhode Island. 2003b: pp74-94.

CHAPTER 3

Inhibition of Bacterial Cell-Cell Signaling by Metabolites

Produced by a Marine *Halobacillus* sp.

Bioassay-guided fractionation led to the isolation of two arylethylamide compounds from the culture extracts of a marine-derived bacterial culture C42, identified as a *Halobacillus* sp. Although these two compounds were previously published, their quorum sensing-antagonistic activity was investigated for the first time in this thesis research. This chapter describes the screening for microbial inhibitors of quorum sensing, optimization of the fermentation conditions of culture C42, bioassay-guided isolation and structural elucidation of two active compounds, and finally the quorum sensing inhibitory properties of these molecules.

3.1 Introduction

Rather than living in isolation, many bacteria form a community by communication with one another using small molecules called autoinducers (Schauder and Bassler, 2001). Autoinducers diffuse through bacterial cell walls, and by sensing the accumulation of autoinducers in their local environment, bacteria are able to determine their own population density. When the population reaches a minimum threshold, back diffusion of autoinducers into the bacterial cells activates specific gene expression (Schauder and Bassler, 2001). Therefore, bacteria can regulate phenotypic expression in response to population density. This process is referred to as quorum sensing (QS).

QS was first discovered in the marine bacterium *Vibrio fischeri*, which uses QS to regulate bioluminescence (Hastings and Nealson, 1977; Nealson and Hastings, 1979). *V. fischeri* lives in symbiotic association with many marine fish and squid (Whitehead *et al.*, 2001), potentially providing light to its hosts for purposes such as attracting prey or camouflage (Schauder and Bassler, 2001). In return, *V. fischeri* obtains a more nutrient rich environment compared to that available in sea water (Ruby, 1996; Visick and McFall-Ngai, 2000). Bioluminescence by *V. fischeri* is regulated by QS, a population-density dependent behavior.

Two model types of Quorum-sensing pathways have been described for bacterial communication: LuxI/LuxR circuits in over 70 species of Gram-negative bacteria using *N*-acyl homoserine lactone (AHL) as autoinducers; and two-component (sensory-transduction) systems in Gram-positive bacteria using oligopeptide or autoinducing peptides (AIPs) as autoinducers (Miller and Bassler, 2001; Federle and Bassler, 2003; Lazazzera and Grossman, 1998). Figure 3.1 shows a typical QS-pathway utilized by Gram-negative bacteria. Specific intra-species communication systems enable bacteria to distinguish themselves from others and to regulate their own particular behaviors in a population of mixed species (Federle and Bassler, 2003). However, the structural similarity of AHL autoinducers does lead to some bacterial cross-talk. For instance, *Vibrio harveyi* has been shown to respond to AHL signals from various bacterial species (Federle and Bassler, 2003). Inter-species communication is believed to allow bacteria to regulate their specific behaviors based on the self-other population ratio (Federle and Bassler, 2003). Autoinducer-2 (AI-2), which is reported to be a furanosyl borate diester (Chen *et al.*, 2002; Federle and Bassler, 2003), has also

been reported to be involved in inter-species communication (Bassler *et al.*, 1997; Bassler *et al.*, 1993; Bassler *et al.*, 1994). Table 3.1 shows representative structures of the different types of autoinducers described above (Schauder and Bassler, 2001; Chen *et al.*, 2002).

QS regulates a number of bacterial behaviors including the expression of virulence, the production of antibiotics and the formation of biofilms (Schauder and Bassler, 2001; Zhu and Mekalanos, 2003; Lindum *et al.*, 1998). It has been hypothesized that some bacteria have evolved chemical mechanisms to disrupt the QS of their competitors (Schauder and Bassler, 2001). A major problem throughout the history of antibiotic drug development is the continual evolution of the drug-resistant strains (Brittain, 1987; Francke and Neu, 1987; Lyon and Skurray, 1987; Schaberg *et al.*, 1991; Smilack *et al.*, 1991; Klein and Cunha, 1995; Geddes, 2000). The biochemical pathways used for QS are widely conserved (Schauder and Bassler, 2001). Thus, the discovery and development of QS antagonists may lead to a new generation of antibiotics possessing broad-spectrum inhibitory activities.

In recent studies, compounds that inhibit QS have been identified. Most notable are brominated furanones produced by the marine red alga *Delisea pulchra* (Rasmussen *et al.*, 2000) and their synthetic analogs. These molecules inhibit QS in Gram-negative bacteria and consequently QS-regulated gene expression. Figure 3.2 shows some representative brominated furanones, both naturally occurring and synthetic. Furanone **1** was reported to inhibit the swarming motility of *Proteus mirabilis* (Gram *et al.*, 1996), as well as inhibit the production of antibiotics and virulence factors by the phytopathogen *Erwinia carotovora* (Manefield *et al.*, 2001). Compound **2** reduces the

swarming motility in *Serratia liquefaciens* MG1 (Rasmussen *et al.*, 2000), while **3** inhibits biofilm formation (Hentzer *et al.*, 2002) and **4** the production of virulence factors by *Pseudomonas aeruginosa* (Hentzer *et al.*, 2003).

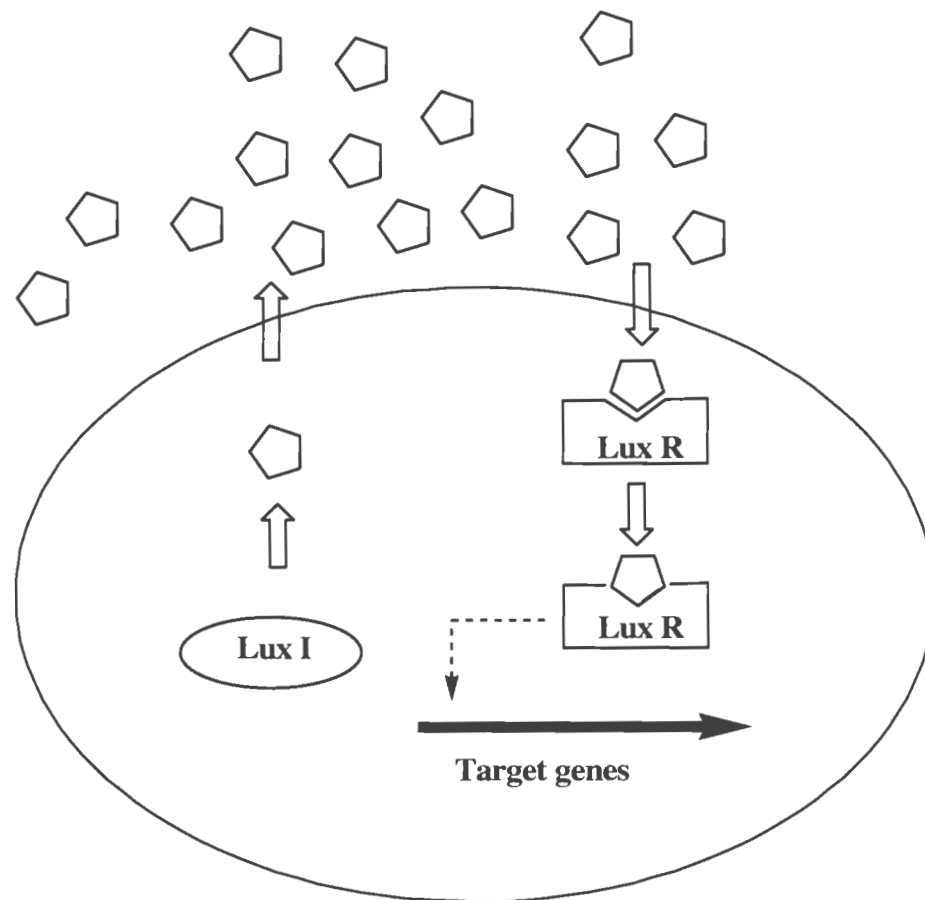
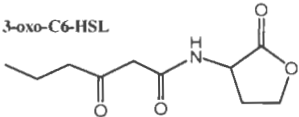
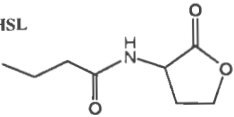
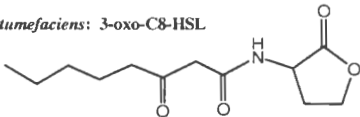
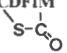
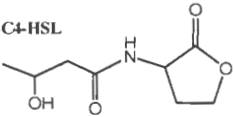
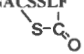
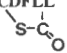
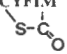
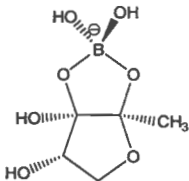


Figure 3.1. A Typical QS Pathway in Gram-negative Bacteria Using LuxI/LuxR Circuit

Note. The AHL autoinducers (open pentagons) are synthesized by the LuxI-like proteins and then diffuse out through the cell wall and accumulate. When the autoinducers reach a minimal threshold concentration, they diffuse back into the cell and bind to the LuxR-like proteins. The formed complexes then bind to the target gene and activate gene expression (Schauder and Bassler, 2001).

Table 3.1

Autoinducers Utilized by Bacteria in Quorum Sensing

A. <i>N</i> -acyl-homoserine lactone autoinducers	B. Oligopeptide autoinducers
<p><i>V. fischeri</i>: 3-oxo-C6-HSL</p> 	<p><i>B. subtilis</i>/ComX ADPITRQWGD</p>
<p><i>P. aeruginosa</i>: C4-HSL</p> 	<p><i>B. subtilis</i>/CSF ERGMT</p>
<p><i>A. tumefaciens</i>: 3-oxo-C8-HSL</p> 	<p><i>S. aureus</i>/subgroup1 YSTCDFIM </p>
<p><i>V. harveyi</i>: 3-hydro-C4-HSL</p> 	<p><i>S. aureus</i>/subgroup2 GVNACSSLF </p>
	<p><i>S. aureus</i>/subgroup3 YINCDFLL </p>
	<p><i>S. aureus</i>/subgroup4 YSTCYFIM </p>
<p>C. Furanosyl borate diester AI-2 <i>V. harveyi</i></p>	
	

Note. A: *N*-acyl-homoserine lactones (AHL) used in Gram-negative bacteria; B: Oligopeptides used by Gram-positive bacteria; C: Furanosyl borate diester (AI-2) hypothesized to be involved in inter-species communication (Schauder and Bassler 2001; Chen *et al.* 2002).

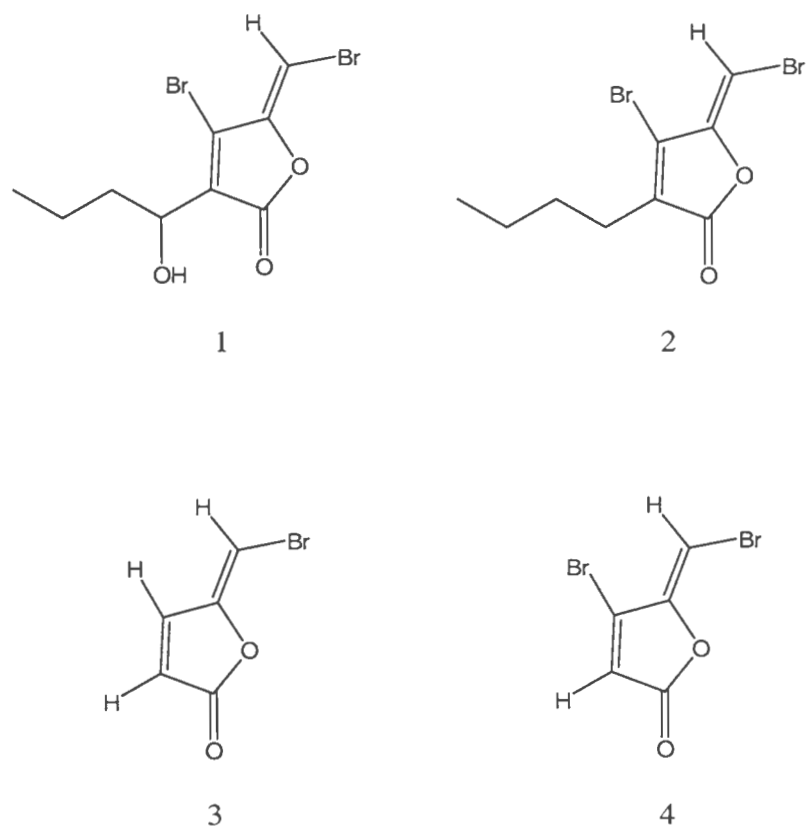


Figure 3.2. Some Brominated Furanones with QS-Antagonistic Activity

Note. **1:** 4-bromo-5-(bromomethylene)-3-(1'-hydroxybutyl)-2(5*H*)-furanone; **2:** 4-bromo-5-(bromomethylene)-3-butyl-2(5*H*)-furanone; **3:** 5-(bromomethylene)-2(5*H*)-furanone; **4:** 4-bromo-5-(bromomethylene)-2(5*H*)-furanone. Compounds **1** and **2** are derived from the benthic marine red alga *D. pulchra*. Compounds **3** and **4** are synthetic.

Oligopeptides that disrupt QS have also been isolated from the post-exponential culture of *Staphylococcus xylosus* (Gov *et al.*, 2001) (Figure 3.3). Called RNAIII-Inhibiting Peptides (RIP), these molecules disrupt QS in the Gram-positive bacterial strains *S. aureus* and *S. epidermis*, consequently preventing toxin biosynthesis. Synergistic activity with other antibiotics to prevent biofilm formation by drug-resistant *Staphylococcus epidermidis* has also been shown (Balaban *et al.*, 2003). In other instances, AHLs with side chains longer than C8, such as *N*-decanoyl-*L*-homoserine lactone (DHL), have been shown to inhibit QS systems that use AHLs with shorter side chains (McClellan *et al.*, 1997).

YSPXTNF YKPITNF YSPWTNF

Figure 3.3. RNAIII-Inhibiting Peptides (RIP) Isolated from Staphylococcus xylosus

3.2 Methods and Results

3.2.1 QS-Antagonism Screening of the Library of Crude Extracts Produced by Marine Bacteria

Four hundred crude extracts derived from marine microbial cultures (Rowley crude extract library, described in Wang, 2003c) were screened for QS antagonist activity. A mutant strain of *Chromobacterium violaceum*, herein referred to as CV026, was used as the bioassay reporter strain and is described below.

The Gram-negative bacterium *Chromobacterium violaceum* produces violacein, a characteristic purple pigment. The biosynthesis of this pigment is regulated by QS using *N*-hexanoyl-*L*-homoserine lactone (HHL) as the autoinducer (McClellan *et al.*, 1997). CV026 is a mini-Tn5 transposon based mutant of the wild-type *C. violaceum* ATCC31532 (Latifi *et al.*, 1996; Throup *et al.*, 1995). This mutant is defective in the production of AHLs, and thus cannot produce violacein (Throup *et al.*, 1995). However, pigment production by CV026 can be restored by exogenous addition of AHLs with side chains from C4-C8 in length (McClellan *et al.*, 1997). The CV026 strain used in this project was graciously provided by Dr. David Nelson (URI).

Synthetic or naturally-derived HHL (Figure 3.4) was used as the autoinducer in the screening assay. Naturally-derived HHL was extracted using dichloromethane from spent liquid cultures of *Serratia liquefaciens* MG1 (McClellan *et al.*, 1997), and is hereafter referred to as SLMG1-HHL. The swarming motility of *S. liquefaciens* MG1 is controlled by QS using HHL (Eberl *et al.*, 1996). To test the ability of SLMG1-HHL to induce violacein production, CV026 was seeded evenly over the surface of LB₁₀ solid agar (composed of 10 g of tryptone, 5 g of yeast extract, 10 g of NaCl and 16 g of agar per liter of deionized water). Paper disks loaded with 0.5 mg of SLMG1-HHL extract were applied to the CV026 lawns. The plate was incubated at 28-30 °C overnight and the resulting pigment production was examined the next day. Figure 3.5 shows a typical assay result. The purple zones surrounding the paper disks indicate violacein production by CV026 in response to diffusion of HHL from the paper disk.

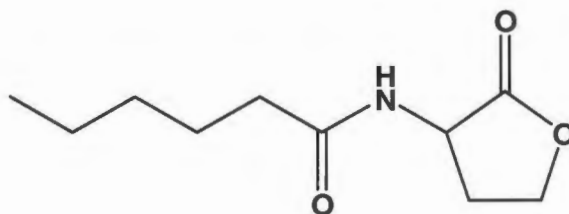


Figure 3.4. *N*-Hexanoyl-*L*-Homoserine Lactone (HHL)

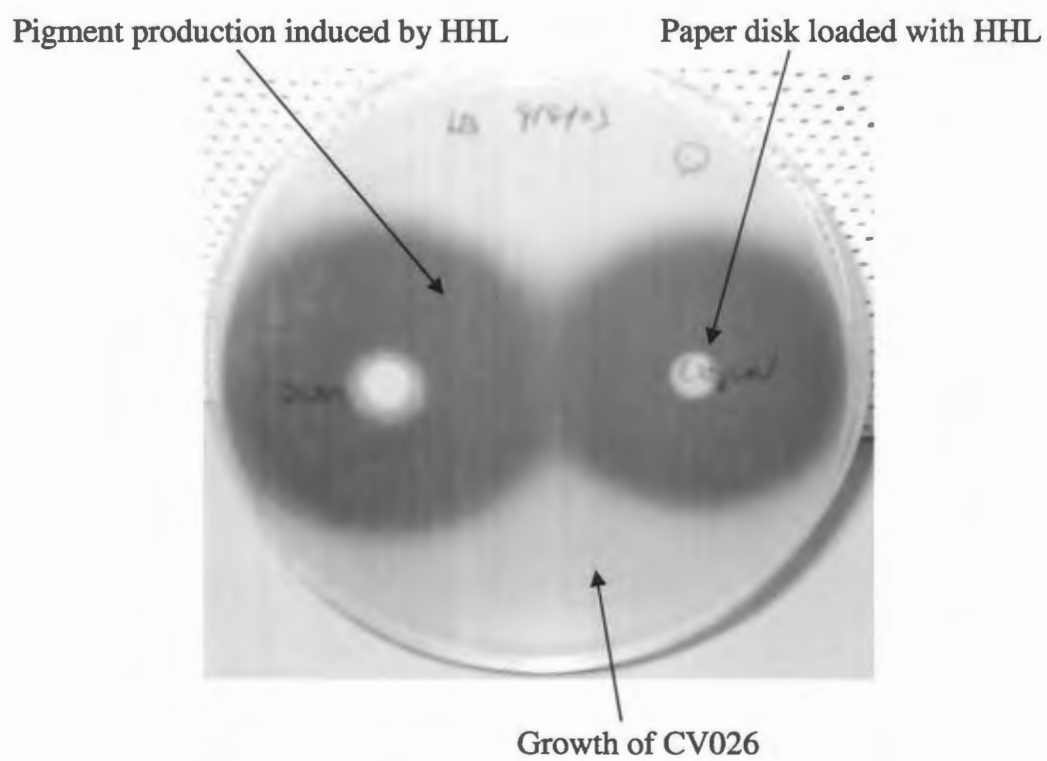


Figure 3.5. HHL Induction of Violacein Production by CV026

3.2.1.1 Agar disk diffusion assay for violacein inhibition.

The frozen stock of CV026 was allowed to thaw at room temperature (23-24 °C). 10 mL of fresh LB₁₀ broth was inoculated with a loop of the thawed CV026 stock and incubated with shaking at 30 °C overnight. On the next day, 50 µL of the overnight CV026 culture and 50 µL of SLMG1-HHL dissolved in dichloromethane (25 mg/mL) were both added to 5 mL of molten 8% semi-solid LB₁₀ agar (39-40 °C). The mixture was vortexed and poured over the top of a LB₁₀ solid agar plate. Five wells were cut from the solidified agar plate. 20 µL of a test sample (25mg/mL in DMSO) was added to one of the five wells. 20 µL of DMSO was added to a different well (solvent control). A total of four test samples could be assayed in one single plate. The plate was then incubated in up-right way at 29-30 °C overnight and the results were examined the next day. The desired assay result should show a purple background with an opaque yellowish halo surrounding the well loaded with a test sample. The purple background is due to violacein production by CV026, while the opaque halo would indicate inhibition of QS-mediated pigment production but not microbial growth. A total of 10 crude extracts were assayed this way.

3.2.1.2 CV026 screening assay in microtiter plates.

Limited by the size of the Petri dish holding the LB₁₀ agar (only four extracts could be tested by using one plate), a screening assay using 96-well microtiter plates was designed for higher throughput. In this assay, turbid CV026 overnight culture (prepared as before) was diluted with fresh LB₁₀ broth by a 1 to 1000 ratio. The SLMG1-HHL solution (25 mg/mL, in DMSO) was added to the diluted CV026 culture

to a concentration of 0.25 mg/mL. This mixture is hereafter referred to as culture-mixture (CM). The assay set up is diagramed in figure 3.6. 150 μ L of CM was added to each well in a 96-well microtiter plate except for wells F11, F12, G11, G12, H11, and H12. 3 μ L of a crude extract (25 mg/mL in DMSO) was added to each well in area 1. A total of 80 crude extracts were tested per plate. 3 μ L of DMSO was added to wells in area 2 (A11, A12, B11, B12, C11 and C12) as the solvent control. 148.5 μ L of the diluted CV026 and 4.5 μ L of DMSO were both added to wells in area 4 (F11, F12, G11 and G12) as violacein-negative controls (no HHL present). 148.5 μ L of LB₁₀ broth plus 4.5 μ L of DMSO was added to each of the wells H11 and H12 as growth-negative control. Wells in area 3 (D11, D12, E11, and E12) contained only CM and served as violacein-positive controls. Assay plates were incubated at 26-27°C with shaking. Over a length of 2 days (48-72 hrs), solvent control (area 2) and violacein-positive control (area 3) displayed turbid bacterial growth and purple color due to violacein production. The culture in the absence of HHL (area 4) showed only turbid bacterial growth. The color of the cultures in the test wells (area 1) were observed carefully. If the color was comparable to those in areas 2 and 3, then test samples were deemed not to inhibit violacein production. However, nine of four hundred test extracts resulted in lesser pigment production.

These nine active crude extracts were further examined using the agar diffusion assay described above. Only two showed obvious opaque halos and were selected for further study. These extracts were derived from cultures C42 and B36. Bacterial strain C42 was isolated from a seaweed sample collected from Point Judith Salt Pond, South Kingstown, Rhode Island in the summer of 2002. Morphologically, single rod-shaped

cells could be observed under microscope (Oil immersion 1000×). Gram staining (Madigan *et al.*, 2003b) and a KOH test (Gregerson, 1978; Halebian *et al.*, 1981) both indicated that this bacterium was Gram-positive. C42 survived heat shock (70 °C, 6 minutes) and grew quickly on YP agar plates (5 g of peptone and 1 g of yeast extract in 1 liter of filtered seawater), but did not grow on the YP agar plates prepared with fresh water (YPF). This bacterium was eventually identified as *Halobacillus* sp. through 16S rRNA sequencing method. In order to explain the chemical mechanism of the violacein-inhibition activity of C42, this bacterial strain was cultured in large scale, and the crude extract was subjected to bioassay-guided fractionation.

	1	2	3	4	5	6	7	8	9	10	11	12
A												
B												2
C												
D												3
E						1						
F												
G												4
H												5

Figure 3.6. The Plating Scheme for QS-Inhibition Broth Assay

Note. Area 1: 150 μL CM* + 3 μL test sample in each well (Test Area); area 2: Solvent Control 150 μL CM* + 3 μL DMSO; area 3: 150 μL CM; area 4: 148.5 μL diluted culture** + 4.5 μL DMSO; area 5: 148.5 μL LB₁₀ + 4.5 μL DMSO. * CM: mixture of the diluted culture and HHL containing MG1 extract; ** Diluted CV026 culture.

**3.2.2 Isolation of Quorum Sensing Inhibitory Compounds C42.191 and C42.205
Produced by Halobacillus sp. Culture C42**

Frozen stock of C42 (-80 °C) was allowed to thaw at room temperature (22-24 °C), inoculated into each of two culture tubes containing 10mL of fresh YP broth, and incubated at 24 °C with shaking overnight. On the next day, the light yellow bacterial culture in two tubes was transferred to two flasks (1 L × 2 flasks, a total of 2 L) of the fresh YP broth and incubated under the identical conditions for eight days. Incremental measurements were taken to determine the optimal fermentation time for the production of QS-antagonistic metabolites by C42. Starting from the second day of the incubation (after one full day of incubation, referred to as day 1), 100 mL of the culture was removed each day from one of the culture flask and extracted with 2 × 75 mL of ethyl acetate. Bioassay of the concentrated extracts from days 1-8 were conducted using the agar diffusion assay. The optimal fermentation time for the production of the QS-inhibitory components by C42 was found to be 5 to 7 days (Figure 3.7).

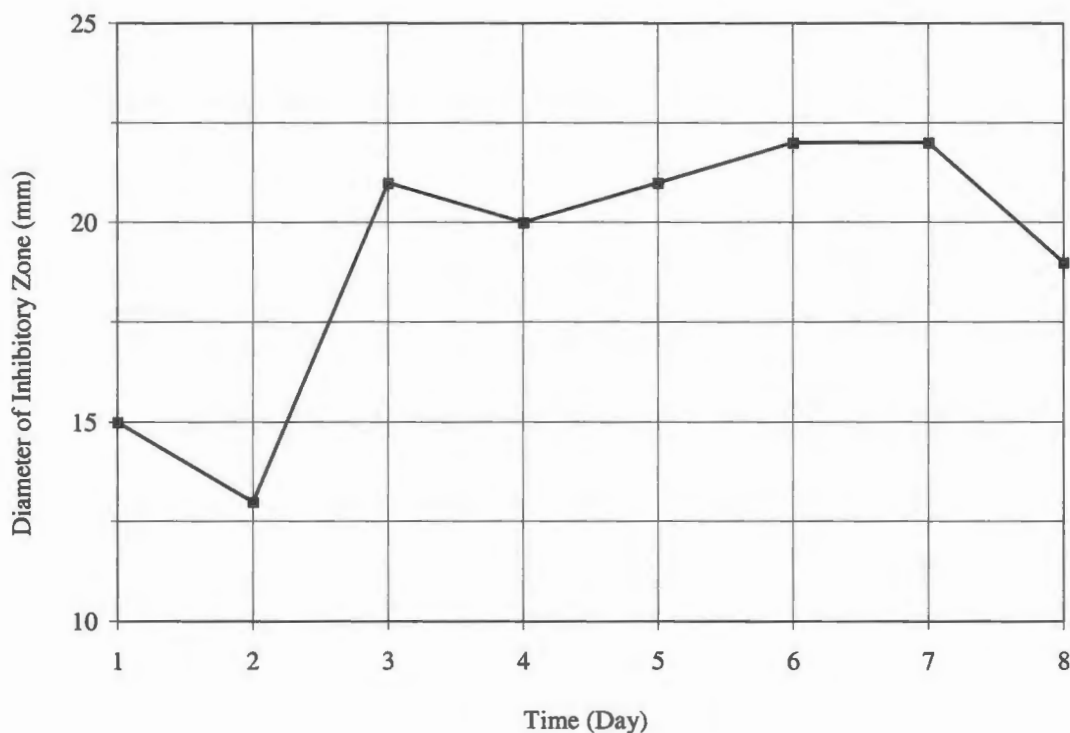


Figure 3.7. QS-Inhibitory Activity of C42 Crude Extracts vs. Fermentation Time

C42 stock was next cultured in 13 L of fresh YP broth (13 × 1 L) for five and a half days under the identical fermentation conditions as used in the optimization experiment. After the fermentation, the 13 L of opaque yellow C42 culture was centrifuged (Sorvall RC-5B, 8000rpm, 15 minutes) to pellet the cells and the clear supernatant was extracted using solid phase chromatography (Kontes[®] Column 600×50mm packed with 700mL of wet resin, Diaion[®] HP-20, Supelco, lot: 1G552) and eluted using an aqueous acetone mixture in gradient concentrations: 25% (1 L) → 50% (1 L) → 75%(1 L) → 100% acetone (3 L). After concentration, the four extracts yielded 6.28 g (25%), 920 mg (50%), 583 mg (75%) and 83.2 mg (100%), of which the 50% fraction showed the desired QS-antagonistic activity. 200 mg of this extract was further

fractionated using size exclusion chromatography (Kontes[®] 500×38 mm column packed with Sephadex LH-20 resin, Fluka[®], Lot: 9041-37-6). A solvent system composed of iso-octane, methanol and toluene (3:2:1) was used to elute the column at a flow rate of one drop every five seconds. The eluent was collected into test tubes using a fraction collector at a rate of 16 minutes per tube. A total of 145 tubes of eluent were collected over the two-day experiment. The individual test tubes of eluent were then combined into eight fractions based on silica gel thin layer chromatography (TLC) (Whatman[®], Lot: 4420222). After vacuum drying, fraction **2** formed a white crystal with yellow impurities. This fraction weighed 173.7 mg while all other fractions were each less than 3 mg. QS inhibition assay showed activity in all eight fractions. Because of the abundant supply, fraction **2** was then selected for further investigation. Recrystallization in iso-octane (TMP) was accomplished by warming the material in TMP to 29-30 °C and allowing to stand at room temperature overnight. White fluffy needle-like crystals were filtered and vacuum dried (72.3 mg).

The purity of the crystal was assessed by analytical HPLC (Hitachi[®] equipped with L-7455 diode array detector, column: X-Terra[®] RP C₁₈ column, 3.0 × 100 mm, λ = 216 nm). Two major peaks were observed with small impurities. Subsequent reversed phase HPLC (X-Terra[®] Prep RP C₁₈ column, 100 × 19 mm, using 20% → 40% acetonitrile gradient in water, λ = 216 nm, flow rate of 10 mL/min) yielded two pure compounds (C42.191, 10 mg; C42.205, 29.7 mg). Figure 3.8 shows a flow chart of the bioassay-guided fractionation of the C42 culture leading to the two pure compounds. These two compounds were both white solids and able to crystallize to form needle-like crystals from TMP.

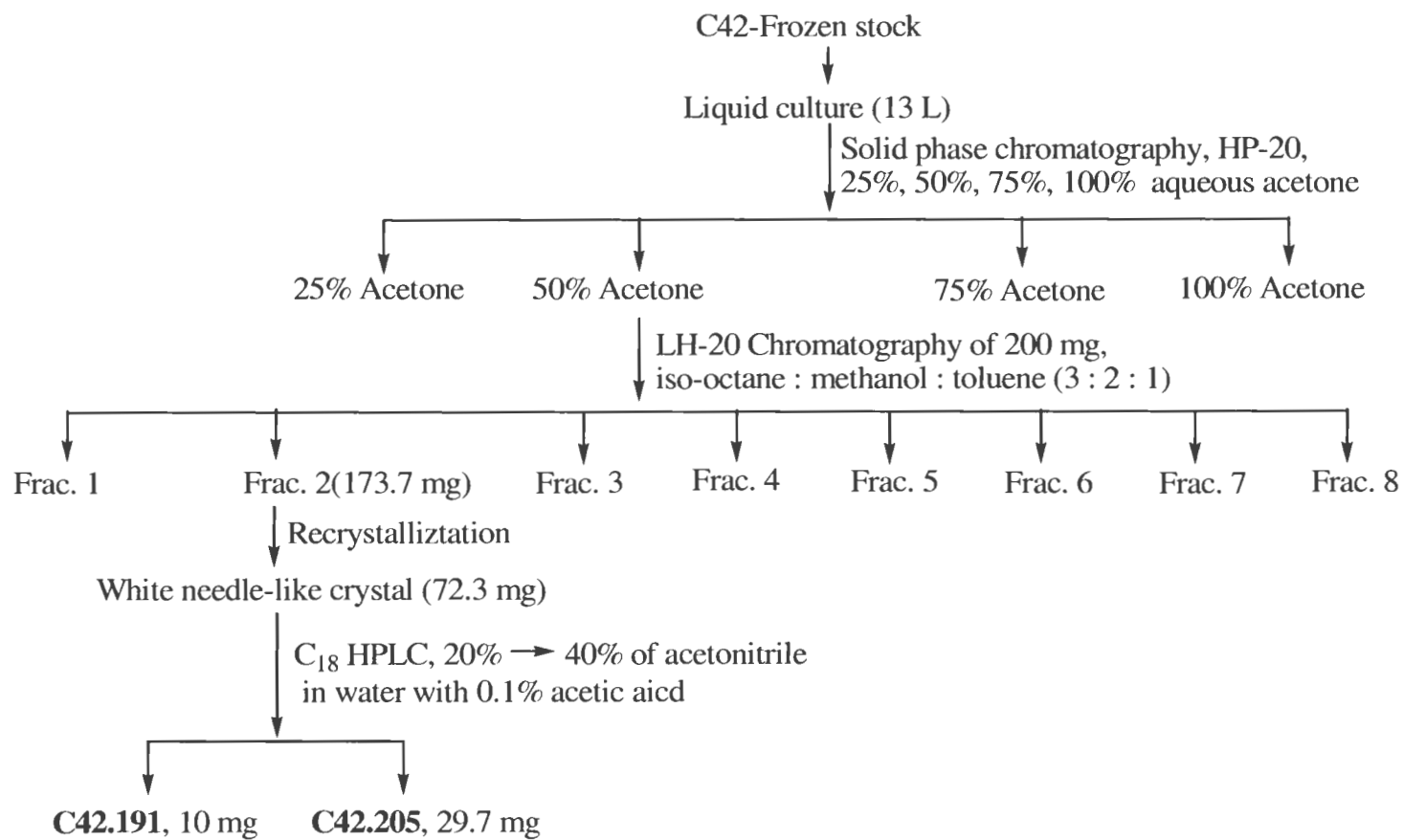


Figure 3.8. Bioassay-Guided Fractionation of C42 Culture

3.2.3 Structural Elucidation of C42.191 and C42.205

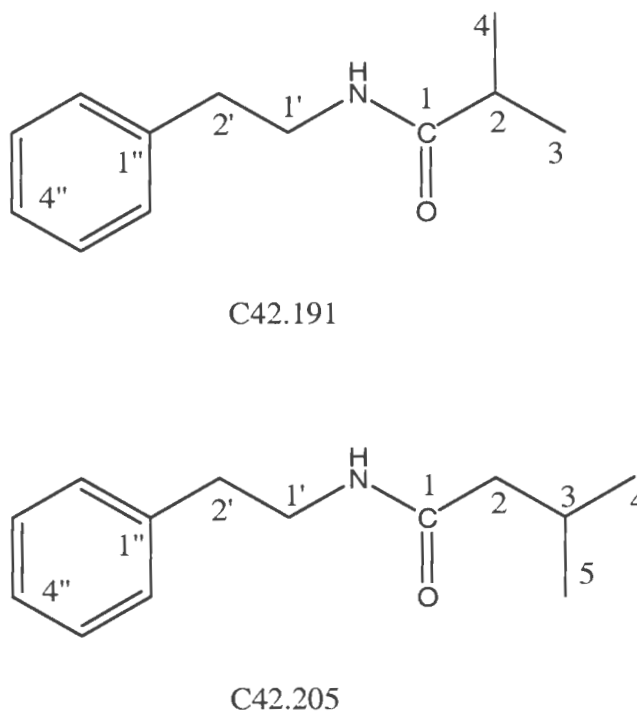


Figure 3.9. The Structures of C42.191 and C42.205

Note. C42.191: *N*-(2'-Phenylethyl) Isobutyramide; C42.205: 3-Methyl-*N*-(2'-Phenylethyl)-Butyramide.

The structures of C42.191 and C42.205 (Figure 3.9) were elucidated using electrospray ionization mass spectrometry (ESI-MS, Mariner Spec[®]) and nuclear magnetic resonance spectroscopy (NMR, Bruker[®]). For ESI-MS, the compounds were dissolved in a methanol : water (1 : 1) + 0.1% acetic acid solvent system at 2 $\mu\text{g/mL}$ to

optimize ionization. NMR experiments were conducted in methanol- d_4 (MeOD) at a concentration of about 15 mg/mL.

The MS spectrum of C42.191 showed the two positive ion peaks: $[M+H]^+$ m/z of 192.1 and $[M+Na]^+$ m/z of 214.1, suggesting a molecular weight of 191 (Figure 3.10). Together with 1H and ^{13}C NMR data, a molecular formula of $C_{12}H_{17}NO$ was deduced, indicating that the molecule would have five degrees of unsaturation. ^{13}C NMR (Figure 3.12) and Dept135 (Figure 3.13) spectra showed that the compound had 12 carbons, including two identical methyls (δ 19.89), two methylenes (δ 36.53 and δ 41.84), one aliphatic methine (δ 36.29), five aromatic methines (δ 127.32, δ 129.43 (2 \times), δ 129.88 (2 \times)) and two quaternary carbons (δ 140.55 and δ 180.07). The more deshielded quaternary carbon represents a carbonyl carbon and accounts for one degree of unsaturation. Integration of the proton NMR spectrum (Figure 3.11) indicated that the molecule possessed 16 hydrogens attached to carbon. Therefore, one of the 17 protons was exchangeable in MeOD (-NH). The doublet at δ 1.06 integrates for six protons and suggests two methyl groups coupled to a common methine. The septuplet (1H) at δ 2.36 represents a proton from a methine coupled to six protons. A multiplet (5H) at δ 7.20 is typical of five conjugated protons from a mono-substituted benzene ring, which accounts for the remaining 4 degrees of unsaturation. The triplet (2H) at δ 2.77 represents a methylene group coupled to another methylene group and the quartet (2H) at δ 3.37 represents a methylene group coupled both to a methylene and to a single proton (exchangeable proton). The coupling constants here were not clear enough to obtain the proton coupling patterns. The two-dimensional COSY (COrrrelation SpectroscopY) spectrum (Figure 3.14) clearly indicated that the two methyl groups

were coupled to a common methine proton and that the two methylene groups formed an isolated spin system. The two-dimensional HMQC (Heteronuclear Multiple Quantum Coherence) spectrum (Figure 3.15) provided information on C-H one bond coupling. All protons and carbons were subsequently assigned (Table 3.2).

Table 3.2

^1H and ^{13}C NMR Assignments for C42.191 in MeOD- d_4

Carbon	δ_{H}	δ_{C}	Dept
1		180.07	C=O
2	2.36	36.29	CH
3, 4	1.06	19.89	CH ₃ (2×)
1'	3.37	41.83	CH ₂
2'	2.77	36.53	CH ₂
1''		140.55	C
4''	7.2	127.32	CH
2'', 6''	7.2	129.43	CH (2×)
3'', 5''	7.2	129.88	CH (2×)

Note. The spectra were recorded in MeOD- d_4 (^1H : 400 MHz, ^{13}C : 100 MHz).

Based on molecular formula, ^1H and ^{13}C NMR chemical shifts, and spin system data, the aryylethylamide compound C42.191 was constructed (Figure 3.9). Subsequent search of the literature showed that this molecule had been previously reported and named as *N*-(2'-phenylethyl) isobutyramide (Maskey *et al.*, 2002).

The MS spectrum of C42.205 also shows two positive ion peaks: $[\text{M}+\text{H}]^+$ m/z of 206.1 and $[\text{M}+\text{Na}]^+$ m/z of 228.1, indicating a molecular weight of 205 and the molecular formula $\text{C}_{13}\text{H}_{19}\text{NO}$ (Figure 3.16) with 5 degrees of unsaturation. ^{13}C and Dept135 NMR spectra (Figures 3.18 and 3.19) show that C42.205 had 13 carbons

including two identical methyls (δ 22.69), three methylenes (δ 36.59 and δ 41.89 and δ 46.36), one aliphatic methine (δ 27.40), five aromatic methine (CH) (δ 127.34, δ 129.47 (2 \times), δ 129.81 (2 \times)) and two quarternary carbons (δ 140.50 and δ 175.54), of which the one with higher chemical shift represented a carbonyl carbon. The integration of the proton NMR (Figure 3.17) showed 18 hydrogens. All the spectra (Figures 3.16 to 3.20) here indicated that C42.205 has the similar structure as that of C42.191 except that C42.205 has one additional methylene. Table 3.3 shows the proton and carbon NMR chemical shift assignment for C42.205. Based on molecular weight and ^1H and ^{13}C NMR chemical shift data, C42.205 was found to be 3-methyl-*N*-(2'-phenylethyl)-butyramide as previously reported in the literature (Maskey *et al.*, 2002).

Table 3.3

^1H and ^{13}C NMR Assignments for C42.205 in MeOD- d_4

Numbering	δ_{H}	δ_{C}	Dept
1		175.54	C=O
2	2.00	46.36	CH ₂
3	2.00	27.40	CH
4, 5	0.90	22.69	CH ₃ (2 \times)
1'	3.39	41.89	CH ₂
2'	2.77	36.59	CH ₂
1''		140.50	C
2'', 6''	7.2	129.47	CH (2 \times)
3'', 5''	7.2	129.81	CH (2 \times)
4''	7.2	127.34	CH

Note. The spectra were recorded in MeOD- d_4 (^1H : 400 MHz, ^{13}C : 100 MHz).

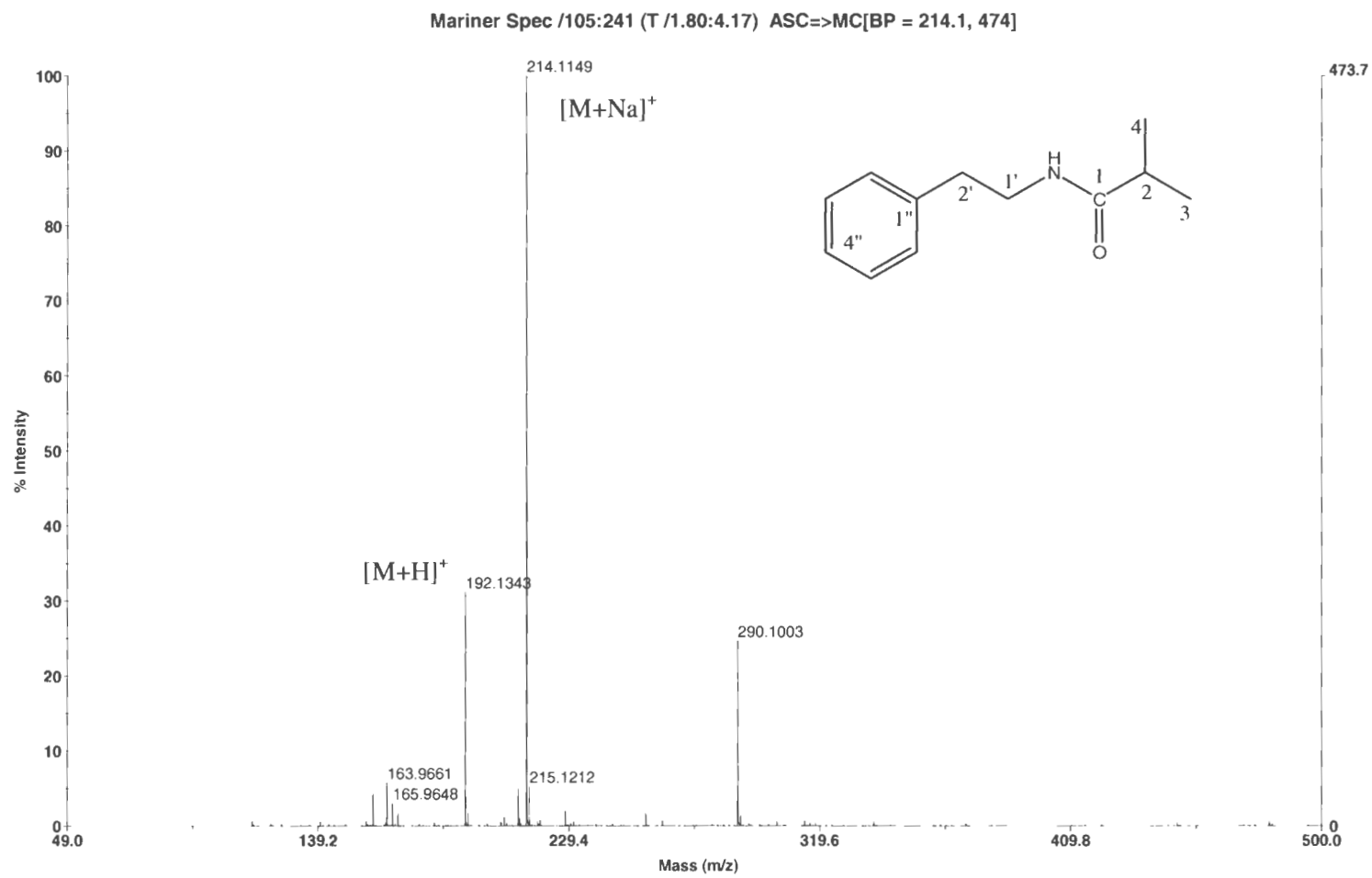


Figure 3.10. Mass Chromatogram (Positive Ion) of C42.191

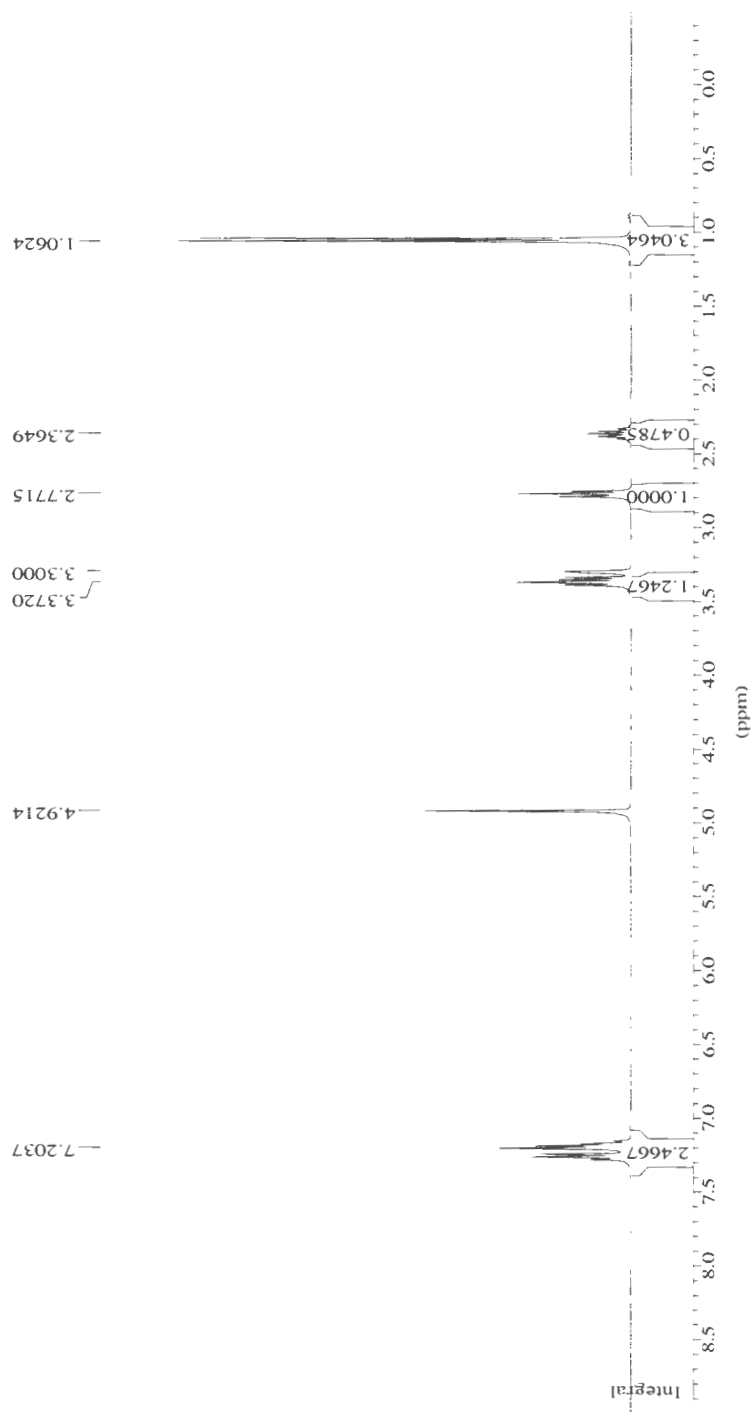


Figure 3.11. ¹H NMR Spectrum (400 MHz) of C42.191 in MeOD-*d*₄.

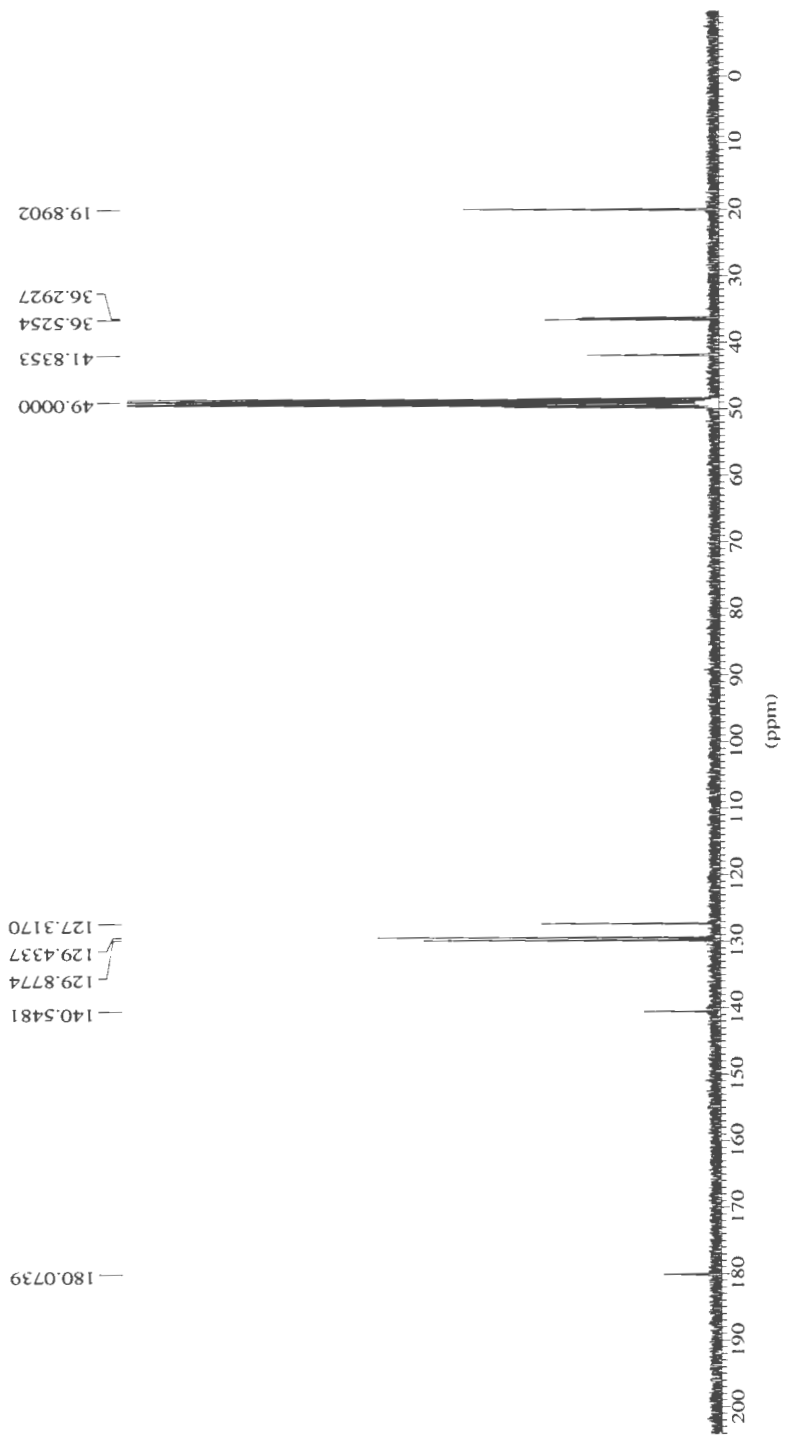


Figure 3.12. ¹³C NMR Spectrum (100 MHz) of C42.191 in MeOD-*d*₄

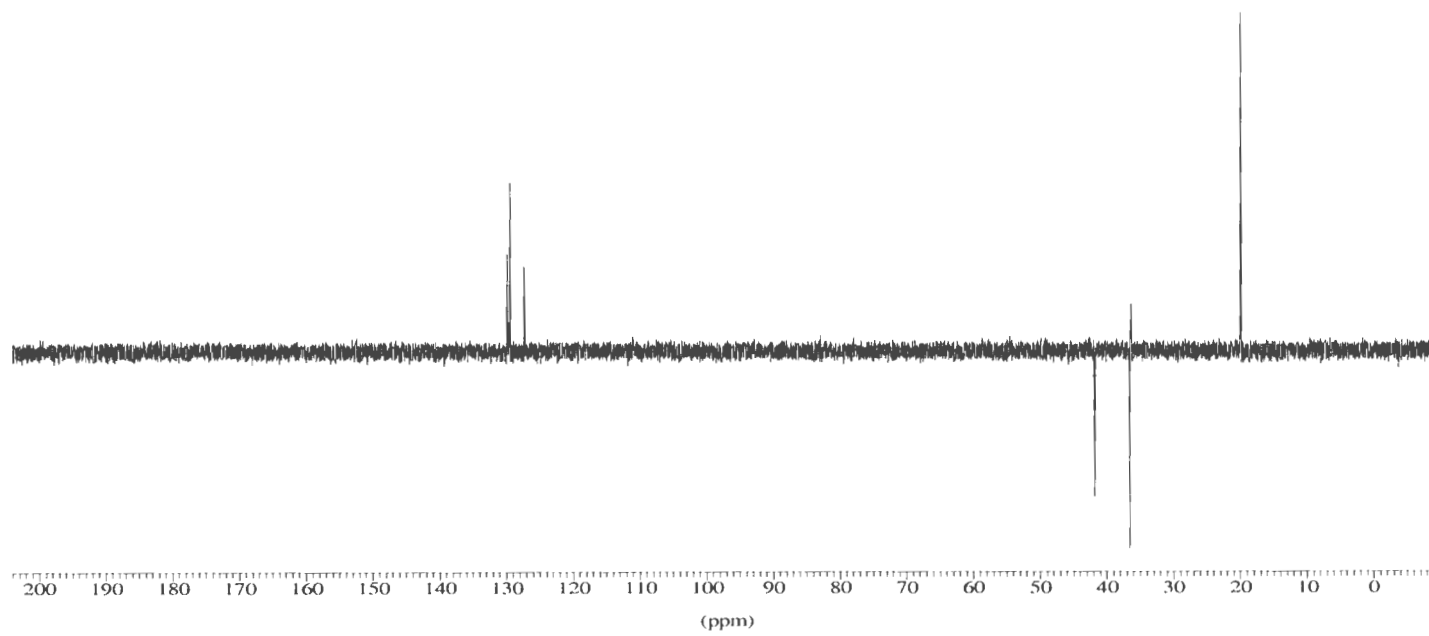


Figure 3.13. Dept135 NMR Spectrum of C42.191 in MeOD- d_4

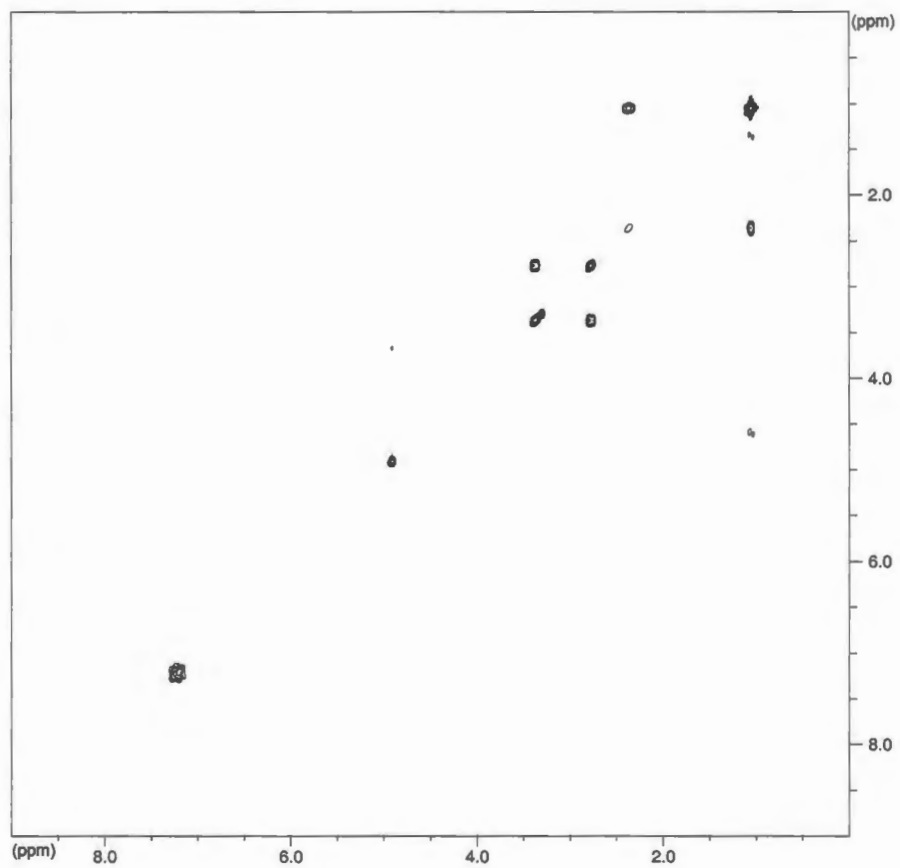


Figure 3.14. COSY Spectrum of C42.191 in MeOD- d_4

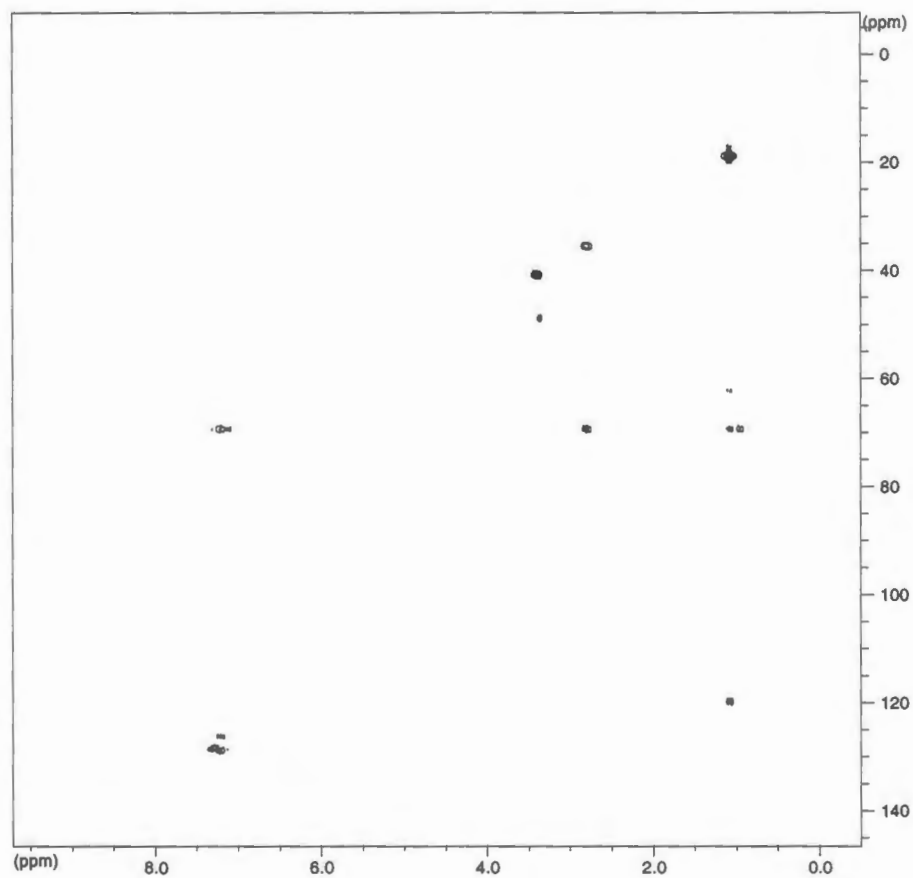


Figure 3.15. HMQC Spectrum of C42.191 in MeOD-*d*₄

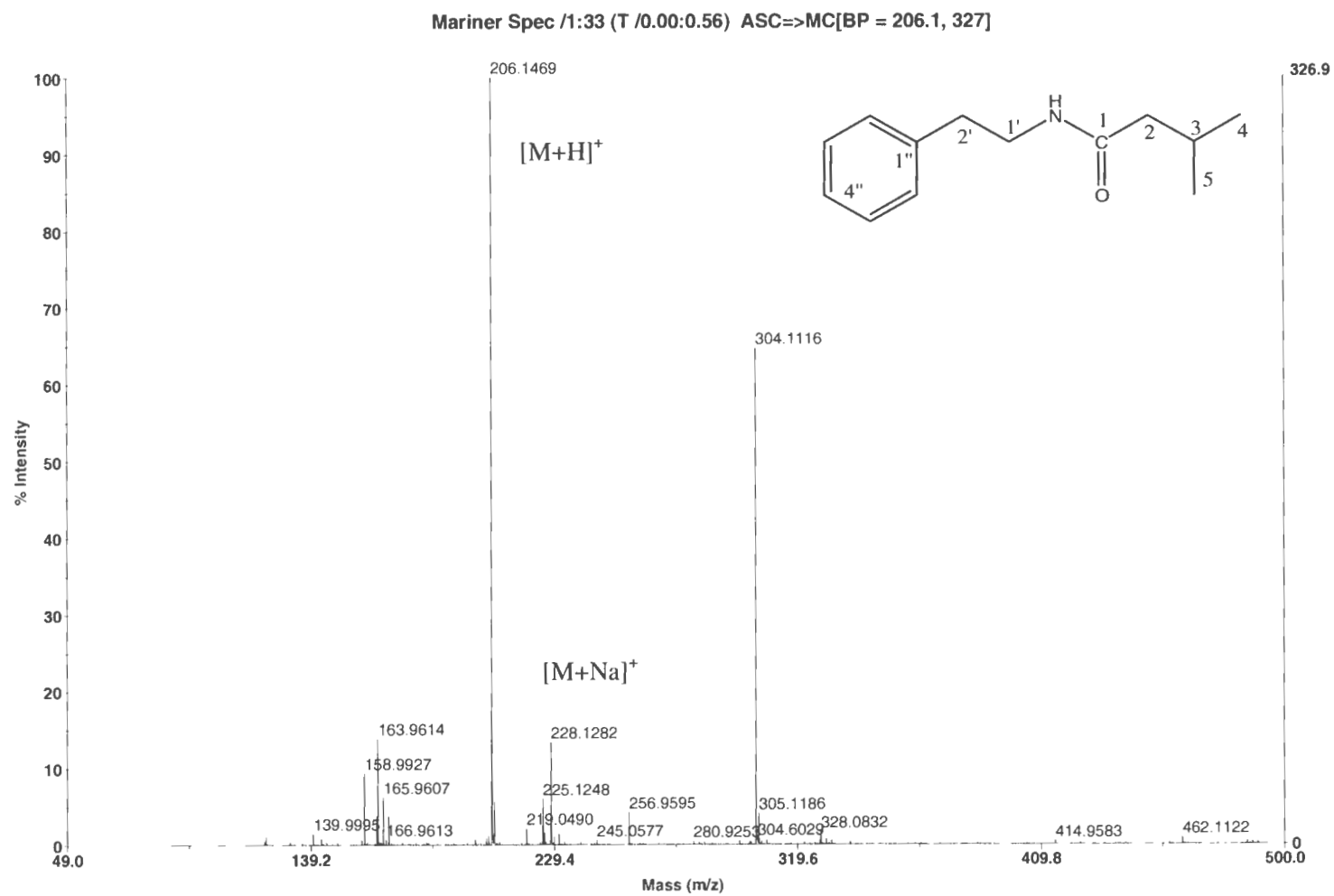


Figure 3.16. Mass Chromatogram (Positive Ion) of C42.205

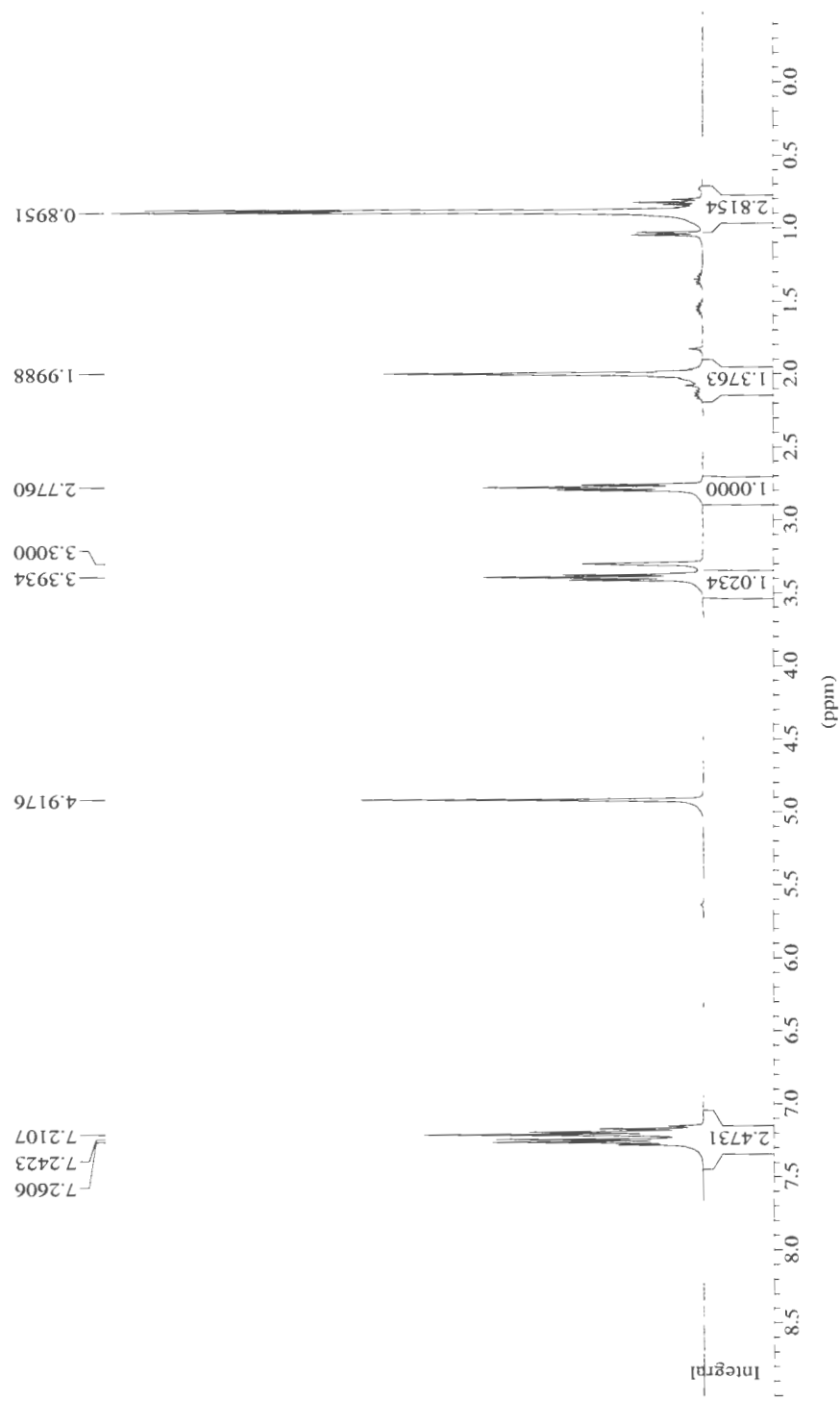


Figure 3.17. ^1H NMR Spectrum (400 MHz) of C42.205 in $\text{MeOD-}d_4$

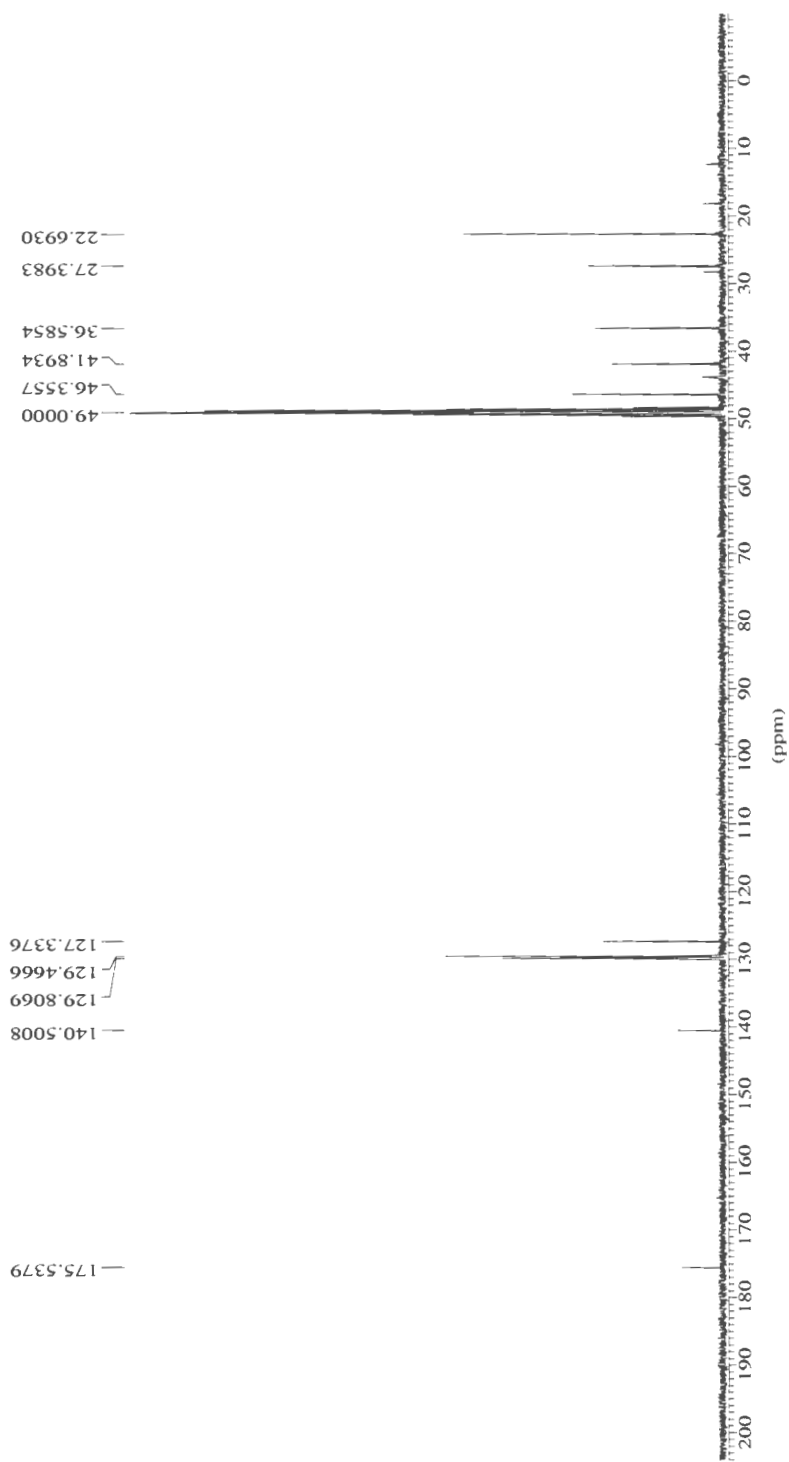


Figure 3.18. ^{13}C NMR Spectrum (100 MHz) of C42.205 in MeOD- d_4

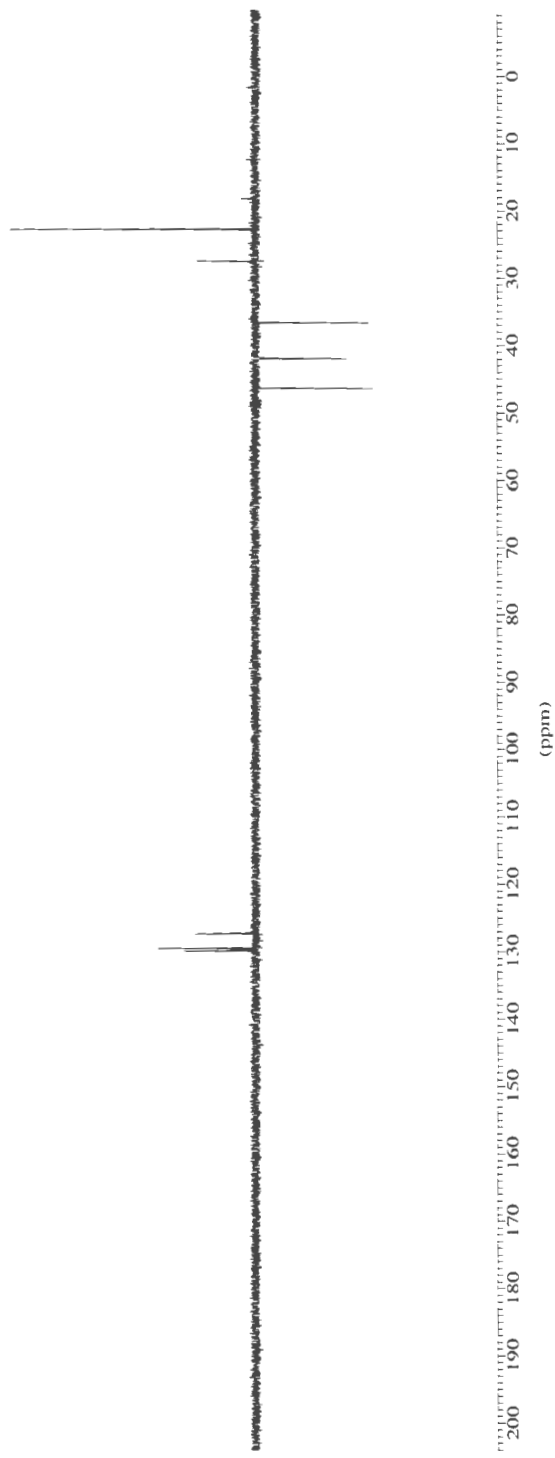


Figure 3.19. Dept135 NMR Spectrum of C42.205 in MeOD-d₄

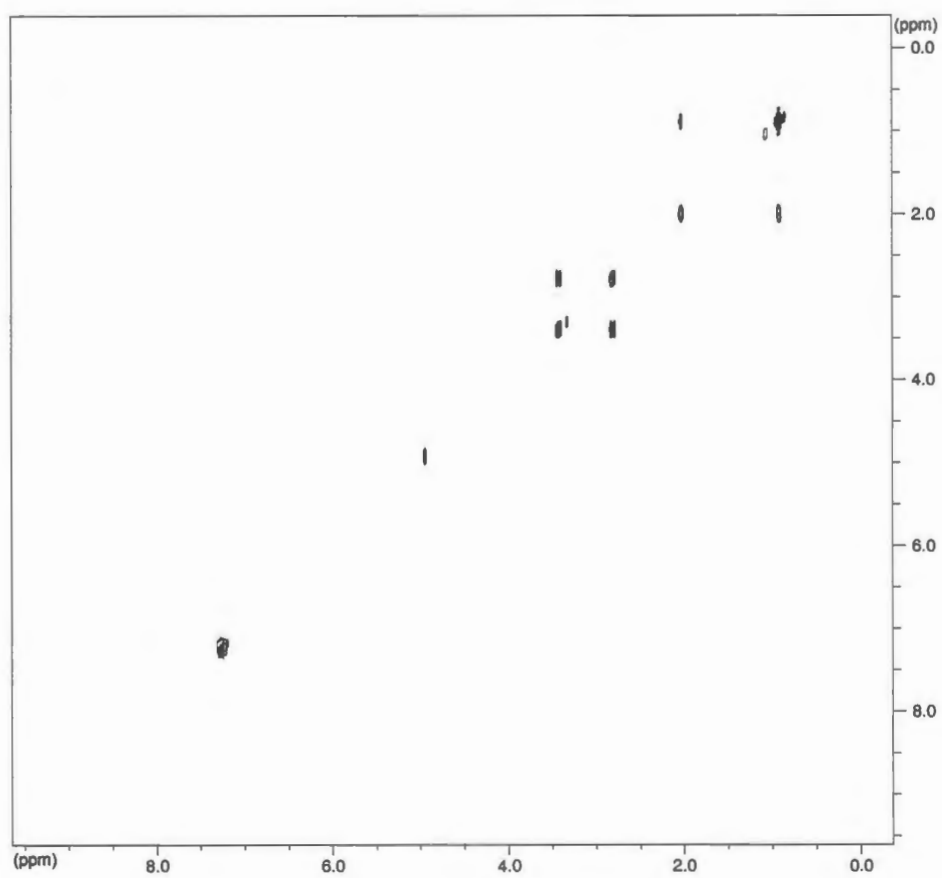


Figure 3.20. COSY Spectrum of C42.205 in MeOD- d_4

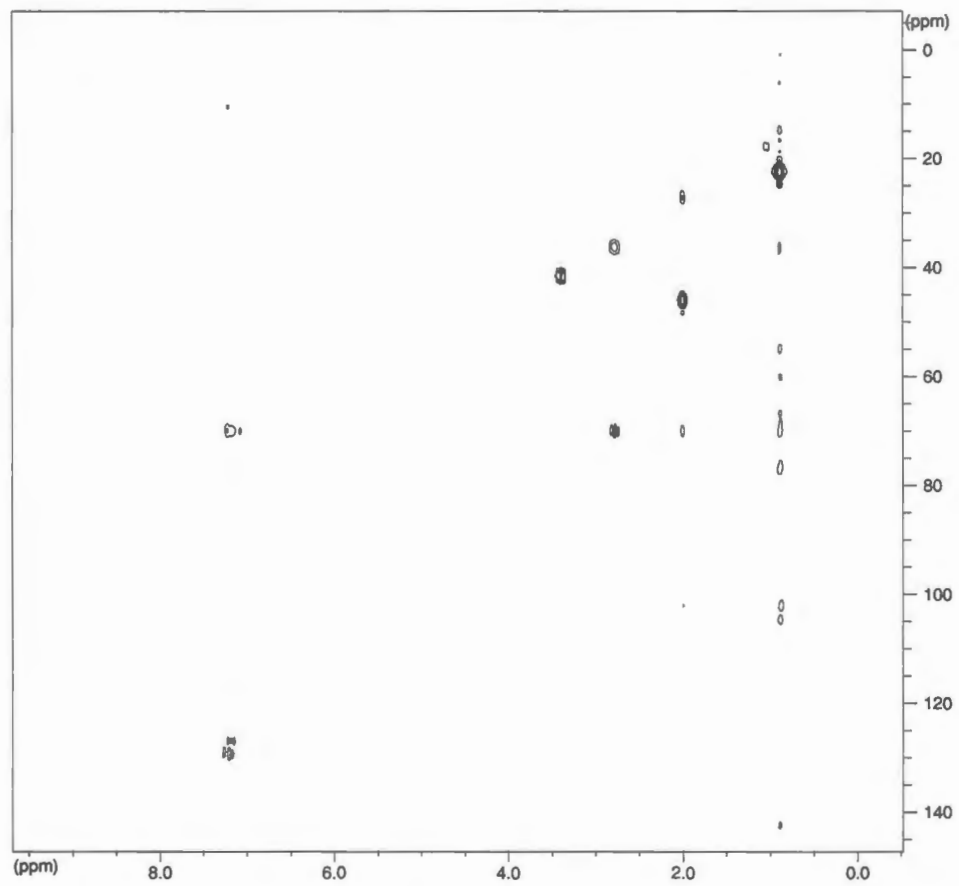


Figure 3.21. HMQC Spectrum of C42.205 in MeOD- d_4

3.2.4 QS-Inhibition Activity of C42.191 and C42.205

3.2.4.1 CV026-violacein inhibition assay.

Both C42.191 and C42.205 inhibited QS-regulated violacein production by the Gram-negative bacterium *C. violaceum* CV026. However, optimization and standardization of the reporter assay were first necessary to accurately assess these properties.

Synthesized HHL was used in the standard assay. Although HHL extracted from *S. liquefaciens* MG1 adequately induced violacein production by CV026, the batch variability of HHL from different *S. liquefaciens* cultures was unknown. Also, severe emulsions were frequently encountered during the extraction process. In order to standardize the CV026 assay, HHL was synthesized *de novo* via a one-step amide-bond formation reaction (Figure 3.22). 728 mg (1 equivalent) of DL-homoserine lactone hydrobromide (ICN Biomedicals, Cat No. 157389), 511.2 mg (1.1 equivalent) of hexanoic acid (ACROS ORGANICS, Lot No. A015866701), and 1.67 g (1.1 equivalent) of HBTU (NOVAbiochem[®] Lot No. A29504) were added to 60 mL of anhydrous acetonitrile and stirred. After 40 minutes, 2.5 equivalents of di-methyl amino pyridine (DMAP) was added and the reaction stirred overnight. The next day, the reaction was concentrated to near dryness and then partitioned between 200 mL of ethyl acetate and 200 mL of 0.5 N HCl (Figure 3.23). The organic fraction was subsequently washed with 200 mL of saturated NaHCO₃ and finally 200 mL of deionized water. The clear ethyl acetate fraction was dried over Na₂SO₄ and concentrated *in vacuo* to yield a slightly-yellow white solid. The solid was dissolved in 15 mL of ethyl acetate and then 60 mL of iso-octane (TMP) was added. White solids were observed to precipitate out of

solution. The solution was cooled (4 °C) for 3 hours, filtered, and washed with TMP. 300 mg of a shiny white solid was obtained after drying *in vacuo*. Comparison of ¹H NMR spectra with literature values (Chhabra *et al.*, 1993) verified the material to be pure HHL.

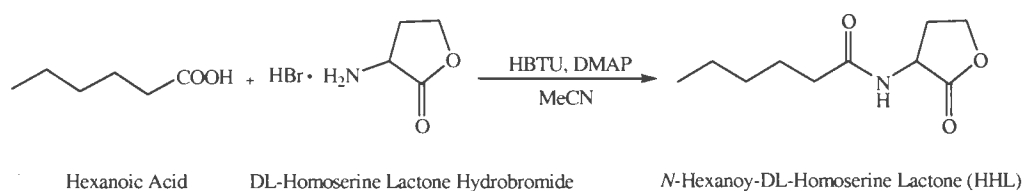


Figure 3.22. Synthesis of HHL

The pure HHL was tested for QS-induction of violacein production. 30 μ L of the HHL dissolved in acetonitrile (2-fold serially dilutions at concentrations from 0.64 mg/mL to 0.32 mg/mL \rightarrow 0.16 mg/mL \rightarrow 0.08 mg/mL \rightarrow 0.04 mg/mL) along with 50 μ L of the overnight CV026 culture were added to 5 mL of molten 8% semi-solid LB₁₀ agar. The mixture was vortexed and poured over the top of a normal LB₁₀ agar plate. The solidified agar plates were then incubated overnight at 29-30 °C. The next day, the plates showed sequentially lighter purple color with decreasing concentrations of HHL. 0.08 mg/mL was the boundary concentration. 0.1 mg/mL was selected to be the concentration of HHL used in the agar diffusion assay.

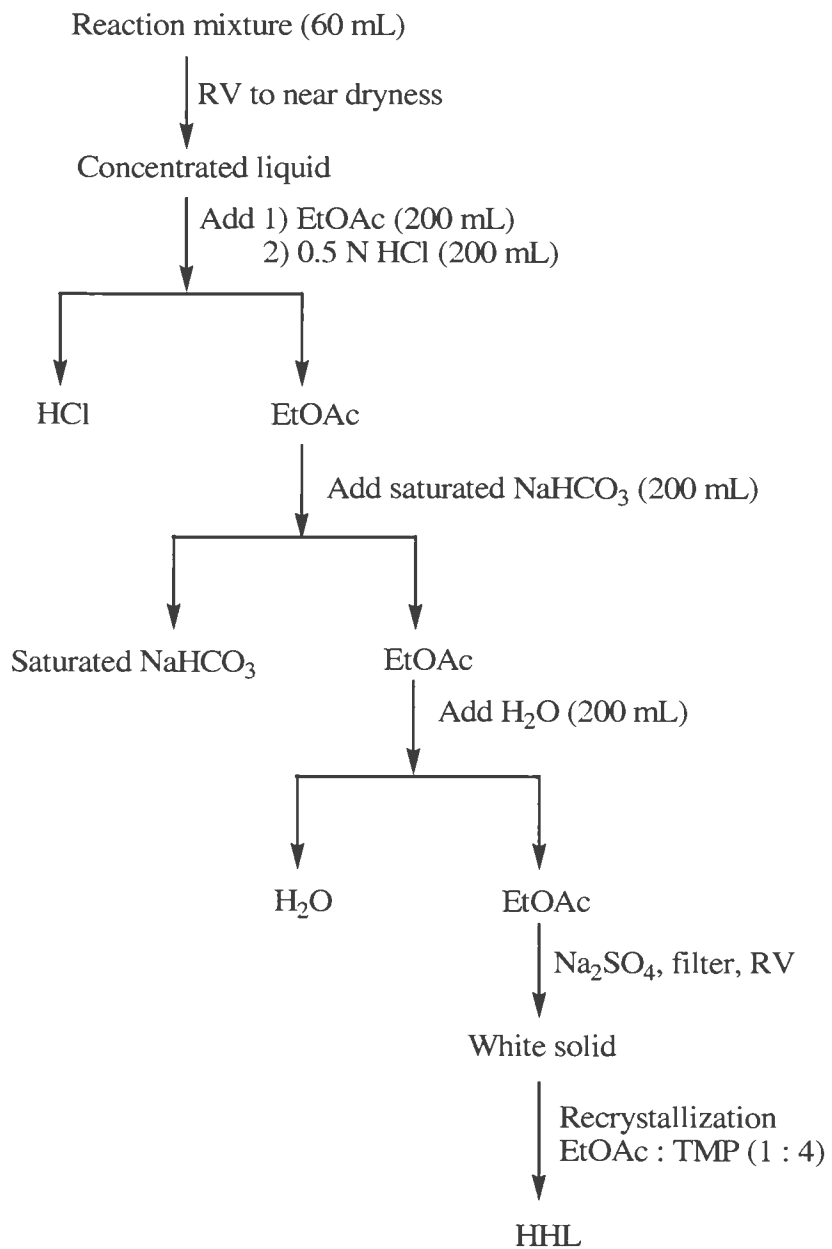


Figure 3.23. Purification of Synthetic HHL

Two quorum sensing inhibitors were synthesized to serve as active controls in the agar diffusion assay. *N*-decanoyl-*L*-homoserine lactone (DHL) (McClellan *et al.*, 1997) was synthesized using the same methodology as was used to prepare HHL, only decanoic acid (ALDRICH[®] Lot No. 03722BA) was used instead of hexanoic acid (Figure 3.24).

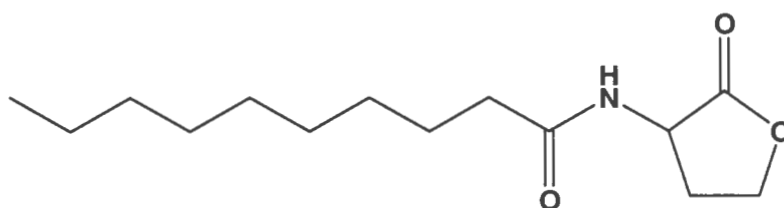


Figure 3.24. *N*-Decanoyl-*L*-Homoserine Lactone (DHL)

A second quorum sensing inhibitor synthesized was 4-bromo-5-(bromomethylene)-2(5*H*)-furanone (Figure 3.25). The two step reaction sequence is shown in figure 3.26 (Manny *et al.*, 1997).

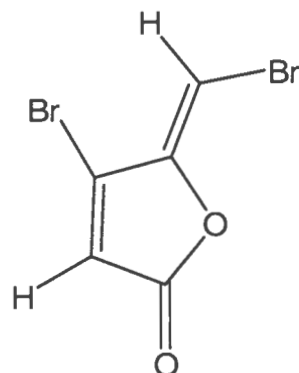


Figure 3.25. 4-Bromo-5-(Bromomethylene)-2(5*H*)-Furanone

The first step was the bromination of keto acid. Br₂ (3.215 mL, 0.062 mol) was diluted with 16 mL of CHCl₃ and added dropwise to a solution of levulinic acid (3.251 g, 0.028 mol) and 12 drops of 30% HBr in AcOH in 30 mL of CHCl₃. The resulting mixture was then heated slowly to 58 °C over 50 minutes, refluxed at 58 °C for 70 minutes, and then cooled to room temperature. The reaction mixture was washed sequentially with 40 mL of H₂O, 40 mL of 0.5 M Na₂S₂O₃, and finally 50 mL of saturated NaCl solution. The organic layer was dried over Na₂SO₄ and concentrated *in vacuo*. This dried material was used directly for the next step.

The second step was acid-promoted lactone formation. 30 mL of H₂SO₄ (98%) was added to the material obtained from the first step. The mixture was heated at 110-125 °C for 25 minutes. The hot acid solution was then slowly poured over crushed ice in a 200 mL-beaker. Dark oil that did not dissolve in the ice water could be observed at the bottom of the beaker. Using a separation funnel, the whole mixture was then extracted with 100 mL × 3 of dichloromethane (DCM). The dark oil material went into the organic solution easily. The DCM extract was then washed with 200 mL of water, dried over Na₂SO₄, and concentrated *in vacuo*.

Proton NMR analysis of the crude product showed it to be a mixture of brominated furanones with different bromo-substitutions (Manny *et al.*, 1997). Therefore, the crude product was purified as shown in Figure 3.27. First it was fractionated by vacuum liquid chromatography on silica-gel (KIMAX[®] funnel Lot No. 28400 packed with silica gel, SELECTO[®] Lot: 306087204, 2 cm thick) by eluting with 200 mL of the solvents as follows: 100% TMP → 5% TMP in EtOAc → 10% TMP in EtOAc → 25% TMP in EtOAc → 50% TMP in EtOAc → 100% EtOAc. The desired

compound shown in figure 3.25 was recognized by proton NMR spectra to reside in the 5% and 10% fractions. These two fraction were therefore combined and 60.5 mg was further purified by silica gel column chromatography (Kontes[®] 300 × 26 mm pack with silica gel of 260 × 26 mm, SELECTO[®] Lot: 306087204, isocratic elution with 1% EtoAc in TMP). 47 tubes of 25 mL each were pooled into 3 fractions based on thin layer chromatography analysis and concentrated *in vacuo*. Proton and carbon NMR spectra verified that the third fraction contained the desired product (Manny *et al.*, 1997).

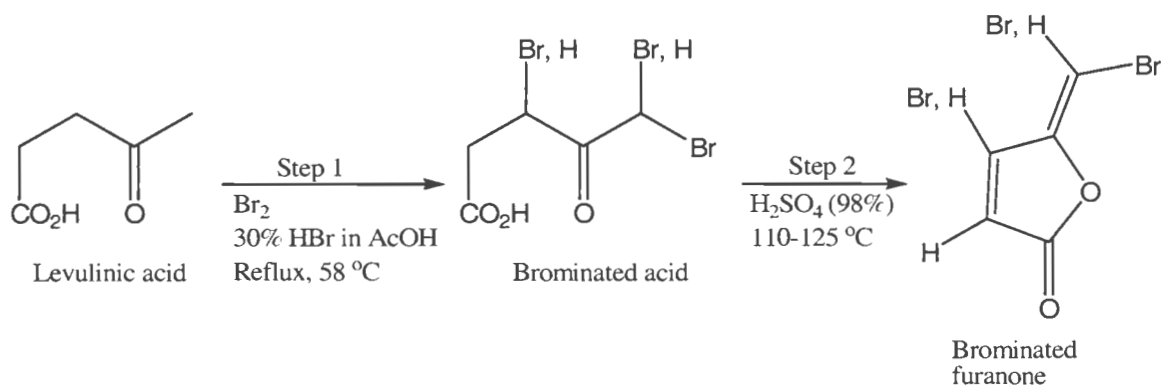


Figure 3.26. Synthesis of Brominated Furanones

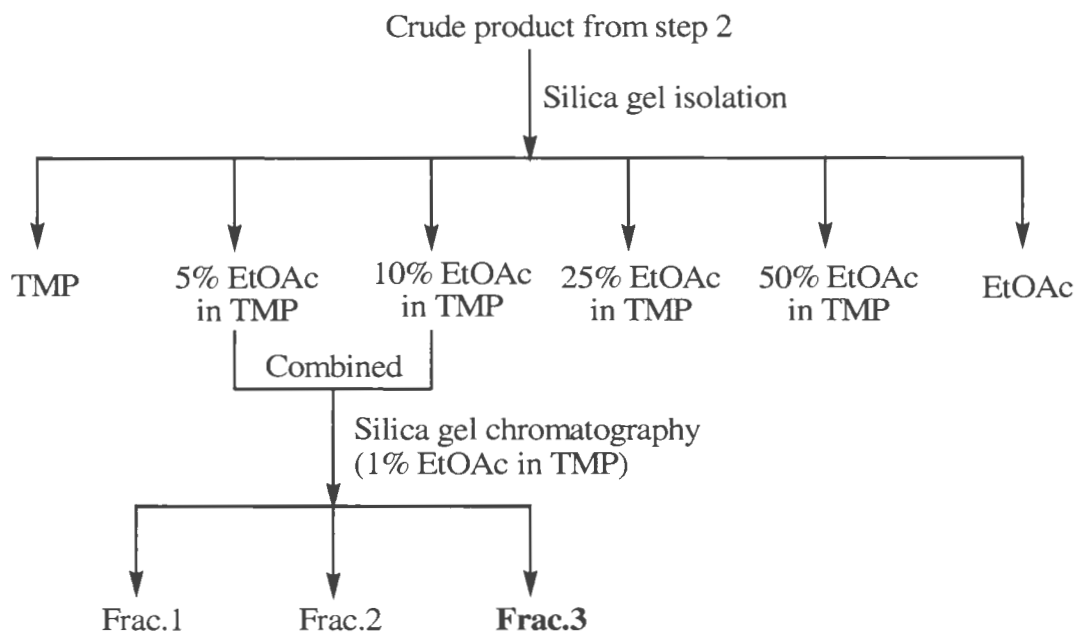


Figure 3.27. Purification of 4-Bromo-5-(Bromomethylene)-2(5H)-Furanone (**Frac.3**)

Inhibition of quorum sensing-mediated violacein production in CV026 by C42.191 and C42.205 was then examined. The assay was conducted as previously described. Synthetic HHL was used to induce violacein production by CV026 (30 μ L of HHL at 0.1 mg/mL in acetonitrile were added to each plate). Synthetic DHL and dibromofuranone served as active controls due to their published QS-inhibitory activity. The paper disks (BBL™ 6mm of diameter) were loaded with 20 μ L of acetonitrile (solvent control), DHL (three disks impregnated with 0.2 mg, 0.02 mg, and 0.002 mg),

dibromofuranone (0.2 mg), C42.191 and C42.205 (four disks each impregnated with 0.5 mg, 0.2 mg, 0.02 mg, and 0.002 mg). The loaded paper disks were air dried and applied over the top of the solidified LB₁₀ plates seeded with 50 μ L of the CV026 culture. The plates were then incubated at 29-30 °C overnight. The assay plates were then monitored for a period of 5 days. On the first day, DHL showed obvious QS-antagonistic activity. In contrast to the purple background, the disk loaded with 0.2 mg DHL displayed a 33.5 mm diameter opaque halo; 0.02 mg of DHL resulted in a 32.5 mm halo, and 0.002 mg of DHL produced a 25.5 mm diameter halo. However, DHL lost its activity gradually over a period of 5 days. Both C42.191 and C42.205 showed QS-antagonistic activity in this assay on disks impregnated with 0.5 mg of compound. Opaque halos of 10 mm and 12.5 mm were observed for C42.191 and C42.205, respectively. Interestingly, bioactivity of both C42.191 and C42.205 were constant over the length of the assay (Figure 3.28). The dibromofuranone at 0.2 mg showed obvious antibacterial activity since it resulted in a clear (killing) zone with a diameter of about 35 mm. Thus, its ability to inhibit QS could not be determined in this assay.

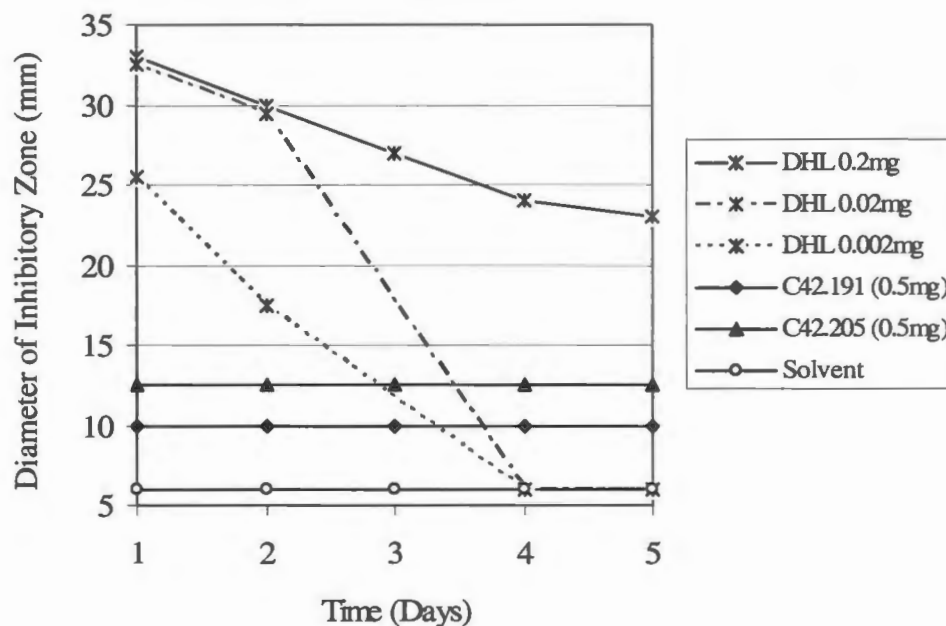


Figure 3.28. QS-Antagonistic Activity of DHL, C42.191 and C42.205

Note. The diameter of the inhibitory zone includes 6mm of the paper disk.

3.2.4.2 Green fluorescence protein assay.

The inhibitory activity of C42.205 against the production of green fluorescent protein (GFP) by *E. coli* JB525 was also examined.

E. coli JB525 harbors plasmid pJBA132 and expresses unstable GFP in response to C6-C8 AHLs (Anderson *et al.*, 2001; Wu *et al.*, 2000). This strain served as a second reporter strain for the studies here. Modified LB broth containing 4 g of NaCl was used to culture *E. coli* JB525 at 30 °C on a rotary shaker overnight. On the next day, the thick opaque culture was diluted to the OD₄₅₀ of 0.242 and then treated with 10 µL of a HHL solution (0.458 mg/mL in DMSO, final concentration of HHL at 100 nM). This cell culture-HHL mixture is hereafter referred to as CC-HHL. Eight culture tubes containing

a 30 mL of CC-HHL each were then treated with different concentrations of C42.205 (Table 3.4) and incubated at 30 °C with shaking. 1mL aliquots were withdrawn from each tube at 0 hr, 1hr, and 2hrs, and measured for optical density (OD₄₅₀) and fluorescence ($\lambda_{ex} = 475 \text{ nm}$, $\lambda_{em} = 515 \text{ nm}$). The results are shown in table 3.5. Relative fluorescent units (RFU) were divided by OD to normalize for cell density as shown in the following equation:

$$\text{RFU/OD} = (\text{FL}_{\text{sample}} - \text{FL}_{\text{blank}}) / (\text{OD}_{\text{sample}} - \text{OD}_{\text{blank}}).$$

Figure 3.29 shows the RFU/OD as a function of time. Over the length of the assay, 1.2 mM of C42.205 completely inhibited GFP production. Activity decreased as a function of concentration decreases, with the lowest concentration tested (1.96 μM) still showing obvious inhibitory activity.

Table 3.4

The GFP Assay Set Up and the Serial Concentration of C42.205

Tube	Preparation	Concentration of C42.205
1	29.8 mL CC-HHL + 0.2 mL DMSO	Solvent Control
2	29.8 mL CC-HHL + 0.2 mL C42.205	6 mM
3	29.8 mL CC-HHL + 0.2 mL C42.205	1.2 mM
4	29.8 mL CC-HHL + 0.2 mL C42.205	240 μM
5	29.8 mL CC-HHL + 0.2 mL C42.205	48 μM
6	29.8 mL CC-HHL + 0.2 mL C42.205	9.6 μM
7	29.8 mL CC-HHL + 0.2 mL C42.205	1.92 μM
8	30.0 mL diluted cell culture	Bacterial Growth

Table 3.5

Measured Fluorescence and Optical Density

Culture tube			0hr		1hr		2hr	
	FL	OD	FL	OD	FL	OD	FL	OD
Tube 1	HHL	100nM	34.883	0.646	52.196	0.809	48.407	0.645
Tube 2	C42.205	6000 μ M	32.817	0.618	32.905	0.766	34.243	0.729
Tube 3	C42.205	1200 μ M	32.296	0.647	33.299	0.775	33.739	0.825
Tube 4	C42.205	240 μ M	32.862	0.619	39.273	0.802	37.379	0.878
Tube 5	C42.205	48 μ M	33.437	0.639	44.788	0.808	44.256	0.972
Tube 6	C42.205	9.6 μ M	35.329	0.656	50.373	0.772	47.615	0.948
Tube 7	C42.205	1.92 μ M	36.265	0.624	51.241	0.845	48.711	0.821
Tube 8	Bacterial growth		32.013	0.675	32.462	0.758	32.676	0.766
Blank	LB ₄ Broth		33.657	0.371	32.850	0.374	33.850	0.383

Note. FL, $\lambda_{ex} = 475\text{nm}$, $\lambda_{em} = 515\text{nm}$; OD, $\lambda = 450\text{nm}$. Values represent an average of three readings.

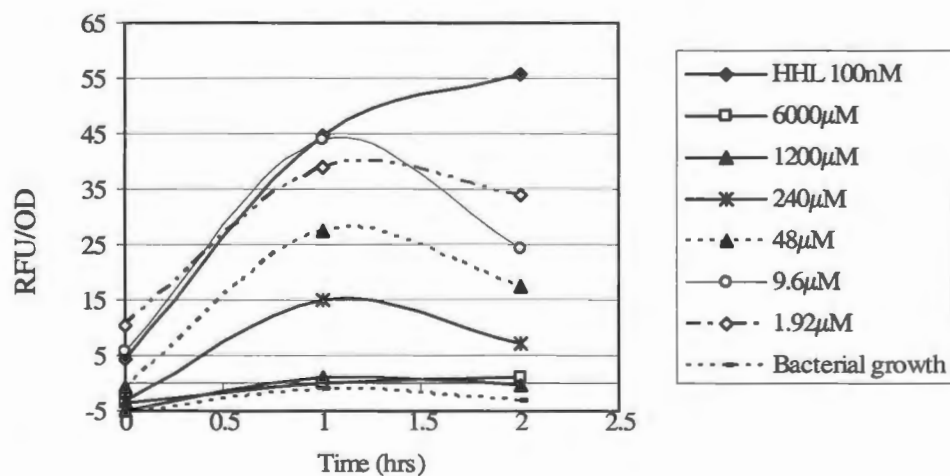


Figure 3.29. C42.205 Inhibition of QS-mediated GFP Production

3.3 Summary and Discussion

Bioassay guided fractionation of the culture of a *Halobacillus* sp. led to the isolation of two arylethylamide compounds herein referred to as C42.191 and C42.205. Both C42.191 and C42.205 were previously reported to be isolated from a possible limnic *Bacillus* sp. culture, but no bioactivity was reported (Maskey *et al.*, 2002). DHL and a dibromofuranone compound were synthesized and utilized as active controls due to their published QS-antagonistic activity. DHL showed obvious QS-inhibitory activity in the CV026 reporter assay. Surprisingly, the dibromofuranone showed antibacterial activity, and no obvious QS-inhibitory activity was observed for this molecule in this assay.

Both C42.191 and C42.205 showed certain QS-antagonistic activity. In the agar diffusion assay, the violacein-inhibitory zones resulted from C42.191 (dia = 10 mm) was slightly less than that from C42.205 (dia = 12.5 mm), both of which were much smaller than that from DHL (dia > 35mm at lower concentrations). This is likely due to DHL being a more potent inhibitor than C42.191 and C42.205. However, the diffusion rate of the three compounds into agar is unknown, and therefore one cannot assess absolutely which is more potent based on this assay. An interesting observation was that the opaque halos resulting from DHL shrank over the period of assay. This implies that CV026 restored its ability to produce the purple pigment over time. In contrast, the halos resulting from C42.191 and C42.205 were maintained over the five-day assay, perhaps indicating the irreversible nature of the inhibition by these two compounds. Alternatively, DHL may not be stable over the length of the assay. In the GFP assay, C42.205 showed obvious QS-inhibitory activity. GFP production was completely

abolished at 1.2 mM of C42.205, while the lowest concentration tested (1.96 μ M) still showed obvious antagonist activity.

Interestingly, Gram-positive bacteria such as C42 are not expected to use AHLs as cell-cell signaling molecules. It is curious that C42 produces secondary metabolites that interfere with a Gram-negative signaling pathway, but does not inhibit bacterial growth. *This is the first time that metabolites from Gram-positive bacterium have demonstrated this type of activity.* This result hints at a possible ecological advantage for bacteria to jam the communication pathways of their competitors.

In future studies, further assays, such as the *Serratia liquefaciens*' swarming motility assay, should be employed to more completely explore the anti-quorum sensing activity of these molecules. Also, synthesis of analogues of these simple molecules should help clarify their important structural features. Like AHLs, arylethylamides also possess a ring system with a side chain connected via an amide bond. These compounds represent a new chemotype for quorum sensing inhibitors, and synthetic manipulation of their unique features may lead to a new generation of molecules to combat antibiotic resistance.

3.4 References

Andersen J. B., Heydorn A., Hentzer M., Eberl L., Geisenberger O., Christensen B. B., Molin S., and Givskov M. *gfp*-based *N*-acyl homoserine-lactone sensor systems for detection of bacterial communication. *Applied and environmental microbiology*. 2001 (67): 575-585.

- Balaban N., Giacometti A., Cirioni O., Gov Y., Ghiselli R., Mocchegiani F., Viticchi C., Prete M.S.D., Saba V., Scalise G., and Dell'Acqua G. Use of the quorum-sensing inhibitor RNAIII-inhibiting peptide to prevent biofilm formation in vivo by drug-resistant *Staphylococcus epidermidis*. *The Journal of Infectious Diseases*. 2003 (187): 625-630.
- Bassler B. L., Greenberg E. P. and Stevens A. M. Cross-species induction of luminescence in the quorum-sensing bacterium *Vibrio harveyi*. *Journal of Bacteriology*. 1997 (179): 4043-4045.
- Bassler B. L., Wright M., Showalter R. E., and Silverman M. R. Intercellular signaling in *Vibrio harveyi*: Sequence and function of genes regulating expression of luminescence. *Molecular Microbiology*. 1993 (9): 773-786.
- Bassler B. L., Wright M., and Silverman M. R. Multiple signaling systems controlling expression of luminescence in *Vibrio harveyi*: Sequence and function of genes encoding a second sensory pathway. *Molecular Microbiology*. 1994 (13): 273-286.
- Brittain D. C. Erythromycin. *The Medical Clinics of North America*. 1987 (71): 1147-1154.
- Chen X., Schauder S., Poteer N., Dorsselaer A. V., Pelczer I., Bassler B. and Hughson F. M. Structural identification of a bacterial quorum-sensing signal containing boron. *Nature*. 2002 (415), 545-549.
- Chharbra S. R., Stead P., Bainton N. J., Salmond G. P. C., Stewart G. S. A. B., Williams P., and Bycroft B. Autoregulation of carbapenem biosynthesis in *Erwinia*

- carotovora* by analogues of *N*-(3-oxohexanoyl)-*L*-homoserine lactone. *The Journal of Antibiotics*. 1993 (46): 441-454.
- Eberl L. Winson M. K. Sternberg C. Stewart G. S. A. B., Christiansen G., Chhabra S. R., Bycroft B. W., Williams P., Molin S. and Givskov M. Involvement of *N*-acyl-*L*-homoserine lactone autoinducers in controlling the multicellular behavior of *Serratia liquefaciens*. *Molecular Microbiology*. 1996 (20): 127-136.
- Federle M. J., and Bassler B. L. Interspecies communication in bacteria. *Journal of Clinicacl Investigation*. 2003 (112): 1291–1299.
- Francke E. L., and Neu H. C. Chloramphenicol and tetracyclines. *The Medical Clinics of North America* 1987(71): 1155-1168.
- Geddes A. Infection in the twenty-first century: Predictions and postulates. *Journal of Antimicrobial Chemotherapy*. 2000 (46): 873-878.
- Gov Y., Bitler A., Dell'Acqua G., Torres J. V., and Balaban N. RNAIII-inhibiting peptide (RIP), a global inhibitor of *Staphylococcus aureus* pathogenesis: structure and function analysis. *Peptides*. 2001 (22): 1609-1620.
- Gram L., Rocky de NYS., Maximilien R., Givskov M., Steinberg P., and Kjelleberg S. Inhibitory effects of secondary metabolites from the red alga *Delisea pulchra* on swarming motility of *Proteus mirabilis*. *Applied and Environmental Microbiology*. 1996(62): 4284-4287.
- Gregerson T. Rapid method for distinction of Gram-negative from Gram-positive bacteria. *European Journal of Applied Microbiology and Biotechnology*. 1978(5): 123-127.

- Haleblian S., Harris B., Finegold S. M. and Rolfe R. D. Rapid method that aids in distinguishing Gram-positive from Gram-negative anaerobic bacteria. *Journal of Clinical Microbiology*. 1981(13): 444-448.
- Hastings J. W. and Nealson K. H. Bacterial bioluminescence. *Annual Review of Microbiology*. 1977 (31): 549-595.
- Hentzer M., Riedel K., Rasmussen T. B., Heydorn A., Andersen J. B., Parsek M. R., Rice S. A., Eberl L., Molin S. HØiby N., Kjelleberg S., and Givskov M. Inhibit of quorum sensing in *Pseudomonas aeruginosa* biofilm bacteria by a halogenated furanone compound. *Microbiology*. 2002 (148): 87-102.
- Hentzer M., Wu H., Andersen J. B., Riedel K., Rasmussen T. B., Bagge N., Kumar N., Schembri M. A., Song Z., Kristoffersen P., Manefield M., Costerton J. W., Molin S., Eberl L., Steinberg P., Kjelleberg S., HØiby N., Givskov M. Attenuation of *Pseudomonas aeruginosa* virulence by quorum sensing inhibitors. *The European Molecular Biology Organization Journal*. 2003 (22): 3803-3815.
- Klein N.C., and Cunha B.A. Tetracyclines. *The Medical Clinics of North America*. 1995(79): 789-801.
- Latifi A., Foglino M., Tanaka T., Williams P., and Lazdunski A. A hierarchical quorum sensing cascade in *Pseudomonas aeruginosa* links the transcriptional activators LasR and VsmR to expression of the stationary phase sigma factor RpoS. *Molecular Microbiology*. 1996 (21): 1137-1146.
- Lazazzera B. A. and Grossman A. D. The ins and outs of peptide signaling. *Trends in Microbiology*. 1998 (6): 288-294.

- Lindum P. W., Anthoni U., Christophersen C., Eberl L., Molin S., and Givskov M. *N*-acyl-*L*-homoserine lactone autoinducers control production of an extracellular lipopeptide biosurfactant required for swarming motility of *Serratia liquefaciens* MG1. *Journal of Bacteriology*. 1998 (180): 6384-6388.
- Lyon B. R., and Skurray R. Antimicrobial resistance of *Staphylococcus aureus*: genetic basis. *Microbiological Reviews*. 1987 (51): 88-134.
- Madigan M. T., Martinko J. M., and Parker J. Light Microscopy. In *Brock Biology of Microorganisms*. Pearson Education, Inc. 2003b (10th Ed): pp56-60.
- Manefield M., Welch M., Givskov M., Salmond G. P. C., and Kjelleberg S. Halogenated furanones from the red alga, *Delisea pulchra*, inhibit carbapenem antibiotic synthesis and exoenzyme virulence factor production in the phytopathogen *Erwinia carotovora*. *FEMS Microbiology Letters*. 2001 (205): 131-138.
- Manny B. J., Kjelleberg S., Kumar N., Rocky de Nys, Read R.W. and Steinberg P. Reinvestigation of the sulfuric acid-catalysed cyclisation of brominated 2-alkyllevulinic acids to 3-alkyl-5-methylene-2(5*H*)-furanones. *Tetrahedron*. 1997 (53): 15813-15826.
- Maskey R. P., Asolkar R. N., Kapaun E., Wagner-Döbler I. and Laatsch H. Phytotoxic arylethylamides form Limnic bacteria using a screening with microalgae. *The Journal of Antibiotics*. 2002 (55): 643-649.
- McClellan K. H., Winson M. K., Fish L., Taylor A., Chhabra S. R., Camara M., Daykin M., Lamb J. H., Swift S., Bycroft B. W., Stewart G. S. A. B. and Williams P. Quorum sensing and *Chromobacterium violaceum*: exploitation of violacein

- production and inhibition for the detection of *N*-acyl-homoserine lactones. *Microbiology*. 1997 (143): 3703-3711.
- Miller, M. B. & Bassler, B. L. Quorum sensing in bacteria. *Annual Review of Microbiology*. 2001 (55): 65–199.
- Nealson K. H. and Hastings J. W. Bacterial bioluminescence: Its control and ecological significance. *Microbiology Review*. 1979 (43): 496-518.
- Rasmussen T. B., Manefield M., Andersen B. G., Eberl L., Anthoni U., Christophersen C., Steinberg P., Kjelleberg S., and Givskov M. How *Delisea pulchra* furanones affect quorum sensing and swarming motility in *Serratia liquefaciens* MG1. *Microbiology*. 2000 (146): 3237-3244.
- Ruby, E. G. Lessons from a cooperative, bacterial-animal association: The *Vibrio fischeri*-*Euprymna scolopes* light organ symbiosis. *Annual Review of Microbiology*. 1996 (50): 591-624.
- Schaberg D. R., Culver D. H., and Gaynes R. P. Major trends in the microbial etiology of nosocomial infection. *The American Journal of Medicine*. 1991(16): 72S-75S.
- Schauder S., Bassler B. L. The languages of bacteria. *Genes and Development*. 2001 (15): 1468-1480.
- Smilack J. D., Wilson W. R., and Cockerill F. R. 3rd. Tetracyclines, chloramphenicol, erythromycin, clindamycin, and metronidazole. *Mayo Clinic Proceedings*. 1991 (66): 1270-1280.
- Throup J., Winson M. K., Bainton N. J., Bycroft B. W., Williams P. and Stewart G. S. A. B. Signalling in bacteria beyond bioluminescence. In *Bioluminescence and*

- Chemiluminescence: Fundamentals and Applied Aspects*, 1995, pp89-92. Edited by A. Campbell, L. Kricka & P. Stanley. Chichester: Wiley.
- Visick K. L. and McFall-Ngai M. J. An exclusive contract: Specificity in the *Vibrio fischeri-Euprymna scolopes* partnership. *Journal of Bacteriology*. 2000 (182): 1779-1787.
- Wang Y., Biologically active secondary metabolites from marine microorganisms. In *A thesis submitted in partial fulfillment of the requirements for the degree of master in pharmacognosy*. University of Rhode Island. 2003c, pp63-65.
- Whitehead N. A., Barnard A. M. L., Slater H., Simpson N. J. L., and Salmond G.P.C. Quorum-sensing in gram-negative bacteria. *FEMS Microbiology Reviews*. 2001 (25): 365-404.
- Wu H., Song Z., Hentzer. M., Andersen J. B. Heydorn A., Mathee K., Moser C., Eberl L, Molin S. Høiby N., and Givskov M. Detection of *N*-acyl-homoserine lactones in lung tissues of mice infected with *Pseudomonas aeruginosa*. *Microbiology*. (2000) 146: 2481-2493.
- Zhu J., and Mekalanos J. J. Quorum sensing-dependent biofilms enhance colonization in *Vibrio cholerae*. *Developmental Cell*. 2003 (5): 647-656.

BIBLIOGRAPHY

- Allredge, A. L., Cole J. and Caron D. A. Production of heterotrophic bacteria inhabiting organic aggregates (marine snow) from surface waters. *Limnology and Oceanography*. 1986 (31): 68-78.
- Andersen J. B., Heydorn A., Hentzer M., Eberl L., Geisenberger O., Christensen B. B., Molin S., and Givskov M. *gfp*-based *N*-acyl homoserine-lactone sensor systems for detection of bacterial communication. *Applied and environmental microbiology*. 2001 (67): 575-585.
- Balaban N., Giacometti A., Cirioni O., Gov Y., Ghiselli R., Mocchegiani F., Viticchi C., Prete M.S.D., Saba V., Scalise G., and Dell'Acqua G. Use of the quorum-sensing inhibitor RNAIII-inhibiting peptide to prevent biofilm formation in vivo by drug-resistant *Staphylococcus epidermidis*. *The Journal of Infectious Diseases*. 2003 (187): 625-630.
- Bassler B. L., Greenberg E. P. and Stevens A. M. Cross-species induction of luminescence in the quorum-sensing bacterium *Vibrio harveyi*. *Journal of Bacteriology*. 1997 (179): 4043-4045.
- Bassler B. L., Wright M., Showalter R. E., and Silverman M. R. Intercellular signaling in *Vibrio harveyi*: Sequence and function of genes regulating expression of luminescence. *Molecular Microbiology*. 1993 (9): 773-786.
- Bassler B. L., Wright M., and Silverman M. R. Multiple signaling systems controlling expression of luminescence in *Vibrio harveyi*: Sequence and function of genes encoding a second sensory pathway. *Molecular Microbiology*. 1994 (13): 273-286.

- Brittain D. C. Erythromycin. *The Medical Clinics of North America*. 1987 (71): 1147-1154.
- Casey M. L., Paulick R. C., and Whitlock H. W. Jr. A carbon-13 nuclear magnetic resonance study of mollisin and its biosynthesis. *Journal of the American Chemical Society*. 1976 (98): 2636-2640.
- Chen X., Schauder S., Poteer N., Dorsselaer A. V., Pelczer I., Bassler B. and Hughson F. M. Structural identification of a bacterial quorum-sensing signal containing boron. *Nature*. 2002 (415), 545-549.
- Chhabra S. R., Stead P., Bainton N. J., Salmond G. P. C., Stewart G. S. A. B., Williams P., and Bycroft B. Autoregulation of carbapenem biosynthesis in *Erwinia carotovora* by analogues of *N*-(3-oxohexanoyl)-*L*-homoserine lactone. *The Journal of Antibiotics*. 1993 (46): 441-454.
- Colwell R. R. Global climate and infectious disease: The cholera paradigm. *Science*. 1996 (274): 2025-2031.
- Eberl L. Winson M. K. Sternberg C. Stewart G. S. A. B., Christiansen G., Chhabra S. R., Bycroft B. W., Williams P., Molin S. and Givskov M. Involvement of *N*-acyl-*L*-homoserine lactone autoinducers in controlling the multicellular behavior of *Serratia liquefaciens*. *Molecular Microbiology*. 1996 (20): 127-136.
- Epstein P. R. Climate and health. *Science*. 1999 (285): 347-348.
- Federle M. J., and Bassler B. L. Interspecies communication in bacteria. *Journal of Clinical Investigation*. 2003 (112): 1291-1299.
- Francke E. L., and Neu H. C. Chloramphenicol and tetracyclines. *The Medical Clinics of North America* 1987(71): 1155-1168.

- Fredenhagen A., Tamura S. Y., Kenny P. T. M., Komura H., Naya Y., and Nakanishi K. Andrimid, a new peptide antibiotic produced by an intracellular bacterial symbiont isolated from a brown planthopper. *Journal of American Chemical Society*. 1987 (109): 4409-4411.
- Geddes A. Infection in the twenty-first century: Predictions and postulates. *Journal of Antimicrobial Chemotherapy*. 2000 (46): 873-878.
- Gov Y., Bitler A., Dell'Acqua G., Torres J. V., and Balaban N. RNAIII-inhibiting peptide (RIP), a global inhibitor of *Staphylococcus aureus* pathogenesis: structure and function analysis. *Peptides*. 2001 (22): 1609-1620.
- Gram L., Rocky de NYS., Maximilien R., Givskov M., Steinberg P., and Kjelleberg S. Inhibitory effects of secondary metabolites from the red alga *Delisea pulchra* on swarming motility of *Proteus mirabilis*. *Applied and Environmental Microbiology*. 1996(62): 4284-4287.
- Gregerson T. Rapid method for distinction of Gram-negative from Gram-positive bacteria. *European Journal of Applied Microbiology and Biotechnology*. 1978(5): 123-127.
- Halebian S., Harris B., Finegold S. M. and Rolfe R. D. Rapid method that aids in distinguishing Gram-positive from Gram-negative anaerobic bacteria. *Journal of Clinical Microbiology*. 1981(13): 444-448.
- Harvell C. D., Mitchell C. E., Ward J. R., Altizer S., Dobson A. P., Ostfeld R. S., and Samuel M. D. Climate warming and disease risks for terrestrial and marine biota. *Science*. 2002 (296): 2158-2162.

- Hastings J. W. and Nealson K. H. Bacterial bioluminescence. *Annual Review of Microbiology*. 1977 (31): 549-595.
- Hentzer M., Riedel K., Rasmussen T. B., Heydorn A., Andersen J. B., Parsek M. R., Rice S. A., Eberl L., Molin S. HØiby N., Kjelleberg S., and Givskov M. Inhibit of quorum sensing in *Pseudomonas aeruginosa* biofilm bacteria by a halogenated furanone compound. *Microbiology*. 2002 (148): 87-102.
- Hentzer M., Wu H., Andersen J. B., Riedel K., Rasmussen T. B., Bagge N., Kumar N., Schembri M. A., Song Z., Kristoffersen P., Manefield M., Costerton J. W., Molin S., Eberl L., Steinberg P., Kjelleberg S., HØiby N., Givskov M. Attenuation of *Pseudomonas aeruginosa* virulence by quorum sensing inhibitors. *The European Molecular Biology Organization Journal*. 2003 (22): 3803-3815.
- Herbert R. B. Polyketides. In *The Biosynthesis of Secondary metabolites*. Chapman and Hall Ltd. 1989a (2nd Ed): pp33-34.
- Herbert R. B. Polyketides. In *The Biosynthesis of Secondary metabolites*. Chapman and Hall Ltd. 1989b (2nd Ed): pp38-42.
- Herbert R. B. Technique for biosynthesis. In *The biosynthesis of Secondary Metabolites*. Chapman and Hall Ltd. 1989c (2nd Ed): pp22.
- Iijima H., Noguchi H., Ebizuka Y., Sankawa U., and Seto H. The biosynthesis of Patulin: the mechanism of oxidative aromatic ring cleavage and loss of side chain protons from aromatic intermediates. *Chemical and Pharmaceutical Bulletin*. 1983 (31): 362-365.
- Klein N.C., and Cunha B.A. Tetracyclines. *The Medical Clinics of North America*. 1995(79): 789-801.

- Latifi A., Foglino M., Tanaka T., Williams P., and Lazdunski A. A hierarchical quorum sensing cascade in *Pseudomonas aeruginosa* links the transcriptional activators LasR and VsmR to expression of the stationary phase sigma factor RpoS. *Molecular Microbiology*. 1996 (21): 1137-1146.
- Lazazzera B. A. and Grossman A. D. The ins and outs of peptide signaling. *Trends in Microbiology*. 1998 (6): 288-294.
- Lindum P. W., Anthoni U., Christophersen C., Eberl L., Molin S., and Givskov M. *N*-acyl-*L*-homoserine lactone autoinducers control production of an extracellular lipopeptide biosurfactant required for swarming motility of *Serratia liquefaciens* MG1. *Journal of Bacteriology*. 1998 (180): 6384-6388.
- Long R. A. and Azam F. Antagonistic interactions among marine pelagic bacteria. *Applied and Environmental Microbiology*. 2001 (67): 4975-4983.
- Lyon B. R., and Skurray R. Antimicrobial resistance of *Staphylococcus aureus*: genetic basis. *Microbiological Reviews*. 1987 (51): 88-134.
- Madigan M. T., Martinko J. M., and Parker J. Cholera, In *Brock Biology of Microorganisms*. Pearson Education, Inc. 2003a (10th Ed): pp943-944.
- Madigan M. T., Martinko J. M., and Parker J. Light Microscopy. In *Brock Biology of Microorganisms*. Pearson Education, Inc. 2003b (10th Ed): pp56-60.
- Manefield M., Welch M., Givskov M., Salmond G. P. C., and Kjelleberg S. Halogenated furanones from the red alga, *Delisea pulchra*, inhibit carbapenem antibiotic synthesis and exoenzyme virulence factor production in the phytopathogen *Erwinia carotovora*. *FEMS Microbiology Letters*. 2001 (205): 131-138.

- Manny B. J., Kjelleberg S., Kumar N., Rocky de Nys, Read R.W. and Steinberg P.
Reinvestigation of the sulfuric acid-catalysed cyclisation of brominated 2-alkyllevulinic acids to 3-alkyl-5-methylene-2(5H)-furanones. *Tetrahedron*. 1997 (53): 15813-15826.
- Maskey R. P., Asolkar R. N., Kapaun E., Wagner-Döbler I. and Laatsch H. Phytotoxic arylethylamides from Limnic bacteria using a screening with microalgae. *The Journal of Antibiotics*. 2002 (55): 643-649.
- McClellan K. H., Winson M. K., Fish L., Taylor A., Chhabra S. R., Camara M., Daykin M., Lamb J. H., Swift S., Bycroft B. W., Stewart G. S. A. B. and Williams P. Quorum sensing and *Chromobacterium violaceum*: exploitation of violacein production and inhibition for the detection of *N*-acyl-homoserine lactones. *Microbiology*. 1997 (143): 3703-3711.
- McMurry J. Intramolecular claisen condensations: the dieckmann cyclization. In *Organic Chemistry*. Brooks/Cole Publishing Company. 1988 (2nd Ed): pp837-839.
- Miller, M. B. & Bassler, B. L. Quorum sensing in bacteria. *Annual Review of Microbiology*. 2001 (55): 65-199.
- Nealson K. H. and Hastings J. W. Bacterial bioluminescence: Its control and ecological significance. *Microbiology Review*. 1979 (43): 496-518.
- Needham J., Kelly M. T., Ishige M., and Andersen R. J. Andrimid and moiramides A-C, metabolites produced in culture by a marine isolate of the bacterium *Pseudomonas fluorescens*: structure elucidation and biosynthesis. *Journal of Organic Chemistry*. 1994 (59): 2058-2063.

- Pascual M., Rodó X., Ellner S. P., Colwell, R. and Bouma M. J. Cholera dynamics and El Niño-Southern oscillation. *Science*. 2000 (289): 1766-1769.
- Ramamurthy T., Garg S., Sharma R., Bhattacharya S. K., Nair G. B., Shimada T., Takeda T., Karasawa T., Kurazano H., Pal A., and Takeda Y. Emergence of novel strain of *Vibrio cholerae* with epidemic potential in southern and eastern India. *Lancet*. 1993(341): 703-704.
- Rasmussen T. B., Manefield M., Andersen B. G., Eberl L., Anthoni U., Christophersen C., Steinberg P., Kjelleberg S., and Givskov M. How *Delisea pulchra* furanones affect quorum sensing and swarming motility in *Serratia liquefaciens* MG1. *Microbiology*. 2000 (146): 3237-3244.
- Renner M. K., Jensen P. R., and Fenical W. Mangicols: structures and biosynthesis of a new class of sesterterpene polyols from a marine fungus of the genus *Fusarium*. *Journal of Organic Chemistry*. 2000 (65): 4843-4852.
- Ruby, E. G. Lessons from a cooperative, bacterial-animal association: The *Vibrio fischeri*-*Euprymna scolopes* light organ symbiosis. *Annual Review of Microbiology*. 1996 (50): 591-624.
- Ruiz G. M., Rawlings T. K., Dobbs F. C., Drake L. A., Mullady T., Huq A., and Colwell R. R. Global spread of microorganisms by ships. *Nature*. 2000 (408): 49-50.
- Schaberg D. R., Culver D. H., and Gaynes R. P. Major trends in the microbial etiology of nosocomial infection. *The American Journal of Medicine*. 1991(16): 72S-75S.
- Schauder S., Bassler B. L. The languages of bacteria. *Genes and Development*. 2001 (15): 1468-1480.

- Shimada T., Nair G., Deb B. C., Albert M. J., Sack R. B., and Takeda Y. Outbreak of *Vibrio cholerae* non-01 in India and Bangladesh. *Lancet*. 1993(341): 1347.
- Singh M. P., Mroczenski-Wildey M. J., Steinberg D. A., Andersen R. J., Maiese W. M., and Greenstein M. Biological activity and mechanistic studies of andrimid. *The Journal of Antibiotics*. 1997 (50): 270-273.
- Smilack J. D., Wilson W. R., and Cockerill F. R. 3rd. Tetracyclines, chloramphenicol, erythromycin, clindamycin, and metronidazole. *Mayo Clinic Proceedings*. 1991 (66): 1270-1280.
- Stretton S., Techkarnjanaruk S., McLennan A. M., and Goodman A. E. Use of green fluorescent protein to tag and investigate gene expression in marine bacteria. *Applied and Environmental Microbiology*. 1998 (64): 2554-2559.
- Throup J., Winson M. K., Bainton N. J., Bycroft B. W., Williams P. and Stewart G. S. A. B. Signalling in bacteria beyond bioluminescence. In *Bioluminescence and Chemiluminescence: Fundamentals and Applied Aspects*, 1995, pp89-92. Edited by A. Campbell, L. Kricka & P. Stanley. Chichester: Wiley.
- Visick K. L. and McFall-Ngai M. J. An exclusive contract: Specificity in the *Vibrio fischeri*-*Euprymna scolopes* partnership. *Journal of Bacteriology*. 2000 (182): 1779-1787.
- Waldor M. K., Colwell R. R., and Mekalanos J. J. The *Vibrio cholerae* O139 serogroup antigen includes an O-antigen capsule and lipopolysaccharide virulence determinants. *National Academy of Sciences Proceedings in USA*. 1994 (91): 11388 -11392.

- Wang Y. Biologically active secondary metabolites from marine microorganisms. A *thesis submitted in partial fulfillment of the requirements for the degree of master in pharmacognosy*. University of Rhode Island. 2003a: pp27-59.
- Wang Y. Biologically active secondary metabolites from marine microorganisms. A *thesis submitted in partial fulfillment of the requirements for the degree of master in pharmacognosy*. University of Rhode Island. 2003b: pp74-94.
- Wang Y., Biologically active secondary metabolites from marine microorganisms. In A *thesis submitted in partial fulfillment of the requirements for the degree of master in pharmacognosy*. University of Rhode Island. 2003c, pp63-65.
- Whitehead N. A., Barnard A. M. L., Slater H., Simpson N. J. L., and Salmond G.P.C. Quorum-sensing in gram-negative bacteria. *FEMS Microbiology Reviews*. 2001 (25): 365-404.
- Wu H., Song Z., Hentzer. M., Andersen J. B. Heydorn A., Mathee K., Moser C., Eberl L, Molin S. Høiby N., and Givskov M. Detection of *N*-acyl-homoserine lactones in lung tissues of mice infected with *Pseudomonas aeruginosa*. *Microbiology*. (2000) 146: 2481-2493.
- Zhu J., and Mekalanos J. J. Quorum sensing-dependent biofilms enhance colonization in *Vibrio cholerae*. *Developmental Cell*. 2003 (5): 647-656.